STRUCTURAL ANALYSIS OF TRANSMISSION TOWERS WITH CONNECTION SLIP MODELING

by
Donovan Kroeker
B.Sc. Civil Engineering

A Thesis
Submitted to the Faculty of Graduate Studies of
the University of Manitoba in Partial Fulfillment
of the Requirements for the Degree of

Master of Science

Department of Civil and Geological Engineering
University of Manitoba
Winnipeg, Manitoba

THE UNIVERSITY OF MANITOBA

FACULTY OF GRADUATE STUDIES

*****

COPYRIGHT PERMISSION PAGE

Structural Analysis of Transmission Towers with Connection Slip Modeling

BY

Donovan Kroeker

A Thesis/Practicum submitted to the Faculty of Graduate Studies of The University of Manitoba in partial fulfillment of the requirements of the degree of Master of Science

ABSTRACT

Self-supporting latticed structures are used in a wide variety of civil engineering applications, most commonly to support transmission lines that transmit and distribute electricity. Manitoba Hydro has approximately 10000 self-supporting latticed transmission towers located throughout the province of Manitoba. The current method for analyzing transmission towers among practicing engineers is to assume linear-elastic behavior and to treat the angle members as pin-ended truss elements. This approach ignores the effects of bolt slippage and local bolt deformation, geometric or material nonlinearity, joint flexibility, and the bending stiffness of the angle members. When the deflections and member axial forces measured in transmission towers in Manitoba are compared with the predictions from linear-elastic programs, there can be a large discrepancy. It is suspected that the bolt slippage and, to a lesser extent, the bending stiffness in the main leg members (not accounted for in linear-elastic programs) are causing the discrepancy between the predicted and the actual structural response. In an effort to improve the structural analysis of transmission towers, this study investigates the effect of bolt slippage on the deflections and member stresses of latticed self-supporting transmission towers. The computer program developed in this study can model tower members as truss and beam elements, can incorporate bolt slippage using an instantaneous slippage model or a continuous slippage model, and can model the connections as semi-rigid (flexible connections) provided moment-rotation data are available. The slippage models require certain parameters, determined from load-deformation experiments on typical angle members, in order to accurately incorporate the effect of bolt slippage. Each member of the transmission tower can have its own slippage properties (most importantly the actual amount of clearance slip and the load which initiates clearance slip) depending on its size and connection configuration. The slippage models are applied to several structural analysis problems: a simple one-dimensional bar element, a double-diagonal plane truss, a double-diagonal plane frame with semi-rigid connections, a simple three-dimensional transmission tower, and a full-scale transmission tower. The instantaneous and continuous slippage models are compared to each other, the no-slip case, and wherever possible, to slippage models of other authors.

ACKNOWLEDGEMENTS

This study was carried out under the direct supervision of Dr. R.K.N.D. Rajapakse, Department Head of Civil Engineering at the University of Manitoba. The author would like to express his gratitude to Dr. Rajapakse for his valuable advice, guidance, and support. This study could not have been completed without his help.

The author would also like to thank Mr. Ben Yue, P.Eng., Section Head of the Transmission and Civil Design Department of Manitoba Hydro and Dr. R. Chandrakeerthy for their guidance, helpful suggestions and for providing valuable journal articles and reference material. Financial Assistance was provided by Manitoba Hydro and the University of Manitoba. Graduate studies would not have been possible without this support.

Finally, the author would like to thank his friends, fellow graduate students, and family for their general support and encouragement.

TABLE OF CONTENTS

LIST OF TABLES

LIST OF FIGURES

Chapter 1

INTRODUCTION

1.1 General

Latticed structures are used in a wide variety of civil engineering applications. A latticed structure is a system of members (elements) and connections (nodes) which act together to resist an applied load. Typical latticed structures include grids, roofing structures, domes, and transmission towers. Latticed structures are ideally suited for situations requiring a high load carrying capacity, a low self-weight, an economic use of materials, and fast fabrication and construction. For these reasons self-supporting latticed towers are most commonly used to transmit and distribute electricity. Manitoba Hydro has approximately 10000 self-supporting latticed transmission towers located throughout the province of Manitoba. Because one latticed tower design may be used for hundreds of towers on a transmission line, it is very important to find an economic and highly efficient design. The arrangement of the tower members should keep the tower geometry simple by using as few members as possible and they should be fully stressed under more than one loading condition. The goal is to produce an economical structure that is well proportioned and attractive (ASCE, 1988). Typical towers have a square body configuration with identical bracing in all faces. Towers range from 30-m to 50-m in height and support wires spanning 200-m to 600-m. Most transmission towers are constructed with asymmetic thin-walled angle sections that are eccentrically connected, are sensitive to material and geometric nonlinearities, and exhibit slippage or semi-rigidity at the joints, making the transmission tower one of the most difficult forms of latticed structures to analyze (Kitipornchai, 1992; Al-Bermani, 1992A). As a result, most computer programs that design and analyze transmission towers make many assumptions to simplify the computations, and ignore any nonlinear effects.

This chapter presents a review of the literature pertaining to computer-aided structural analysis of transmission towers. Current advances in tower analysis are discussed, specifically: nonlinear effects such as joint slippage, semi-rigid-joints, material

and geometric nonlinearity, and sophisticated data input schemes. Finally, the scope and objectives of the present study are outlined.

1.2 Literature Review

Before the computer was applied to structural analysis problems, highly indeterminate transmission towers were separated into determinate planar trusses with loads that acted in the same plane as the truss (Bergstrom, 1960). These approximate methods (algebraic or graphical) required conservative assumptions that resulted in over-designed towers.

Several computer programs have been developed to analyze a tower as an entire structure, which take into account the elastic properties of the members and calculate the displacements and axial forces using the stiffness method of analysis (Marjerrison, 1968). These first-order linear elastic programs assumed the angle members were idealized truss elements, pin-connected at the joints. The members were capable of carrying tension and compression, and the loaded configuration of the structure was identical to the unloaded configuration – the secondary effects of the deflected shape were ignored. Secondary (redundant) members, used to provide intermediate bracing points along primary members, need not be considered in this type of analysis since they have no effect on the forces in the load-carrying primary members (ASCE, 1988).

The next improvement in the structural model of the transmission tower included the tension-only member (ASCE, 1988; Rossow, 1975; Lo, 1975; Yue, 1994). Long bracing members, with L/r ratios greater than 300, are not capable of sustaining any significant compressive force once the member has reached its buckling load. Consequently, the strength of such a member is not the same in compression as it is in tension. After the compression strength of such a member is reached, the loads are redistributed to adjacent members. The process requires several iterations to determine which members have exceeded their buckling load, and to remove such members from the analysis. These programs also incorporate data generating schemes to minimize the amount of manual input. Making use of transmission tower symmetry (placing the Z-axis vertically through the center of the tower and the X-axis and Y-axis parallel to the

transverse and longitudinal directions of the tower), the known coordinates of one node may be used to generate the coordinates of up to three more nodes. The same data generation also applies to tower elements. Once the geometry has been generated, most programs produce a three-dimensional view of the tower to check the correctness of the input. These programs often include the automatic detection of planar nodes and mechanisms. In the space truss model, some nodes may have all of the connecting members lying in the same plane – causing instability normal to this plane. The program would search for such nodes and stabilize them by attaching springs normal to the planes. This has the effect of eliminating the singular stiffness matrix, without materially changing the characteristics of the structure (Lo, 1975).

When transmission tower displacements are large, the first-order elastic analysis techniques can be improved by using a second-order elastic analysis (ASCE, 1988; Roy, 1984). A second order analysis (nonlinear in the geometric sense) produces forces that are in equilibrium in the deformed geometry, not the initial geometry. The geometry of the structure is usually updated at the end of each iteration. Self-supporting latticed transmission towers are usually sufficiently rigid to assume small-displacement theory. However, as the tower flexibility and the applied loads increase, the secondary effects may become more significant.

One assumption that is often made in transmission tower analysis is that the angle-to-angle bolted connections are pinned. If no rotation between connected members is expected, the joint is traditionally modeled as a rigid connection. In reality, however, the connection behavior lies somewhere in between these two idealizations, possessing some degree of rotational stiffness as a function of the applied load. Knight (1993) investigated the secondary effects of modeling the connections as rigid instead of pinned and found that the secondary effects may lead to premature failure of transmission towers. Chen and Lui (1987) developed a procedure to modify a two-dimensional beam-column element for the presence of flexible connection springs. Al-Bermani and Kitipornchai (1992C) extended this formulation to a three-dimensional beam-column element. In both studies, a two node zero length connection element is used to model a flexible joint. The connection element is attached to the end of a beam-column element

via kinetic transformation and static condensation. Both studies showed that the structural response of a flexibly jointed structure is very sensitive to joint behavior.

Al-Bermani and Kitipornchai (1992A) have combined several nonlinear effects into one computer program (AK TOWER) that predicts the structural response of latticed structures up to the ultimate load. Sources of nonlinearity include geometric nonlinearity, material nonlinearity, joint flexibility, and joint slippage. Geometric nonlinearity can be accounted for by incorporating the effect of initial stresses and geometrical variations in the structure during loading. Modeling of material nonlinearity for angle members is based on a lumped plasticity model coupled with the concept of a yield surface in force space. The angle members in the tower are treated as asymmetrical thin-walled beam-column elements with rigid connections. The effect of joint flexibility can be incorporated by modifying the tangent stiffness of an element using an appropriate moment-rotation relationship for a flexible joint, provided joint flexibility information is known. The effect of bolt slippage can also be included. This program also uses the formex formulation to generate the geometry, the loading conditions and the support conditions of towers. Formex algebra is used to greatly reduce the amount of manual input, and acts as a preprocessor to the nonlinear AK TOWER program.

Bolt slippage has long been recognized as a factor that can influence the deflections of transmission towers, but until recently no research has been conducted. Peterson (1962) concluded that up to one-half of the measured deflection in transmission towers could be due to bolt slippage while the remainder was due to elastic deformation. Marjerrison (1968) realized that the deformation in holes and in the shanks of bolts could account for the measured deflection being approximately three times the theoretical deflection. Williams and Brightwell (1987) were the first researchers to present a stochastic method of assessing the effect of joint deformation on bolted latticed towers. They proposed a method for including joint movement in the axial strain of bracing or leg members and compared their results with a linear elastic analysis. They concluded that there was no deterministic way in which the amount of joint deformation can be specified for each member of the structure. Their idealized bearing stress joint movement relationship was not based on experimental data. Dutson and Folkman (1996) also investigated the effect of bolt clearances in a cantilevered truss. The clearance in the

joints was found to significantly change the structure's dynamic behavior by altering the damping characteristics of the truss. Kitipornchai, Al-Bermani, and Peyrot (1994) presented two idealized slippage models to investigate the effect of bolt slippage on the ultimate behavior of latticed structures. They proposed an instantaneous slippage model and a continuous slippage model. Their numerical study showed that bolt slippage increases structural deflection, but does not significantly influence the ultimate strength in transmission towers.

1.3 Objectives and Scope

The current method for analyzing self-supporting latticed transmission towers among practicing engineers is to assume linear elastic behavior and to treat the angle members as pin-ended truss elements. This approach ignores the effects of bolt slippage and local bolt deformation, geometric or material nonlinearity, joint flexibility, and the bending stiffness of the angle members. When the actual deflections and axial forces measured in transmission towers in Manitoba are compared with the predictions based on linear elastic analysis, there can be a large discrepancy. These differences are generally accepted to be due to joint slippage and deformation. Some researches have argued that the magnitude of the slippage may be as large as the elastic elongation of the connected members (Kitipornchai, 1994) and therefore an accurate analysis of a latticed structure was not possible.

Manitoba Hydro engineers have recognized the need to improve current tower analysis practices. Some of the towers in northern Manitoba, subjected to large differential settlements due to frost heave, are performing normally while the results from tower analysis software indicate that some of the main legs are stressed well beyond their load carrying capacity. It is suspected that the bolt slippage at the connections and the bending stiffness of the main leg members, not accounted for in the software, are causing the discrepancy between the predicted and the actual structural response. In an effort to provide practicing engineers with a better understanding of the structural behavior of transmission towers, this study investigates the effect of bolt slippage on the deflections and member stresses of latticed self-supporting transmission towers. The computer

program developed in the present study (TAP) is able to model the angle members as truss or beam elements, can incorporate bolt slippage using an instantaneous slippage model or a continuous slippage model, and can model the connections as semi-rigid (flexible connections) provided moment-rotation data are available. The analysis assumes that the displacements are not large enough to warrant a computationally costly geometrically nonlinear analysis, therefore equilibrium is based on the initial geometry. The program was developed to include all of the important factors governing the working-load behavior of a transmission tower since the load that typically initiates slippage in a member is much less than the ultimate load. As a consequence, buckling and yielding considerations are not considered. Furthermore, the material properties remain linear-elastic throughout the loading process.

The slippage models require certain parameters, determined from load-deformation experiments on typical angle members, in order to accurately incorporate the effect of bolt slippage. Each member of the transmission tower can have its own slippage properties, depending on its size and connection configuration. An independent study has recently been conducted at the University of Manitoba to determine the load-slip relationship of typical tower angles (Ungkurapinan, 2000). Most importantly, the experiments are able to determine the load at which the members initiate clearance slip, and the actual amount of clearance slip. These values can be used to model the slippage characteristics of transmission tower members with similar connection configurations. The validity of the theoretical slippage models can be verified with the experimentally determined load-slip relationships.

Chapter 2 introduces the finite element method of structural analysis, with descriptions and formulations of typical transmission tower elements including nonlinear finite element techniques. Two models for bolt slippage are presented. Model I represents an instantaneous slippage, with all of the slip occurring at a specified load level and model II assumes slippage is a continuous process starting from the first load increment. Chapter 3 describes the Tower Analysis Program (TAP) developed for investigating the effects of bolt slippage. The main program and several subroutines are described in detail. Chapter 4 discusses the application of the software developed in this study to several structural analysis problems: a simple one-dimensional bar element, a

double-diagonal plane truss, a double-diagonal plane frame with semi-rigid connections, a simple three-dimensional transmission tower, and a full-scale transmission tower. The instantaneous and continuous slippage models are compared to each other, the no-slip case, and wherever possible, to slippage models of other authors. The comparisons are made in terms of nodal deflections and member stresses. The summary and conclusions of the present study are given in chapter 5.

Chapter 2

STRUCTURAL ANALYSIS OF TRANSMISSION TOWERS

2.1 General

This chapter introduces the finite element method of structural analysis, with descriptions and formulations of elements typically used for modeling transmission towers. Nonlinear finite element techniques and load incrementing procedures are discussed in preparation for the sections concerning axial bolt slippage and the semi-rigid behavior of connections. Two models are presented to incorporate the effect of bolt slippage into a typical structural analysis program.

2.2 The Finite Element Method in Tower Analysis

The finite element method (FEM) is a mathematical procedure, most often computer aided, which is used to obtain approximate solutions to the governing equations of complex problems. In some cases, solutions to these problems cannot be obtained analytically. An analytical solution is a mathematical expression that can give an exact value of the field variable (displacement, temperature) at any location in the body. In the finite element method, the field variable is approximated using interpolation functions pieced together between discrete points. Most practical engineering problems involve complicated geometry, material properties, or loading conditions, and therefore require a numerical solution procedure such as the finite element method.

The finite element method can be considered as an extension or generalization of the stiffness method (with reference to framed structures) to two-dimensional and three-dimensional continuum problems, such as plates, shells and solid bodies (Ghali, 1978). The finite element concepts used in continuum problems can be used to formulate the stiffness method of analysis treating the member of a framed structure as an element (Krishnamoorthy, 1996). Therefore, the element stiffness matrices derived for truss and beam elements using the stiffness method of analysis are identical to the stiffness matrices derived using finite element concepts.

For each problem utilizing the finite element method, several steps must be followed. The physical system must be discretized into smaller finite elements. The elements may be one-dimensional, two-dimensional, or three-dimensional depending on the nature of the problem. For transmission towers, each angle member is usually modeled as a one-dimensional element, or line element, with one node at each end of the element. The unknown degrees of freedom, or the primary unknowns, are evaluated at these nodal points. An interpolation function must be selected which approximates the distribution of the unknown variable within an element. The function is expressed in terms of the nodal values of the element. For example, the unknown quantity within a beam element (the transverse displacements) can be fully described once the degrees of freedom for each end node are known. The governing equations and constitutive relations are then defined. The element equations are formulated using the direct equilibrium method, energy methods, or the method of weighted residuals. For the 2-node line elements used in transmission towers, the direct equilibrium method is usually performed. The equation of equilibrium for each element can be written as

$$[k]\cdot\{d\}=\{f\} \tag{2.1a}$$

where $[k]$ is the element stiffness matrix, $\{d\}$ is the element displacement vector consisting of the unknown degrees of freedom, and $\{f\}$ is the element nodal force vector.

The equations for each element are assembled to obtain the global system of equations, and appropriate boundary conditions are applied. The assembled global system of equations can be written as

$$[K]\cdot\{q\}=\{F\} \tag{2.1b}$$

where $[K]$ is the global stiffness matrix obtained by assembling all element stiffness matrices $[k]$, $\{q\}$ is the displacement vector consisting of the unknown global degrees of freedom, and $\{F\}$ is the global force vector obtained by assembling all element force vectors $\{f\}$. The primary unknowns, $\{q\}$, are determined by solving the global system of equations, often by Gauss elimination, from which the secondary unknowns, such as element forces and moments, can be calculated.

The same steps are followed for any type of problem; the end result is always a matrix equation in the form of equation 2.1b. The same steps are followed for one-

dimensional heat conduction, two-dimensional flow through porous media, or three-dimensional stress analysis. Because of its versatility, the finite element method has become the most popular computer analysis tool available to engineers today. Chapter 3 describes the computer implementation of the finite element method, with each step separated into a subroutine of the main computer program developed for analyzing transmission towers.

2.2.1 Truss Elements

Latticed transmission towers are often modeled as linear-elastic truss elements, since the angle members of the tower primarily resist axial loading with minimal bending resistance. The joints at the ends of truss members are idealized as frictionless pins, free to translate in any direction unless externally constrained by a specified boundary condition. In reality, however, the idealized pin connection seldom occurs. Truss elements are used in situations where the bending stresses are negligible compared to the axial stresses. Appendix A shows the stiffness matrices for two-dimensional and three-dimensional truss elements. Krishnamoorthy (1996) describes their formulation in detail. If the angle members in a tower are modeled as truss elements, then they cannot resist lateral loading. Any wind load or dead load acting over the truss element must be distributed to the two connecting joints. It is standard practice to concentrate half of the self-weight of the member to each of the two joints the member connects.

A problem with the truss element in modeling transmission towers is the possibility that a collapse mode may occur. Collapse modes are caused by out-of-plane instability at planar joints or by in-plane instability due to unstable subassemblies called mechanisms. A planar joint occurs when all the members terminating at one joint lie in the same plane, causing instability at the joint in the direction normal to this plane. In Figure 2.1, joints 1, 2, 3, 4 are planar joints, and if the bracing member *ab* is removed, joints 5 and 6 are also planar joints. A planar joint can displace in some direction without resistance, resulting in a loss of equilibrium. In order to correct out-of-plane instability, artificial restraints can be connected to planar joints, which are fixed at one end and normal to the plane of all connecting members at the planar joint. The artificial restraint

has a small cross-sectional area so as to provide enough stiffness to the joint to prevent collapse, but without significantly altering the physical characteristics of the tower.

An example of an in-plane instability is shown in cross-section A-A of Figure 2.1. The diaphragm in section A-A becomes a mechanism if the stabilizing member is removed from the analysis. The stabilizing member, or dummy member (not actually present in the real tower), again has a small cross-sectional area so as to provide enough stiffness to the unstable subassembly to prevent collapse. In both cases, the minimum number of restraints required to prevent rigid body movements have not been provided, resulting in a singular stiffness matrix (not possessing an inverse) if artificial restraints or dummy members are not provided. This problem is associated with pin-connected members only, and does not occur with towers modeled with beam elements. In-plane and out-of-plane instabilities are prevented in actual towers by the bending stiffness of continuous members that pass through the joints (ASCE, 1988).

2.2.2 Beam Elements

The linear-elastic truss assumption is an accurate model for tower members that are subjected to only axial tension or compression. In real transmission towers, eccentrically applied loads, lateral wind and dead loads, initially crooked members, connection rigidity, members not connecting at a single point, and the continuity of the main members may cause bending moments and shearing forces to develop. The bending moments in tower members caused by joint rigidity and member continuity, widely ignored despite experimental evidence, can be as significant as axial stresses in certain cases (Roy, 1984). The conventional linear-elastic truss model should be replaced with a beam element model when significant bending stresses are present in tower members.

Some structural analysis programs allow several different types of elements to model the same problem. The stiffer main leg members, subjected to the largest bending stresses, could be modeled as continuous beam elements while the smaller angle members could use the conventional truss model. Some researchers assume that the multiple-bolted end connections offer enough restraint to regard the connection as rigid, and model the entire transmission tower as an assembly of beam elements (Al-Bermani,

1992A). Appendix A shows the stiffness matrices for two-dimensional and three-dimensional beam elements. Krishnamoorthy (1996) describes their formulation in detail. The beam elements considered here do not include the effects of shear deformation or secondary moments (the beam-column effect). In more advanced inelastic analysis, tower members may be modeled as general thin-walled beam-column elements, capable of yielding and buckling.

2.2.3 Boundary Elements

Boundary elements are used to specify displacement boundary conditions (zero and non-zero values), to provide artificial restraints at planar nodes, and to compute the values of the support reactions. A boundary element is a spring with axial stiffness to resist translation and torsional stiffness to resist rotation. In a three-dimensional transmission tower problem, a boundary element is attached to each footing joint in each of the global X, Y, and Z directions. If the specified displacements at the footing joints of a tower are input as zero, the footings are prevented from translating or rotating in any of the global directions. If a non-zero displacement is specified (negative translation represents a foundation settlement and positive translation represents a foundation uplift due to frost heave) the amount of translation or rotation is read as a property of the boundary element.

To get the value of a reaction in the direction of one of the global axes, a very large stiffness coefficient is added to the corresponding diagonal coefficient. This produces a very small but finite displacement in that direction, which when multiplied by the very large stiffness, k, gives the desired reaction (Krishnamoorthy, 1996).

When a non-zero displacement, b, is specified at a degree of freedom, q, the load vector is modified as

$$k \cdot q = k \cdot b \tag{2.2}$$

where k is very large (10^{10}). When equation 2.2 is added to the global system (equation 2.1), the solution at the degree of freedom q will always equal the specified displacement. If the nodal displacement is specified, the external reaction cannot be specified and remains unknown. When the boundary element is used to model an artificial restraint at a

planar node, the stiffness must be reduced to a much smaller value, generally less than the stiffness of the smallest tower member.

2.3 Nonlinear Finite Element Analysis

In the previous section it was assumed that the constitutive relations, used to derive the element equations, remained linear throughout the analysis. In some cases the stress-strain relationships do not obey the simple linear elastic assumption, and the non-linearity of the material properties must be considered. In other problems the linear strain-displacement relationship cannot be used accurately due to large displacements and large strains altering the geometry of the elements. These types of problems are said to be geometrically non-linear. This section describes non-linear finite element problems that have only material non-linearity; the assumption of small displacements and small strains is still made.

In nonlinear problems, the stiffness matrix depends on the unknown quantity. A direct solution procedure is no longer possible, and an iterative solution scheme is required. For structural analysis problems, where the stiffness is a function of the displacements and the loading history, the tangential stiffness method is usually performed along with a load increment procedure. The nonlinear problem is essentially linearized over a small portion, or increment, of the total structural load. Equation 2.1 is revised as

$$[K(q)]\cdot\{q\}=\{F\} \tag{2.3}$$

When employing an iterative solution scheme, equation 2.3 will not be satisfied and a system of residual forces exist, $\{\Psi\}$, that essentially measures the deviation of equation 2.3 from equilibrium (Owen, 1980)

$$\{\Psi\}=[K(q)]\cdot\{q\}-\{F\}\neq 0 \tag{2.4}$$

Since the stiffness is a function of the displacements, so is the residual force vector, $\{\Psi\}=\{\Psi(q)\}$. An initial solution vector is assumed; for structural problems the most common initial solution is $\{q^0\}=\{0\}$. The tangential stiffness can then be

evaluated and the residual forces can be calculated using equation 2.4. The initial solution must be corrected by an amount $\{\Delta q^0\}$ using

$$\{\Delta q^r\} = -[K(q^r)]^{-1} \cdot \{\Psi(q^r)\} \tag{2.5}$$

to obtain an improved approximation

$$\{q^{r+1}\} = \{q^r\} + \{\Delta q^r\} \tag{2.6}$$

This procedure is repeated until the residual forces converge to a tolerably small value. Once convergence has occurred, the next load increment is applied and the iterative process is repeated. The solution vector calculated in the current load increment is added to the solution vector of the previous load increment to get the current total. The secondary unknowns, the member forces and bending moments for example, are accumulated in a similar fashion.

If the load increments are made small enough, the non-linear relationship within the load increment will closely resemble a linear relationship. Consequently, the residual forces calculated using equation 2.4 will be very small, and any iteration performed will only slightly improve the solution. If the total load is separated into enough increments, the residual forces can be neglected without sacrificing any accuracy in the final solution. The program developed in this study uses this piecewise-linear technique. For a problem using a continuous bolt slippage model, the total structural load must be divided into small increments since the slippage is a function of the member's axial force.

In other cases, the non-linear effect may only occur once a certain condition has been satisfied. In these cases, such as instantaneous bolt slippage or elastic-plastic problems, the stiffness is only modified once a prescribed load level or strain level has been exceeded. For a problem using an instantaneous bolt slippage model, the total structural load must be divided into small increments in order to detect when a member first exceeds its slippage load, and to prevent a member from exceeding the specified maximum allowable slippage in the following load increments. Any iteration scheme performed within these small loading increments will not improve the solution significantly.

2.4 Modeling Joint Slippage

The bolt slippage contribution to transmission tower deflections has long been recognized. Past research (Peterson, 1962; Marjerrison 1968) has found that bolt slippage, and the deformation in the bolts and bolt holes, accounts for part of the large discrepancy between observed deflections and theoretically predicted deflections. Only recently have bolt slippage considerations been included in transmission tower analysis software. Kitipornchai realized that the magnitude of the slippage may be as large as the elastic elongation of the connected members and, as a result, modified the stiffnesses of members to include the effect of bolt slippage.

The bolted connections of transmission towers always experience some degree of slippage. Slippage occurs in bolted connections since the bolt holes punched in typical tower angle members are oversized, in comparison to the bolt diameter, in order to provide erection tolerance. With oversize holes, slip into bearing at or below design loads cannot be prevented (Winter, 1956). The tolerance is usually 1.5-mm (1/16 of an inch) for the connections used in transmission towers. This would allow a possible slip of 1.5-mm at a joint in any direction, depending on the magnitude and direction of the member force, and the starting position of the bolt (Kitipornchai, 1994). In a member with a slipping connection at both ends, both joint tolerances could combine to provide a maximum member slippage of approximately 3-mm. In order to produce the maximum slippage at one end of a member, the bolt must be in a position of maximum clearance (see Figure 2.2). The theoretical maximum clearance slip is unlikely to be achieved in a multiple-bolt connection since some bolts go into bearing before others due to minor dimension deviations. If the bolt is bearing initially against the bolt hole, a position of zero clearance, then no clearance slippage can take place at that joint. Figure 2.3 shows the load-slip relationship for a two-bolt connection with the bolts in a position of maximum clearance, clearly indicating a 2 to 3-mm rigid-body slippage until bearing is established. Before this clearance slip begins, the connection behaves linearly. As loading is increased, the joint behavior becomes non-linear as the bolts slip through the maximum clearance. As the displacement increases, the joints behave linearly until the

limit of elasticity of their material is reached. Mercadal (1989) has also observed this behavior in tension and compression tests on pinned joints.

Even in situations where the bolt is initially bearing against the bolt hole, a deformation slip at the connection is also observed (Winter, 1956; Ungkurapinan, 2000). Deformation slip arises from the plastic deformation of the joined elements and the bolt, and represents a large portion of the total slip. Deformation slip occurs after clearance slip, at loads much larger than the load that initiates clearance slip, and continues until the metal on the bearing side of the hole begins to yield.

Many tests have been conducted on bolted connections to determine the load that produces a significant slippage, or to determine the entire load-slip relationship of the connection (Winter, 1956; Lobb, 1971; Gilchrist, 1979; Ungkurapinan, 2000). Past research has indicated that the strength of a connection can be predictable and the possibility of failure is remote if it is designed correctly. However, the possibility that the connection will slip before ultimate load is reached is very likely (see Table 2.1).

Bolts may slip continuously throughout the loading process or instantaneously once a certain load has been reached. Some typical load-slip relationships are shown in Figure 2.4. The slippage load in curve A is normally defined as the maximum load reached before major slippage begins. The slippage load in curve B is defined as the load at which the deflection rate suddenly increases. For curve C, no obvious slippage load can be observed, and a slip load is selected once a certain amount of slippage has occurred (0.5-mm for example).

The load-slip relationship for bolted connections is highly variable and depends on such factors as the applied loading, workmanship, the torque used to tighten the bolts, the properties of the bolts and joining members, the number of bolts, the position of the bolt relative to the bolt hole, and the friction coefficient between the slipping surfaces. Table 2.2 shows the variability in the slippage load by comparing the minimum and maximum values for several tests conducted by Winter.

In a real transmission tower, it is impossible to know precisely how much the bolts actually slip and at what load level. The position of the bolt relative to the bolt hole is not known for each tower member, and the torque used to tighten the bolts is not identical for each connection. For this reason, certain assumptions must be made about

the position of the bolt relative to the bolt hole. The bolt may be initially bearing, positioned exactly in the center of the hole, or in a position of maximum clearance. The slippage model may assign random bolt positions for each connection in a tower, or the model may assume each connection will slip the same amount.

Two models are presented which attempt to incorporate the effect of bolt slippage on the behavior of latticed structures. These models require certain slippage parameters for each element that experiences slippage. The number of bolts in the connection, the position of the bolt with respect to the bolt hole, and the size of the angle member, affect the maximum slippage allowed, the slippage load, and the load-slip relationship. For an accurate model, this input must be based on experimental slippage studies. Figure 2.5 shows an idealized load-deformation curve for joints with maximum clearance at assembly for connections with 1 to 4 bolts. The actual experimental results shown in Figure 2.3 are represented in this idealized curve to provide the necessary input for the slippage models. The most important parameters for the slippage models are the amount the connection slips and the slippage load. This information can be read directly from such an idealized curve. If the effect of bolt slippage was to be investigated in bracing members with two-bolts per joint with the bolts in a position of maximum clearance, a slippage load of 20.14-kN and a maximum slippage of 2.21-mm would be input into the slippage model.

2.4.1 Model I - Instantaneous Slippage

This slippage model, proposed by Kitipornchai, Al-Bermani and Peyrot (1994), assumes that all the slippage occurs at a certain load level. In model I, it is assumed that the ends of the truss or beam member, under tension or compression, slip relative to one another by an amount Δ_s when the axial force in the member exceeds the slippage load, P_s (see Figure 2.6). The member length after slipping may be expressed as

$$\overline{L} = L + \Delta_s \tag{2.7}$$

for a tension member, and

$$\overline{L} = L - \Delta_s \tag{2.8}$$

for a compression member, where L is the length before slipping and $\overline{L}$ is the length after slipping. These changes in length are small (2 to 3 mm) when compared to the member's original length and their effect on the member stiffness after slippage is complete is very small. While slippage is taking place, however, a substantial change in the member stiffness occurs. In the instantaneous slippage model, once the force in the member has reached or exceeded the slippage load, P_s, by adding the applied structural load in small increments, no additional load increment is carried by the member until the assumed slip, Δ_s, is completed. Essentially, the stiffness of the member is reduced to zero and the force in the member remains equal to the slippage load as the member slips (Figure 2.7). When a member's stiffness is reduced to zero it is "removed" from the structure and the load it was carrying is distributed to the other members in the structure.

Slippage model I does not work if the removal of slipping members produces a geometrically unstable structure, creating a singular stiffness matrix. In order to correct this problem, the stiffness of the slipping member should be reduced by two or three orders of magnitude instead of reducing it completely to zero. The same concept is applied when a tension-only member is subjected to a compression load. Experience has shown that this technique is successful for modeling tension-only members and eliminates the problem of a singular stiffness matrix (Rossow, 1975). By greatly reducing the slipping member's stiffness, the deflections at the joints of the slipping member increases while the internal force in the member remains relatively constant. Because the stiffness is not zero, but some reduced value, the internal force in the member increases by a very small amount as the member slips. The joint deflections continue until the assumed slip is complete. Once this occurs, the member stiffness is restored to its original value, but the member length is based on the modified length, $\overline{L}$. In some cases, the total structural load is not divided into enough load increments, causing the member to exceed the maximum specified allowable slippage, Δ_s. When this occurs, the number of load increments must be increased until the difference between the computed slippage and the specified slippage is tolerably small. In other cases the assumed slippage is not completed after the last load increment is added, and the member stiffness remains in its reduced form.

The total axial deformation of the slipping member is equal to the elastic deformation before slippage occurs, the amount the member slips, and any elastic deformation after the member has reached the specified maximum slip, if it reaches the specified maximum slip before the last load increment. The total axial deformation for the continuous slippage model has the same two components (elastic deformation and slippage deformation), but they are present at all load increments and not discretized as in slippage model I.

2.4.2 Model II - Continuous Slippage

This slippage model (Figures 2.6 and 2.7), borrowed from concepts developed by Kitipornchai, Al-Bermani and Peyrot (1994), assumes that slippage is a continuous process from the first load increment to the last, as opposed to a sudden slip event once the slippage load is exceeded as in the instantaneous slippage model. A Ramberg-Osgood type function, which has been used successfully in modeling non-linear moment-rotation curves, is used to describe the continuous slip behavior. At any load increment, if the axial deformation in the member is Δ, it is assumed that the incremental slip in the member, Δ_s, may be expressed as

$$\Delta_s = \Delta(\nu - \nu^m) \tag{2.9}$$

in which

$$\nu = \frac{P}{P_s} \cdot \frac{1}{\left(1 + \left(\frac{P}{P_s}\right)^n\right)^{\frac{1}{n}}} \tag{2.10}$$

where P is the axial force in the member, P_s is the slippage load, and m and n are parameters that control the amount of slip required and the sharpness of the curve. As m increases, the slippage increases (Figure 2.8) and is spread out over a larger range of axial forces. Figure 2.9 shows that at the slippage load, only 20% of the total slippage is complete for an m value of 100, but for an m value of 4, almost 90% of the total slippage is complete. Varying the n parameter has the inverse effect. For larger n values, the slippage decreases (Figure 2.10) but most of the slippage occurs near the slippage load.

As the n parameter is decreased, the force-slip relationship changes significantly, distributing the total slippage over much larger axial forces. As seen in Figure 2.11, as the n parameter increases, model II begins to resemble model I, with most of the slippage occurring at or near the slippage load.

It can be shown, using equations 2.9 and 2.10, that the axial slip is always less than the axial deformation. However, when the axial force in a slipping member is near the slippage load and the m parameter is large, the $(\nu - \nu^m)$ term in equation 2.9 approaches unity and most of the axial deformation in this case is due to axial slippage.

Similar to elasto-plastic problems where the total strain is separated into elastic and plastic components, in the continuous slip model the total axial deformation is comprised of an elastic deformation component, Δ_e, and a slippage component, Δ_s. Therefore,

$$\Delta = \Delta_e + \Delta_s \tag{2.11}$$

For a non-slipping member loaded with a force P, the following relationship can be written

$$\frac{P}{\Delta} = \frac{AE}{L} \tag{2.12}$$

For a slipping member however, the slippage component does not contribute to the axial force in the member, only the elastic deformation component does. Therefore,

$$P = \frac{AE}{L} \cdot \Delta_e \tag{2.13}$$

or using equations 2.9 and 2.11

$$P = \frac{AE}{L} \cdot \left[\Delta - \Delta \cdot \left(\nu - \nu^m\right)\right] \tag{2.14}$$

The stiffness of a slipping member can now be calculated as the total axial force divided by the total axial deformation as in equation 2.12

$$K_{slip} = \frac{AE}{L} \cdot \left[1 - \left(\nu - \nu^m\right)\right] \tag{2.15}$$

The stiffness of a slipping member is very similar to a non-slipping member initially, but decreases significantly as additional loading increments are applied and as the axial force in the member approaches the slippage load. Once the prescribed slip has been attained

or when the incremental slip in equation 2.9 approaches zero at axial forces much greater than the slippage load, the stiffness returns to that of a non-slipping member. Again, as in slippage model I, the member stiffness is now based on the modified length, $\overline{L}$.

2.5 Semi-Rigid Connections

The angle-to-angle bolted connections in transmission towers are traditionally modeled as pinned connections, completely free to rotate. If no rotation between intersecting members with multiple-bolt connections is expected, the joint is traditionally modeled as a rigid connection. In reality, however, the connection behavior lies somewhere in between these two idealizations; a pinned joint has a certain amount of rigidity and a rigid joint has a certain amount of flexibility. Therefore, every connection in any structure is actually a semi-rigid connection, although most design and analysis techniques ignore this fact. This type of joint flexibility can be considered a form of slippage, only instead of in the axial direction as in the previous section, the joint slips rotationally.

If a connection is to be modeled as a semi-rigid connection then the moment-rotation relationship of the connection must be known. Mathematically, this relationship can be expressed in a general form as

$$M = f(\theta_r) \tag{2.16}$$

where M is the moment transmitted by the connection and θ_r is the relative angle of rotation between the connecting members. This relationship, which best fits the experimental data available for a particular connection, is implemented into the finite element method to model the non-linear connection stiffness. Typically the function is an exponential function, since connection stiffness decreases as load increases, and this type of function avoids the possibility of negative stiffness values – encountered in some polynomial models.

The method for incorporating connection flexibility involves attaching a two-node zero length connection element at both ends of a standard beam element. The tangent stiffness of a connection at a particular load increment is given by

$$R = \frac{dM}{d\theta_r} \tag{2.17}$$

For a three-dimensional problem, a connection element has three rotational degrees of freedom at each node. The behavior of a connection element in its three directions (in-plane bending, out-of-plane bending, and torsion) are governed by their own specified moment-rotation relationship.

By enforcing equilibrium and compatibility at the junction of a beam element and a connection element, and by statically condensing the internal degrees of freedom (Chen and Lui 1987, Al-Bermani and Kitipornchai 1992) a modified beam stiffness can be computed. A semi-rigid beam element can easily represent the perfectly pinned or perfectly rigid idealizations by modifying the parameters of the moment-rotation relationship to produce zero connection stiffness or infinite connection stiffness respectively. Any intermediate connection stiffness corresponds to a semi-rigid connection. The structural analysis program described in chapter 3 has the capability to model semi-rigid connections. Appendix B presents the formulation of a semi-rigid beam element in two and three dimensions.

Gage (Galvanized)	Slip Load (lbs)	Ultimate Load (lbs)	Slip Load / Ultimate Load (%)
26	260	720	36
26	220	610	36
26	200	585	34
24	225	850	26
24	275	875	31
24	130	830	16
22	210	1030	20
22	275	965	28
22	170	940	18

Table 2.1: Slippage and ultimate loads for single 1/4 inch bolt specimens securing a lap joint in tension (Gilchrist, 1979)

Gage	Shear Type	1/4	3/8	1/2	5/8	3/4	1
20	SS Min	230	600	1550	1700	2600	-
	SS Max	900	1600	2000	2100	3300	-
	DS Min	600	840	1600	1740	2690	-
	DS Max	1300	2200	2300	3070	3980	-
14	SS Min	300	370	1200	-	2650	5530
	SS Max	900	1060	2450	-	6540	6570
	DS Min	300	640	1960	5100	3700	5680
	DS Max	1240	1260	3300	6300	5800	7460
10	SS Min	-	720	1800	-	3100	6900
	SS Max	-	1200	3600	-	5600	8000
	DS Min	-	600	2400	-	4200	10200
	DS Max	-	1900	3000	-	5100	14200

Table 2.2: Ranges of observed slip loads (lbs) for various bolt sizes tested in single shear (SS) and double shear (DS) for three gage thicknesses (Winter, 1956)

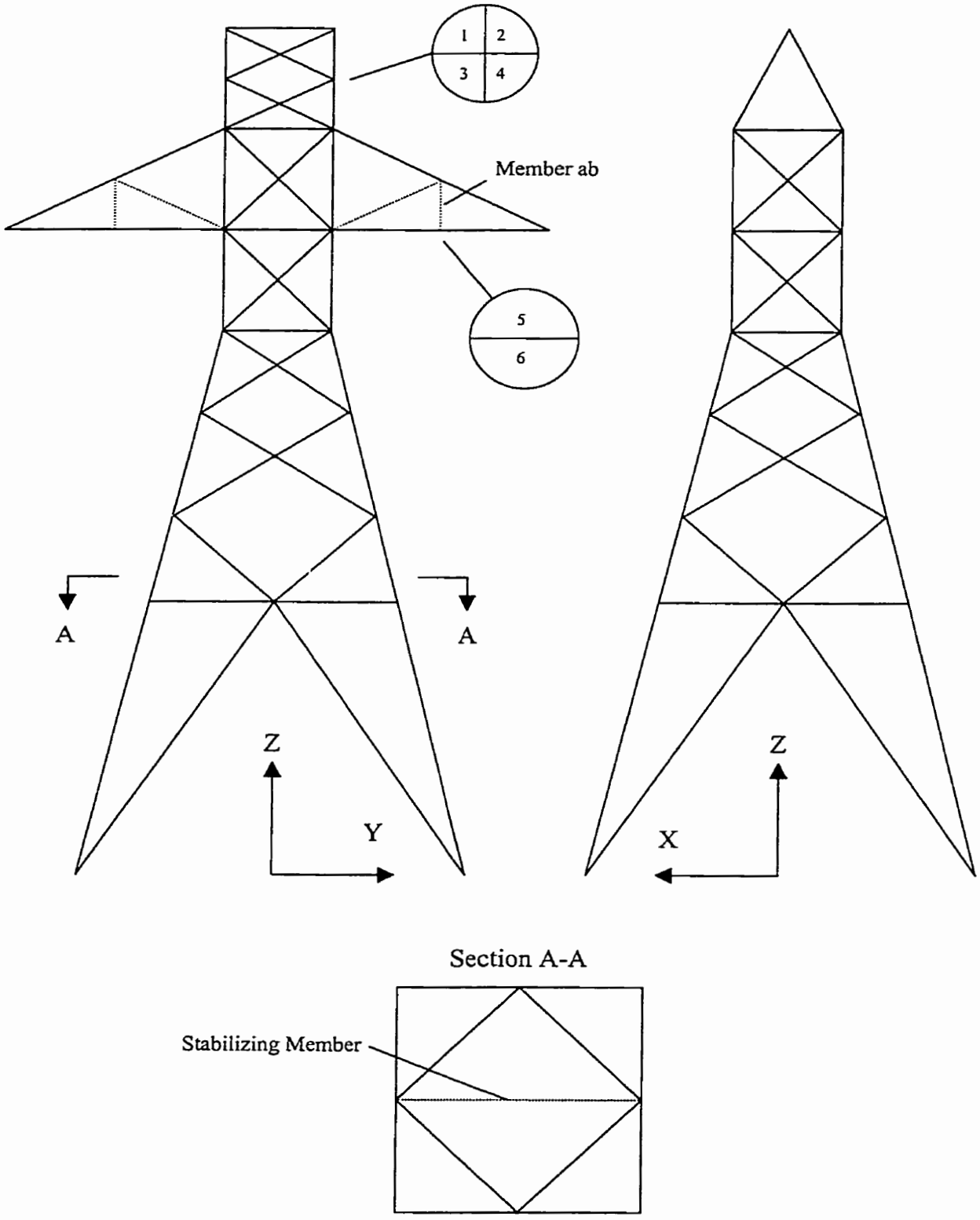

Figure 2.1: Simplified transmission tower model

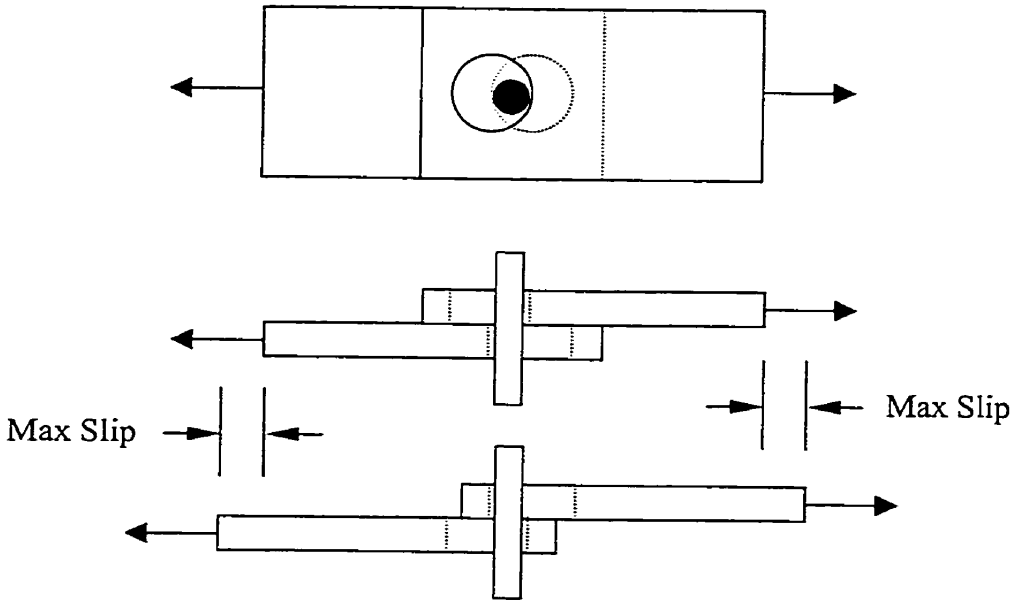

Figure 2.2: Maximum clearance producing maximum slip after loading

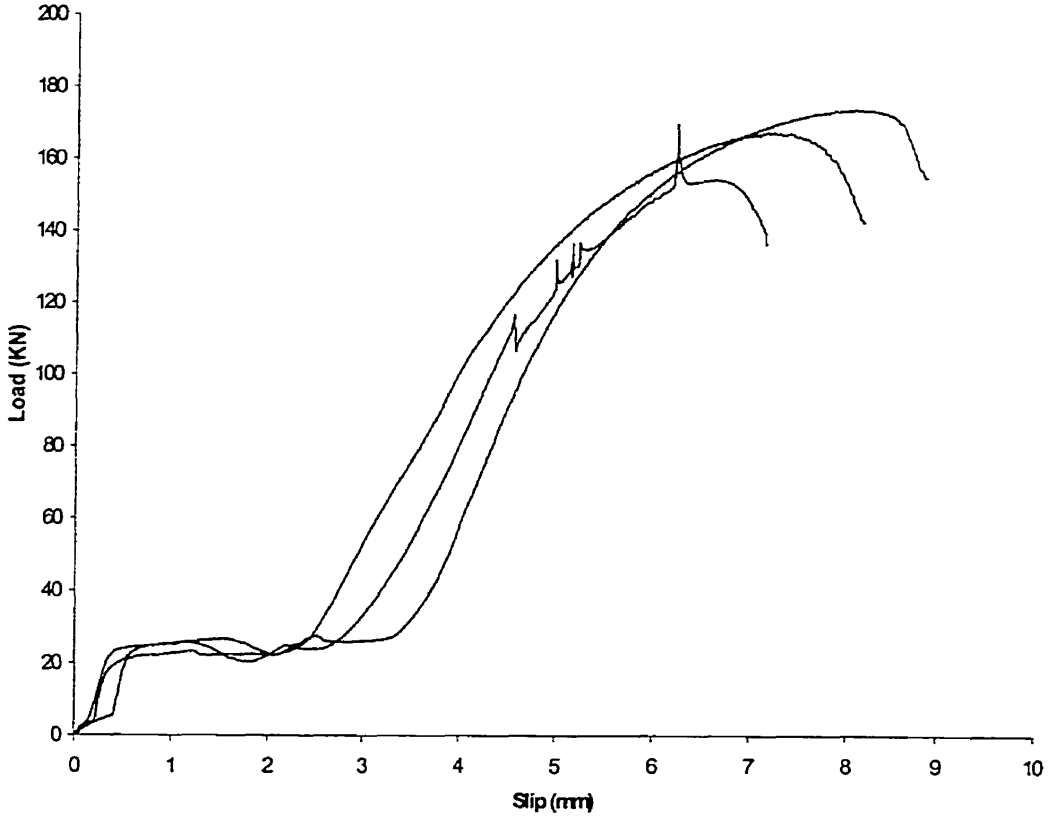

Figure 2.3: Load-Slip relationship for specimens with a two-bolt connection and bolts in a position of maximum clearance (Ungkurapinan, 2000).

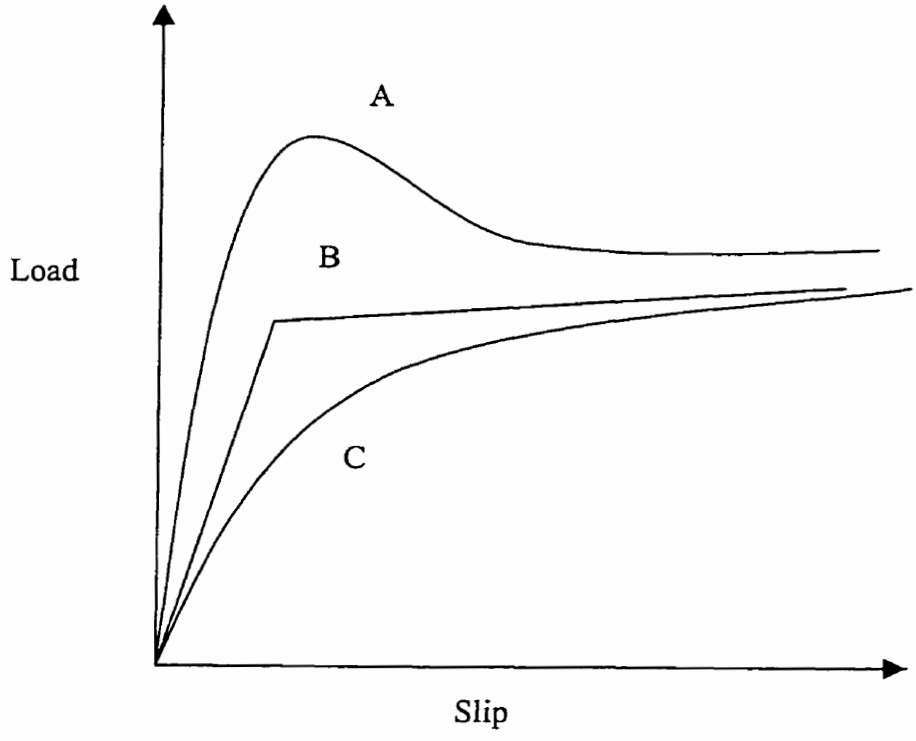

Figure 2.4: Typical load-slip relationships (FHWA, 1981)

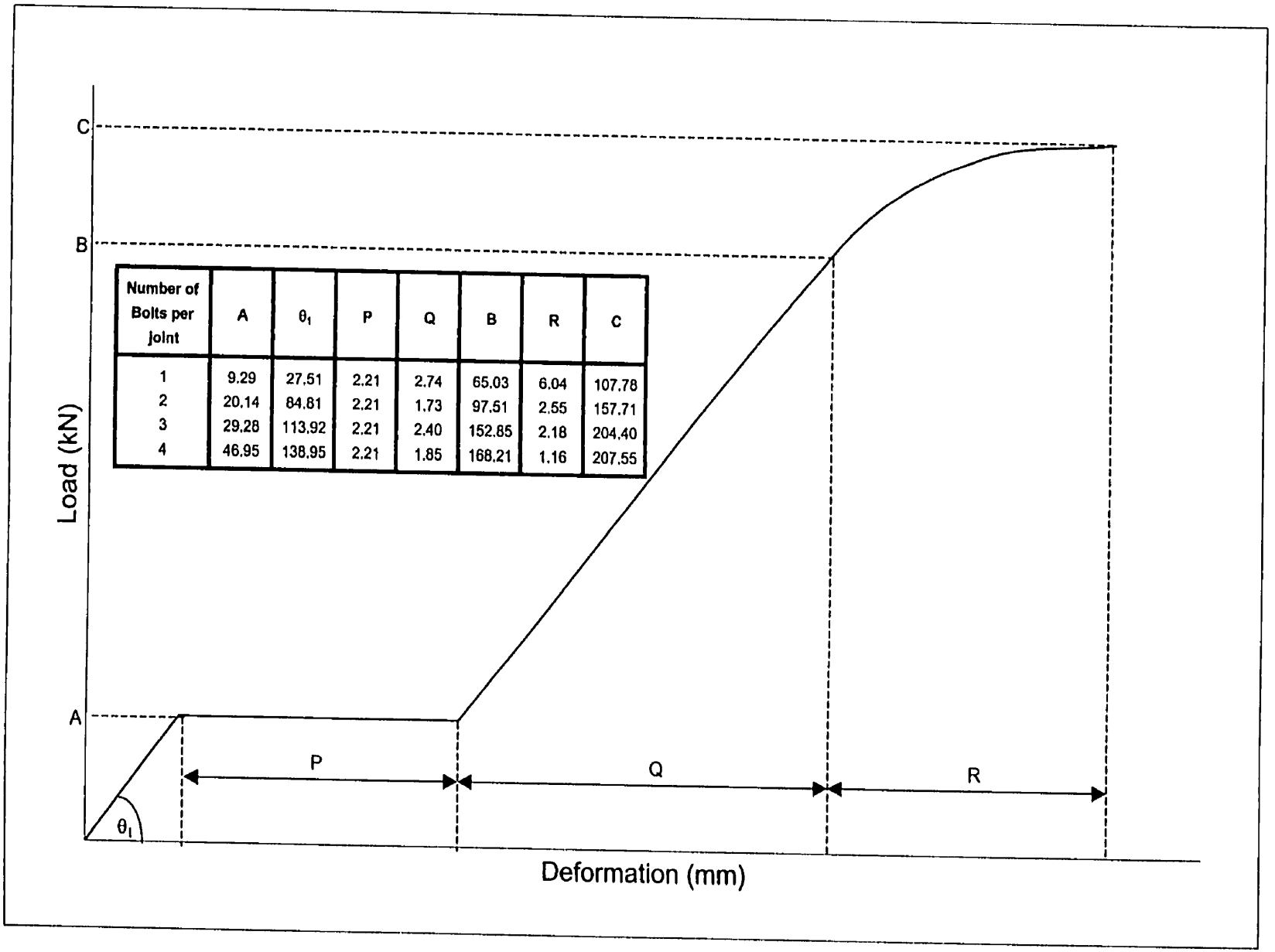

Number of Bolts per joint	A	θ_1	P	Q	B	R	C
1	9.29	27.51	2.21	2.74	65.03	6.04	107.78
2	20.14	84.81	2.21	1.73	97.51	2.55	157.71
3	29.28	113.92	2.21	2.40	152.85	2.18	204.40
4	46.95	138.95	2.21	1.85	168.21	1.16	207.55

Figure 2.5: Idealized curve for joints with maximum clearance at assembly (Ungkurapinan, 2000)

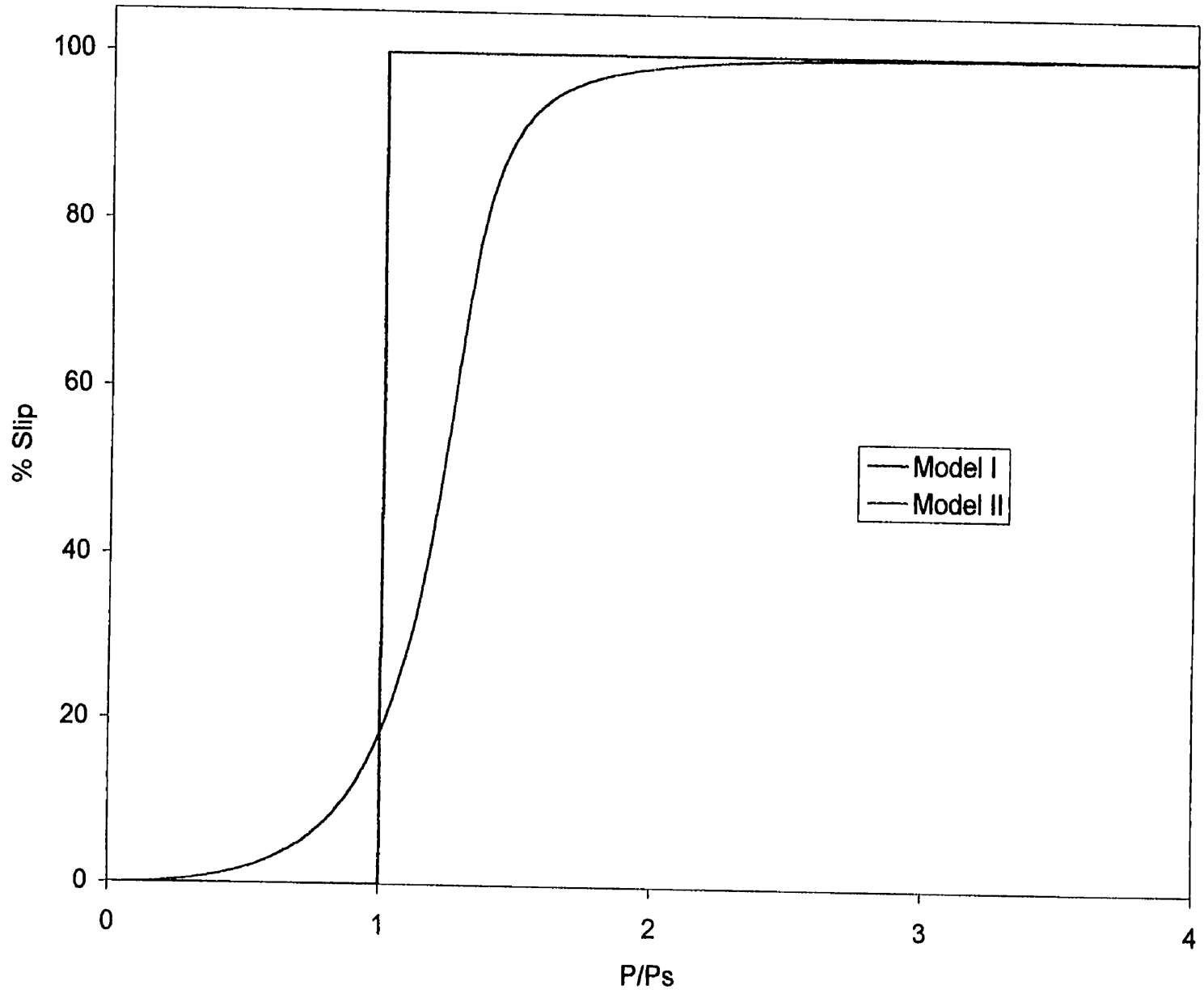

Figure 2.6: Bolt slippage models

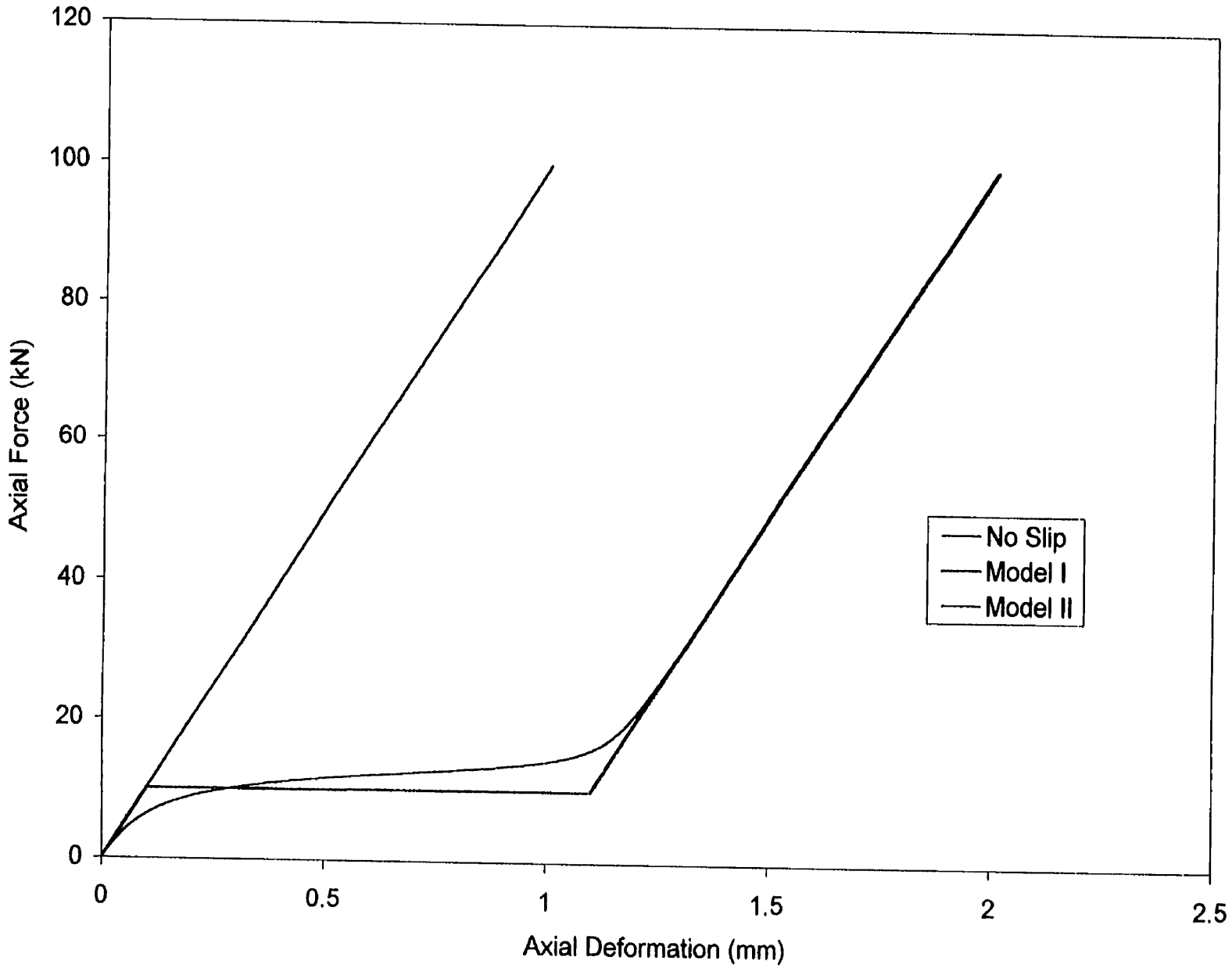

Figure 2.7: Force-Deformation relationships (Ps = 10-kN)

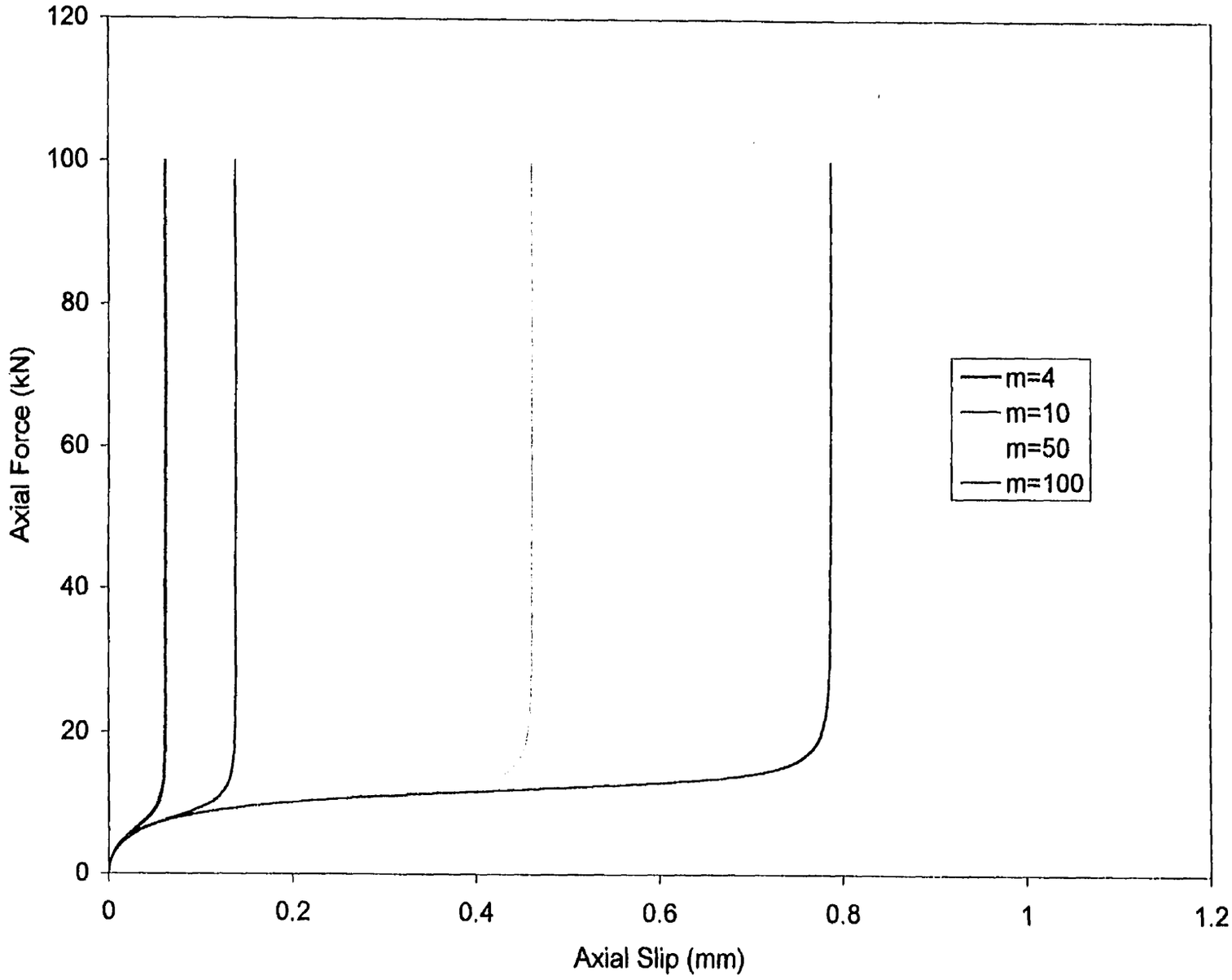

Figure 2.8: Axial force-slip relationship for several m values (Ps = 10-kN, n = 6)

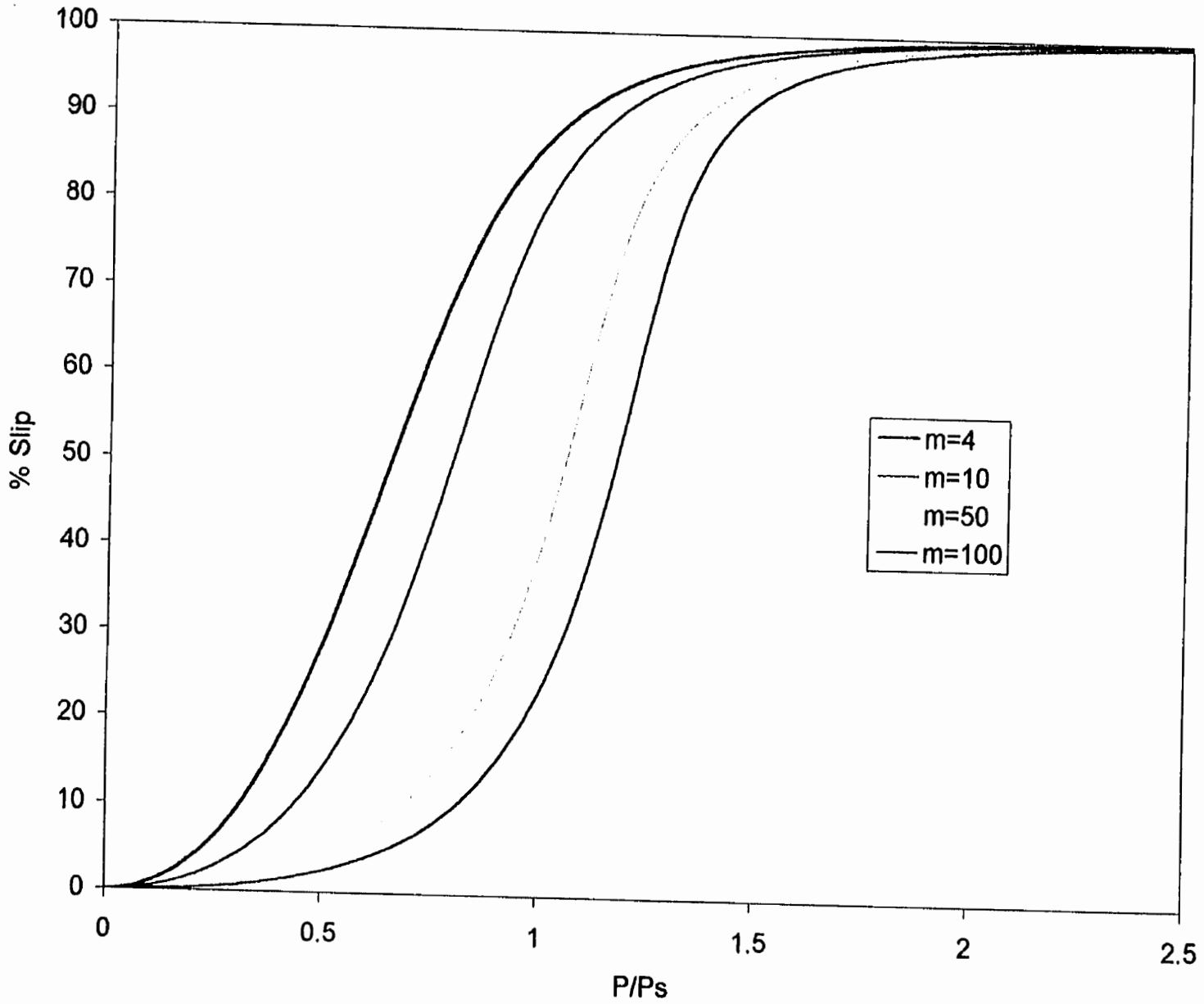

Figure 2.9: Slippage model II for several m values (n = 6)

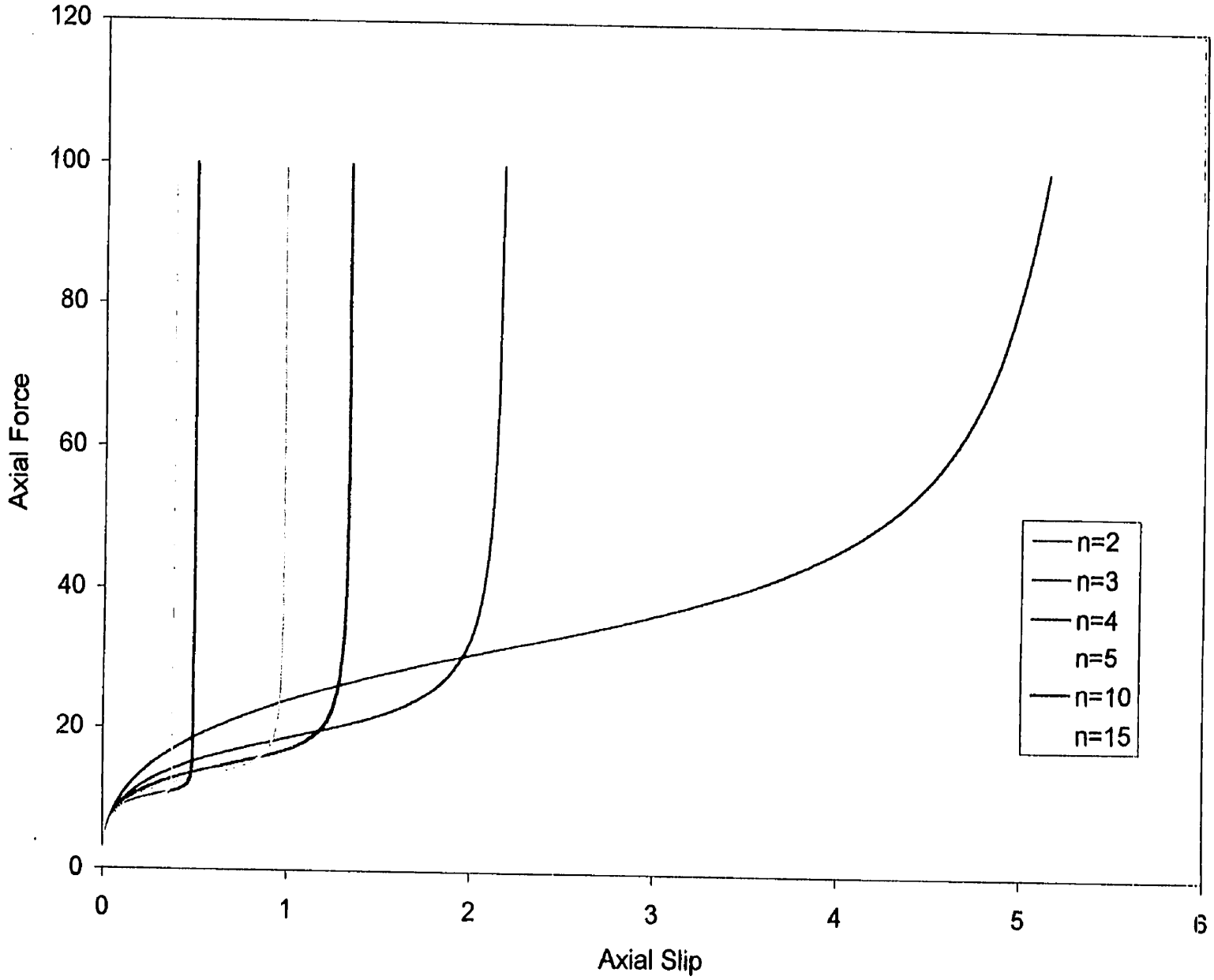

Figure 2.10: Axial force-slip relationship for several n values (Ps = 10-kN, m = 100)

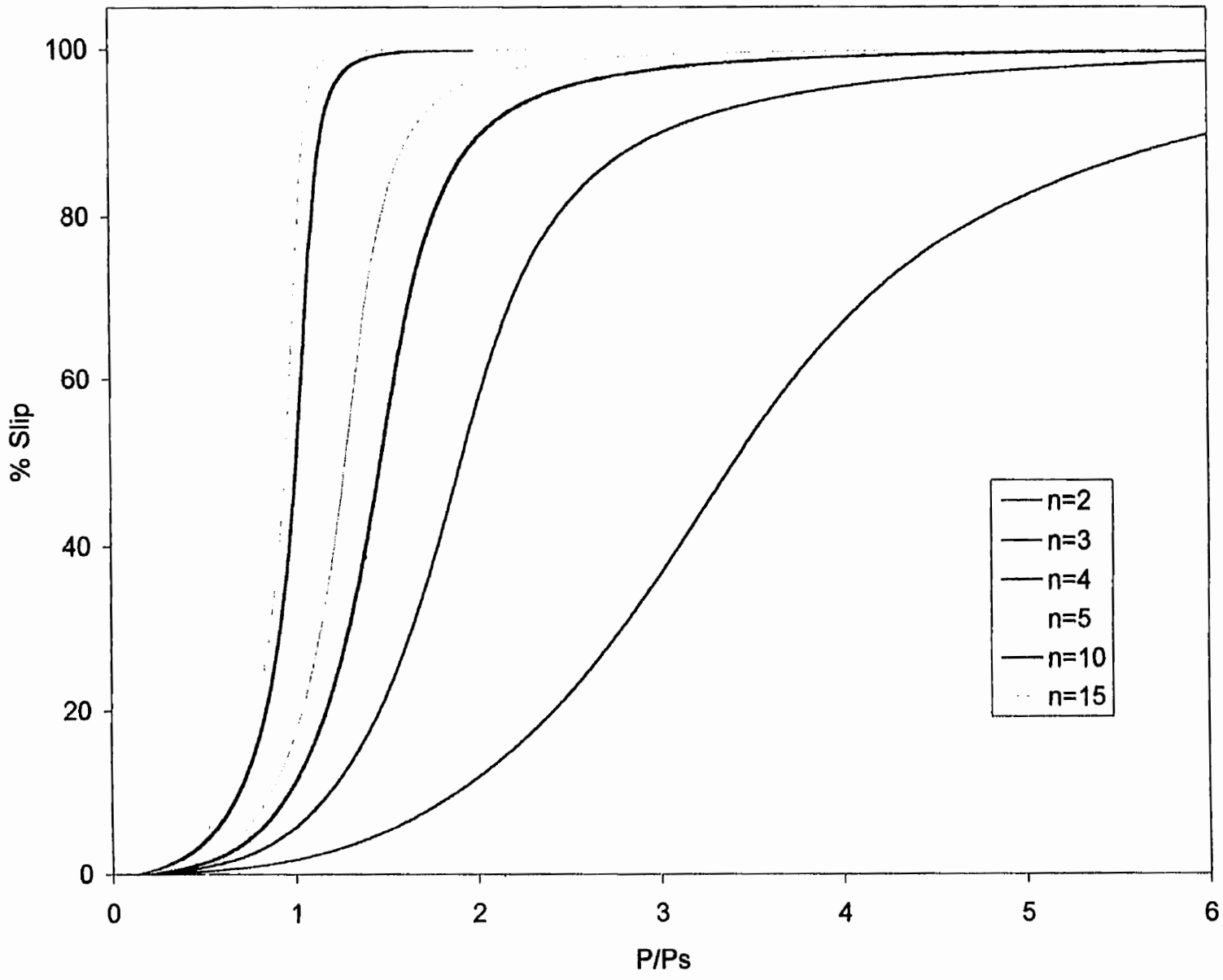

Figure 2.11: Slippage model II for several n values (m = 100)

Chapter 3

TRANSMISSION TOWER ANALYSIS PROGRAM

3.1 General

This chapter describes the Tower Analysis Program (TAP) developed for investigating the effect of bolt slippage on the structural behavior of latticed self-supporting transmission towers. The program was written using the Microsoft Developer Studio, an integrated development environment used to develop Fortran 90 applications. It includes a text editor, resource editors, project build facilities, an optimizing compiler, an incremental linker, a source code browse window, and an integrated debugger in one application. The main program and each of the subroutines are described in detail.

3.2 Tower Analysis Program (TAP)

The tower analysis program (TAP) calculates the nodal deflections and the member stresses of a two-dimensional or three-dimensional structure comprised of beam and/or truss elements. The program can consider instantaneous or continuous axial bolt slippage and can include the effect of semi-rigid connections. Figure 3.1 shows the structure of the program, listing all of the subroutines called by the main program. Some of these main subroutines call other subroutines themselves, but are not shown in the figure. TAP, like most finite element programs, uses an element library subroutine that is called several times during the analysis. Many procedures in the finite element method require different treatment depending on which type of element is being considered (truss element, beam element, boundary element, or semi-rigid beam element); the element library directs the main program to the correct element-specific procedure. Each subroutine marked with an asterisk in Figure 3.1 calls the element library for its element-specific procedure. Material properties (IND = 1), assembling the self-weight load vector (IND = 2), assembling the stiffness matrix (IND = 3), and calculating stresses (IND = 4), are all element specific. The IND parameter is a flag to indicate which segment of the

element routine to execute. The general form of any element subroutine is shown in Figure 3.2.

The first step of the program is to read the control data for the problem being analyzed. The control data include the number of nodes, the number of elements, the number of material sets, the number of dimensions, the maximum number of degrees of freedom per node, the number of load increments, and the slippage model to be used. After the program reads this information, the input file can be accessed.

3.2.1 Input Subroutine

The input subroutine reads and generates nodal coordinates, element connectivity data, element material set data, and element specific material properties. All of this information is echoed back into the output files along with the eventual nodal displacements and element stresses of the structure at the final load increment. Intermediate displacements and stresses can also be monitored. The generation of data can be carried out along a straight line. For example, if the coordinates of the exterior nodes along a straight line are specified manually, all internal nodal coordinates at a specified interval are automatically generated. For certain transmission towers, linear interpolation may not be the best method, and a generation scheme utilizing tower symmetry about the Z-axis may be the most efficient. If the Z-axis is placed vertically through the center of the tower and the X-axis and Y-axis are oriented parallel to the longitudinal and transverse faces of the tower respectively, then when the coordinates of one node are input manually, up to three more nodes may be automatically generated using the tower's symmetry. This coordinate system is highly recommended for either of these generation schemes. This type of coordinate system assumes that gravity acts in the negative Z-direction. This is important when considering the self-weight of tower members. If the analyzed structure occupies only two dimensions, gravity is assumed to act in the negative Y-direction. If the user assumes a different gravity direction, the self-weight load vector will be incorrect.

When reading the element specific material properties, the element library must be used. If analyzing a two-dimensional truss element, the Young's modulus, the cross-

sectional area, and the self-weight must be read along with all of the slippage parameters. If analyzing a two-dimensional beam element, the program must also read the moment of inertia from the input file. The element library is called for each material set specified in the control data.

The input subroutine also has the important function of determining the number of unknowns in a problem, or, the number of equations that must be solved simultaneously. This is done by summing the number of degrees of freedom for every node of the structure. If the structure only uses one type of element, this is a simple procedure. But when two types of elements meet at one joint, the element with the maximum number of degrees of freedom must be used. When these two elements are assembled into the global stiffness matrix, special care must be taken to ensure that the matrix assembly is performed correctly. If a member capable of transmitting moments to a node is coupled at that node to a truss element, it is necessary to complete the stiffness matrix of the truss element by insertion of zero coefficients in the rotation or moment positions (Zienkewicz, O. C., 1989). By storing the maximum number of degrees of freedom at every node, the global matrix can be assembled correctly.

3.2.2 Concentrated Load Subroutine

This subroutine reads and generates the concentrated nodal load data and assembles the global load vector $\{F\}$. One node may have up to six different concentrated loads, one for each degree of freedom for a three-dimensional beam element. Concentrated loads may also be generated using liner interpolation. The sign of the applied loads are with respect to the global coordinate system. No concentrated loads may be applied to nodes which may experience a collapse mode (at planar joints if only modeling the tower with truss elements).

3.2.3 Distributed Load Subroutine

This subroutine computes the element force vector in global coordinates, $\{f\}$, due to the self-weight of an element and any applied distributed loads (for beam

elements) and assembles the global force vector $\{F\}$. Distributed loads may also be automatically generated for elements with the same loading. For truss elements, since no transverse loading is acceptable, the self-weight of the truss member (calculated by multiplying the dead load of the member [kN/m] by its length) is concentrated equally onto the connecting nodes. For beam elements, the self-weight and any applied distributed loads must be added together when forming the element force vector

$$\{f\} = [T]^T \cdot \{\{f_m\} + \{Selfweight\}\} \tag{3.1}$$

The member force vector, $\{f_m\}$, is transformed into global coordinates by the transformation matrix $[T]$, see Appendix A. The member self-weight vector must first be converted into its equivalent nodal loads in the member axis before it is transformed into global coordinates by the transformation matrix. It is important to realize that the self-weight, or the dead load of the member, acts in the negative global *Y*-direction in two-dimensional problems and in the negative global *Z*-direction in three-dimensional problems. For a two-dimensional beam element with a linearly varying distributed load and a uniformly distributed self-weight, the element force vector is written as

$$\{f\} = [T]^T \cdot \left\{ \begin{Bmatrix} 0 \\ \dfrac{(7 \cdot p_1 + 3 \cdot p_2) \cdot L}{20} \\ \left(\dfrac{p_1}{20} + \dfrac{p_2}{30}\right) \cdot L^2 \\ 0 \\ \dfrac{(3 \cdot p_1 + 7 \cdot p_2) \cdot L}{20} \\ -\left(\dfrac{p_1}{30} + \dfrac{p_2}{20}\right) \cdot L^2 \end{Bmatrix} + \begin{Bmatrix} -\sin\theta \cdot \dfrac{Sw \cdot L}{2} \\ -\cos\theta \cdot \dfrac{Sw \cdot L}{2} \\ -\cos\theta \cdot \dfrac{Sw \cdot L^2}{12} \\ -\sin\theta \cdot \dfrac{Sw \cdot L}{2} \\ -\cos\theta \cdot \dfrac{Sw \cdot L}{2} \\ \cos\theta \cdot \dfrac{Sw \cdot L^2}{12} \end{Bmatrix} \right\} \tag{3.2}$$

where p_1 and p_2 are the intensities of the linearly distributed load per unit length at nodes one and two respectively with respect to the member *y*-axis, and *Sw* is the intensity of the self-weight per unit length. For a three-dimensional beam element, additional

parameters, p_3 and p_4, are used to specify the intensities of a linearly distributed load per unit length at nodes one and two respectively with respect to the member z-axis.

Once the self-weight and distributed load vector is computed for an element, it is assembled into correct location in the global force vector. This process is repeated for all elements. When this subroutine returns to the main program, the complete global force vector, $\{F\}$, is divided into the number of load increments specified in the control data line. The solution procedure can then begin. For each increment in load, the stiffness matrix must be updated and the incremental displacements and stresses must be accumulated.

3.2.4 Assemble Subroutine

This subroutine forms the element stiffness matrix for each element (each time calling the element library) and assembles the global stiffness matrix. If displacements are specified for a particular problem, they are first divided into the same number of increments as the force vector, and the global stiffness matrix and the global force vector are modified according to equation 2.2. For every element in the structure, the length is calculated and its material properties are either retrieved from memory or recalculated based on the modified stiffness of slippage model I or model II. Once the element stiffness matrix is formed, it is transformed from the member coordinate system to the global coordinate system. Control returns to the assembling subroutine where each element stiffness matrix is placed in the proper location in the global stiffness matrix.

3.2.5 Gauss Elimination Subroutine

This subroutine uses the gauss elimination method to solve a set of simultaneous equations in the form $[K]\cdot\{q\}=\{F\}$. The set of equations are manipulated until an upper triangular matrix is formed. If the maximum value for any element on the main diagonal is close or equal to zero, then the error message "no unique solution exists" appears, and the subroutine is terminated. The program identifies which main diagonal node has a stiffness coefficient less than 1E-10. This error occurs when the stiffness matrix is

singular, most likely due to a planar node or a collapse mechanism in a truss structure. The geometry of the model can be modified with stabilizing members or dummy members once the source of instability is detected, or certain truss elements can be replaced with beam elements. If a unique solution does exist, the values of $\{q\}$ can be determined by a process of back-substitution, starting from the last equation in the upper triangular matrix. These solutions are accumulated to predict the nodal displacements for the current load increment.

3.2.6 Stresses Subroutine

This subroutine calculates the incremental stress resultants (forces, bending moments) and the incremental axial slippage of every element, which are accumulated at every load increment. The incremental nodal displacements, $\{d\}$, calculated in the gauss elimination subroutine, are used to calculate the incremental stress resultants in an element by using

$$\{S\} = [k_m] \cdot \{d_m\} + \{S_o\} \tag{3.3}$$

and

$$\{d_m\} = [T] \cdot \{d\} \tag{3.4}$$

where $\{S_o\}$ represents the stress resultants corresponding to the nodal degrees of freedom due to loads on the member under fully restrained end conditions (Krishnamoorthy, 1996). The axial slippage is calculated according to the specified slippage model in the control data line (instantaneous slippage, continuous slippage, or no slippage). All results are printed to an output file.

3.2.7 Equilibrium Subroutine

After the final load increment is applied, but before the program ends, the equilibrium subroutine is called. This subroutine checks if each node is in equilibrium by summing the forces and moments in the global *X*, *Y*, and *Z* directions. All the element stress resultants that contribute to the equilibrium of a particular node are added together.

The total stress resultant for each degree of freedom at each node should equal zero if the structure is in equilibrium.

3.3 Sample Input File

The text file shown on the following page, **input.dat**, illustrates the input format required by TAP. This is the input file used for the double-diagonal truss example in the next chapter. Only the left column of numbers is required by the program. The right column gives the variable name that stores the data in the program, and is used to help the programmer identify what the input represents. The input is separated into five main components: the control data, nodal coordinates, element data, material properties, and the loading conditions. The input file shows these components separated into five sections for clarity, but in the actual input file no blank lines are allowed.

The control data is the first line in the input file. It stores the number of nodal points (NUMNP), elements (NUMEL), material sets (NUMAT), dimensions (NDM), degrees of freedom per node (NDF), load increments (INCREM), and the slippage model used (MODEL). The structure in the sample input file is a plane truss since NDM and NDF are equal to two.

The nodal coordinates are the next component in the input file, one node per line (unless nodal generation is used) starting with one and ending with NUMNP. The input uses the following format: node number, node generation increment, *X*-coordinate, *Y*-coordinate, and *Z*-coordinate. In the sample input file, node 3 does not generate additional nodes, and has an *X*-coordinate and *Y*-coordinate of 250-mm. Since this problem is only two dimensions the *Z*-coordinate is not required.

The element data input uses the following format: element number, element generation increment, the element's material set, and the nodal points i, j, and k that define the element's length and direction. Nodal point k is only required for three-dimensional beam elements. It serves to orient the member about its own axis, and therefore cannot be located along the line joining points i and j. Nodal points i, j, and k define the member x-y plane. Point k is chosen to produce a positive y-coordinate with respect to the member's coordinate system. Point k must already be a defined node in the

input.dat

```
4,9,4,2,2,1000,3          NUMNP,NUMEL,NUMAT,NDM,NDF,INCREM,MODEL

1,0,0,0                   N,NX,X(1,N),X(2,N)
2,0,0,250                 N,NX,X(1,N),X(2,N)
3,0,250,250               N,NX,X(1,N),X(2,N)
4,0,250,0                 N,NX,X(1,N),X(2,N)

1,0,1,1,2,0               M,MX,MSET(M),NP(1,M),NP(2,M),NP(3,M)
2,0,1,2,3,0               M,MX,MSET(M),NP(1,M),NP(2,M),NP(3,M)
3,0,1,3,4,0               M,MX,MSET(M),NP(1,M),NP(2,M),NP(3,M)
4,0,2,1,3,0               M,MX,MSET(M),NP(1,M),NP(2,M),NP(3,M)
5,0,1,2,4,0               M,MX,MSET(M),NP(1,M),NP(2,M),NP(3,M)
6,0,3,1,0,0               M,MX,MSET(M),NP(1,M),NP(2,M),NP(3,M)
7,0,4,1,0,0               M,MX,MSET(M),NP(1,M),NP(2,M),NP(3,M)
8,0,3,4,0,0               M,MX,MSET(M),NP(1,M),NP(2,M),NP(3,M)
9,0,4,4,0,0               M,MX,MSET(M),NP(1,M),NP(2,M),NP(3,M)

1,1                       MA,IEL
1000,10,0,0,2,4,6         E,A,SW,SLIPMAX,PSLIP,SLIPM,SLIPN
2,1                       MA,IEL
1000,10,0,1,2,4,6         E,A,SW,SLIPMAX,PSLIP,SLIPM,SLIPN
3,5                       MA,IEL
1,1,0,0,0,1E20            AXIS,DISP-CODE,ROT-CODE,DISP,ROT,STIFFNESS
4,5                       MA,IEL
2,1,0,0,0,1E20            AXIS,DISP-CODE,ROT-CODE,DISP,ROT,STIFFNESS

2,0,10,0                  N,NX,CL(1,N),CL(2,N)
3,0,10,0                  N,NX,CL(1,N),CL(2,N)
0,0,0,0                   N,NX,CL(1,N),CL(2,N)
0,0,0,0,0,0               M,MX,P(1,M),P(2,M),P(3,M),P(4,M)
```

structure. For transmission towers, angle members are oriented such that their principal axes are in line with existing structural nodes, therefore, defining the *k* node is not difficult. In the sample input file, elements 1-5 are truss elements (element type 1) and elements 6-9 are boundary elements (element type 5). Element 3 belongs to material set 1 and is connected to nodes 3 and 4; nodes 1 and 4 are restrained in the *X* and *Y*-directions.

The next component in the input file is the material properties of the elements. Each material set is associated with one element type, and each element type has a certain number of material properties that are needed to form the element stiffness matrix. A two-dimensional truss element requires the following properties: Young's Modulus, cross-sectional area, self-weight, maximum slip, slip load, *m* parameter, and *n* parameter. A boundary element requires the following properties: the global axis direction (1 = *X*, 2

= *Y*, 3 = *Z*), displacement code (1 = restrained, 0 = free), rotation code (1 = restrained, 0 = free), specified displacement, specified rotation, and spring stiffness. In the sample input file, element 4 has a maximum slip of 1-mm while element 5 has a maximum slip of 0-mm.

The last component in the input file is the loading conditions – concentrated and distributed. The format for concentrated loads is: node number, generation increment, load at the first degree of freedom, load at the second degree of freedom, ... , load at the maximum number of degrees of freedom. Nodes 2 and 3 have a 10-kN load applied in the *X*-direction. The concentrated load data must terminate with a line of zeros – indicating that there are no more concentrated loads. The format for distributed loads (only applicable to beam elements) is: element number, generation increment, intensity at node-*i* in the member *y*-direction, intensity at node-*j* in the member *y*-direction, intensity at node-*i* in the member *z*-direction, intensity at node-*j* in the member *z*-direction. The distributed load data must terminate with a line of zeros – indicating that there are no more distributed loads and the end of the input file has been reached. The input file is not accessed again. With all input read and stored, the first increment of displacements can be calculated with the first load increment.

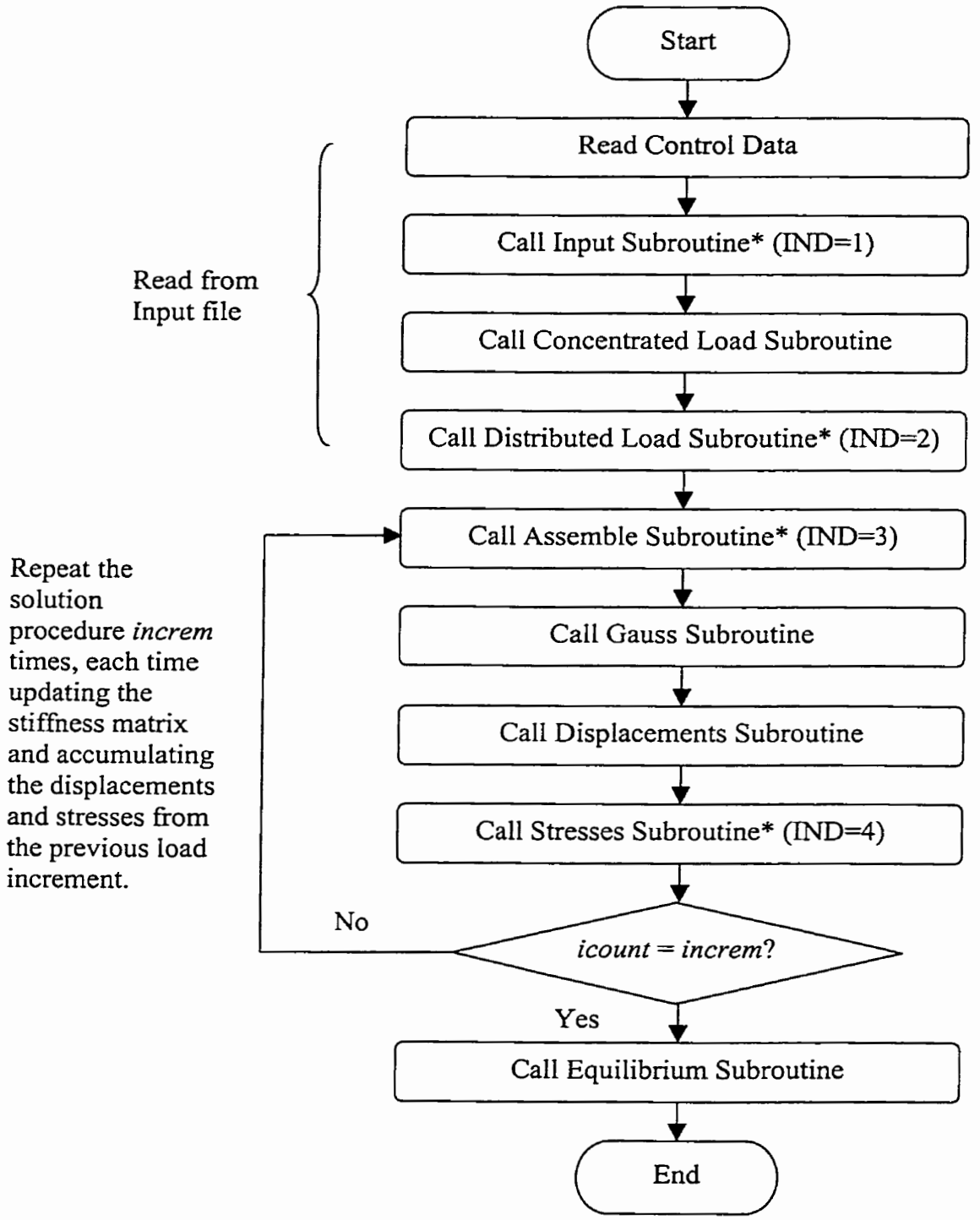

Figure 3.1: Flowchart of TAP program

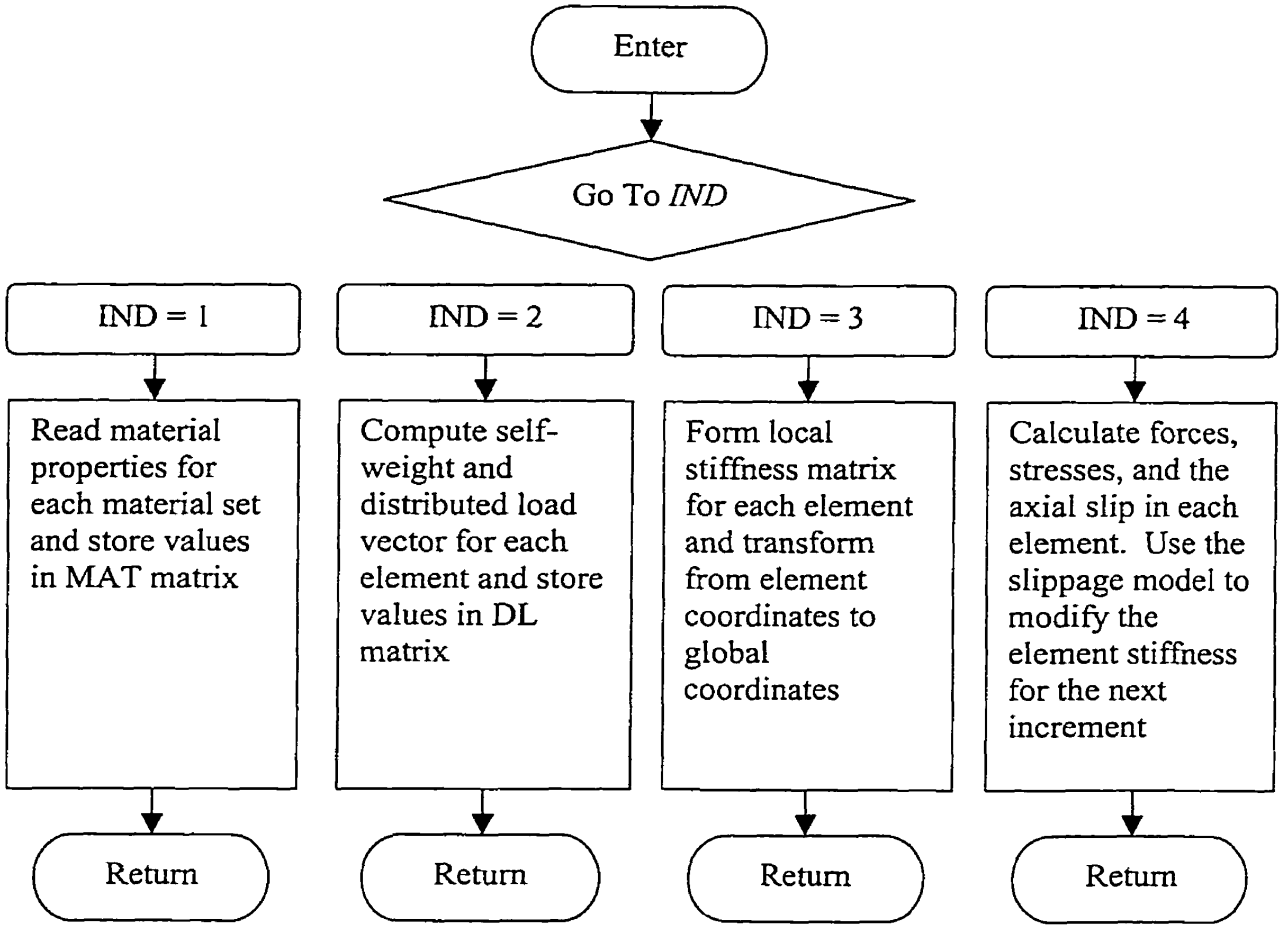

Figure 3.2: Element subroutine called by main program

Chapter 4

MODEL VERIFICATION AND APPLICATION

4.1 General

This chapter verifies the slippage models developed in chapter 2 and investigates the effect of bolt slippage on the general behavior of latticed structures. The linear no-slip aspects of TAP are first validated followed by a comparison of the results from bolt slippage analyses using TAP and the program AK TOWER. The comparisons are made in terms of nodal deflections and member stresses. The number of slipping elements and the parameters of both the instantaneous and continuous slippage models are varied in order to investigate the effect of bolt slippage on a simple one-dimensional bar element, a double-diagonal plane truss, a double-diagonal frame with flexible connections, and a simple three-dimensional transmission tower using beam elements. Finally, a full-scale transmission tower is analyzed. Before the slippage analysis was conducted on the full-scale tower, the most suitable element configuration was determined by trying several models (all truss elements, all beam elements, or a combination of truss and beam elements). The effect of bolt slippage is investigated on a full-scale transmission tower using truss and beam elements with experimentally determined slippage parameters.

4.2 Model Verification

Several example problems are analyzed in this section in order to establish the validity of the developed TAP program. The linear no-slip results of the TAP program are first compared to solutions obtained from PASSFEM, a *p*rogram for the *a*nalysis of *s*tructural *s*ystems by *f*inite *e*lement *m*ethod developed by Krishnamoorthy (1996) and the popular *s*tructural *a*nalysis *p*rogram SAP IV. The only program available for comparison of the results from bolt slippage analyses was AK TOWER (Al-Bermani and Kitipornchai, 1994). Unfortunately, this program combines several nonlinear effects into the same program (geometric and material nonlinearity, joint flexibility, and joint slippage). In the TAP program, only joint slippage produces the nonlinear response.

Therefore, a direct comparison between the TAP results and the AK TOWER results is not possible. Several conclusions can be made, however, from the results of TAP, AK TOWER, and the no-slip case.

4.2.1 Plane Truss, Space Truss, Plane Frame, and Space Frame

Before any nonlinear effects are incorporated into a structural analysis program, the linear-elastic capabilities must be functioning correctly. In order to verify the linear (no-slip) aspects of TAP, several simple analyses of framed structures were conducted. A two-dimensional truss, a three-dimensional truss, a two-dimensional frame, and a three-dimensional frame were analyzed by TAP. The geometry, material properties and loading conditions of the structures are given in Appendix C (taken from Krishnamoorthy, 1996). Comparisons of axial forces and end moments from selected members using various analysis programs are shown in Tables 4.1 to 4.4. Clearly TAP is able to reproduce the results of standard structural analysis programs, and all truss, beam, and boundary elements are functioning correctly.

4.2.2 Double-Diagonal Plane Truss with Slippage

The nonlinear aspects of TAP were investigated by analyzing a simple double-diagonal truss as shown in Figure 4.1. Kitipornchai, Al-Bermani, and Peyrot (1994) investigated the effect of instantaneous bolt slippage and continuous bolt slippage on the same double-diagonal truss. Figure 4.1 indicates the element material properties and the element slippage properties that Kitipornchai selected for the analysis. For this structure, the slippage load is 2-kN and slipping members are allowed to slip 1-mm. The continuous slippage parameters m and n for the AK TOWER program and the TAP program were assigned values of 4 and 6 respectively.

The vertical deflection of node 2 is shown in Figure 4.2 for the no-slip case and for slippage model I and slippage model II when the tension diagonal (element 4) slips and when the compression diagonal (element 5) slips. The deflections are greater when

the compression diagonal slips because it is directly connected to node 2. In other words, node 2 would deflect more if element 5 were removed than if element 4 were removed.

The AK TOWER results along with the output from TAP are shown in Table 4.5. AK TOWER computed the ultimate load of the truss, and the deflections shown in Table 4.5 are taken at 95% of the calculated ultimate load. Although the results from the two programs should not be compared directly (since Kitipornchai's program includes geometric and material nonlinearity, and treats the angle members as general asymmetric thin-walled beam-column elements) some observations can be made. For the no-slip case, both programs predict the same vertical deflection at 95% of the ultimate load - before the compression member buckles. Also, for any slippage model, the vertical deflection of node 2 is always more than the no-slip case. The results for the continuous slippage models are fairly similar (a 3% difference), but there is a significant discrepancy between the instantaneous slip models. Even though the absolute difference is only 0.17-mm, the instantaneous slip results from TAP are 50% larger when the compression diagonal slips. The differences between the predicted deflections are most likely due to the geometric and material nonlinearities not accounted for in the TAP program, and the different methods used to modify the stiffness of the slipping member. Kitipornchai's method for updating the stiffness matrix and the actual amount of member slip was not available for comparison (Kitipornchai, 1994).

The TAP deflections reported in Table 4.5, were the values obtained once the solution had converged. For the relatively simple double-diagonal truss example, the difference between the solution at 100 load increments and the solution at 10000 load increments was less than 2%. In fact, the accuracy of the solution did not improve after 1000 load increments (much less than 1%). Figure 4.3 shows the solution convergence as the number of load increments are increased for the instantaneous slip model when the tension diagonal slips – this vertical deflection value was entered in Table 4.5.

4.2.3 Simple Transmission Tower with Slippage

A simplified model of a transmission tower is shown in Figure 4.4 along with the angle sizes and slippage properties. Kitipornchai, Al-Bermani, and Peyrot (1994)

investigated the effect of instantaneous bolt slippage and continuous bolt slippage on the same structure. Four vertical loads, two transverse loads, and two lateral loads are applied to the top of the 8-m tower. The tower cross section remains square and the bracing is symmetrical on all faces, typical of most transmission towers. For this structure, Kitipornchai assumed a slippage load one tenth of the yield load, which is a fairly reasonable assumption (see Figure 2.3 or Figure 2.5), and all members are allowed a maximum bolt slip of 1-mm. The slippage load was calculated as 81.55-kN for the members in the four main legs and 23.18-kN for all other members using the yield stress and the cross-sectional area of each type of angle. The same m and n parameters that were used for slippage model II in the double-diagonal truss example (4 and 6 respectively) were selected by Kitipornchai for the simplified transmission tower. All members are modeled as three-dimensional beam elements. In the input file, the usual two end nodes are not enough to completely define the length and orientation of each beam element. A third node must also be entered to define the orientation of the principal planes of bending (the member y-axis and the member z-axis). This is only necessary for three-dimensional beam elements.

The transverse deflection at A is shown in Figure 4.5 for the no-slip case and for slippage model I and slippage model II when all members of the tower are allowed to slip 1-mm. The load factor on the tower was increased to a maximum of 30; the ultimate load of the simplified transmission tower (calculated by AK TOWER) occurred at a load factor of 29.35. The transverse deflection at A at 95% of the ultimate load is shown in Table 4.6 for the AK TOWER program and the TAP program. Again, as in the double-diagonal truss example, a direct comparison of the deflections cannot be made since the two computer programs use different analysis techniques. However, as seen from Table 4.6, no matter what technique or what computer program is used, instantaneous or continuous bolt slippage produces significantly larger deflections than the no-slip case. In this example, the transverse deflection at A was increased by over 30% by using the instantaneous slippage model from TAP, and the continuous slippage model from AK TOWER resulted in a 20% increase in transverse deflection (Kitipornchai, 1994). The model I deflections are greater than the model II deflections in Table 4.6 (and Table 4.5) since the low m parameter in model II does not produce the 1-mm member slip which is

achieved instantaneously in model I. As discussed later, when the members slip the same amount, both models predict the same structural response.

Figure 4.6 illustrates the convergence of the transverse deflection at A (using model I) as the number of load increments are increased up to 1000. The no-slip case has been included for comparison. The solution does not change significantly (less than 1%) for load increments greater than 1000, as shown in Figure 4.7. It is interesting to note that the general shape of the load-deflection relationship remains fairly consistent, no matter how many load increments are used. This implies that the tower members slip at the same load level (the specified slippage load, P_s) but the members that are analyzed with fewer load increments exceed the maximum allowable slip and cause larger transverse deflections. When the axial force exceeds the slippage load for a member using model I, a large stiffness change results in a large change in displacement. In some cases, this large slip displacement exceeds the maximum allowable slip, Δ_s, specified in the input file, and the analysis must be repeated with a smaller load increment. Until the member slip is approximately equal to the specified allowable slip, the number of load increments must be increased. This aspect of model I is shown in Table 4.7; as the number of load increments increase, the actual member slip approaches the specified member slip. For this simple transmission tower example, model I required 1000 load increments before all of the member's slipped an amount equal to the specified maximum slippage. Because of the large slip displacement associated with instantaneous slip, model I usually requires more load increments than model II before the solution converges. In terms of computational efficiency, model II is superior to model I.

4.3 Slippage Effects on the General Behavior of Structures

The program verification in the previous section has shown that linear examples analyzed with TAP produce the same results as standard structural analysis programs and that the slippage models compared favorably to the only known solutions to structural analysis problems incorporating bolt slippage. In this section, the number of slipping elements and the parameters of both the instantaneous and continuous slippage models are varied in order to observe the effect on the general behavior of several structures and

to compare the results of the instantaneous slippage model to the continuous slippage model. The investigations are conducted in order to arrive at a suitable slippage model for a full-scale transmission tower.

4.3.1 Simple Bar Elements

The most basic of latticed structures, a single one-dimensional bar with one node restrained and one end axially loaded is shown in Figure 4.8. This simple case can easily measure the effects of bolt slippage without complicating the analysis with a large input mesh. The bar element may be modeled as a truss or a beam – both representations give identical results since the bar is only subjected to axial forces. The following analysis of the simple bar element was based on 1000 load increments; no change in the output was observed if the number of load increments was increased above this amount for either slippage model (see Figure 4.9).

The axial force-deformation relationship shown in Figure 4.10 is based on a single bar element with the material properties and loading conditions given in Figure 4.8. In this example, the slippage load is 10-kN (one-tenth the total load) and the maximum amount of slip is 1-mm. It can be seen that the m parameter has a significant effect on the results, as mentioned earlier in chapter 2. If the m parameter is increased above 135, however, the axial force-deformation relationship does not change. Any value above 135 produces an axial slip equal to the specified slip (1-mm), and any value below 135 produces an insufficient amount of slip (less than 1-mm). This is illustrated in Figure 4.11. Therefore, in order to produce the same slippage effect for models I and II, the m parameter must be at least 135.

For the no-slip case, the elastic axial deformation (Δ_e) in the bar is 1-mm at the final load level. For a specified slippage (Δ_s) of also 1-mm, the total axial deformation (Δ) should equal 2-mm according to equation 2.11. As can be seen in Figure 4.10, both slippage models have a final axial deformation of 2-mm (if a large enough m value is selected for model II). Furthermore, if an additional bar is attached to the bar shown in Figure 4.8, with the same material properties and with an m parameter that produces a 1-mm slip in both members, then the deflection of the end node is equal to each member's

elastic deformation and each member's slippage. This produces a 4-mm end node deflection compared to only 2-mm for the no-slip case (see Figure 4.12). This summation of elastic and slippage deformations for a structure with many members can produce nodal displacements that are much larger than a similar structure without connection slip. Alternatively, the same amount of slip shown in Figure 4.12 for a two-bar assembly is produced when a single bar element is capable of slipping 2-mm instead of 1-mm. By applying this concept to a full-scale transmission tower, the tower deflections would be considerably larger with the bolts in a position of maximum clearance than with the bolts positioned in the center of the bolt hole or bearing against the bolt hole.

Altering the slippage load also has a significant effect on the axial force-deformation relationship. Figure 4.13 shows the force-deformation relationship for model I and model II for slippage loads of 10-kN, 30-kN, and 50-kN. Altering the value of the slippage load only effects the load which initiates slippage (model I) or the load at which most of the slippage occurs (model II), but the end result is not affected. A structure comprised of elements that slip at 10-kN and a structure comprised of elements that slip at 50-kN would produce identical nodal displacements, as long as the axial force in all members is greater than 50-kN.

Another interesting feature of a member capable of slipping is its ability to absorb a specified displacement. To illustrate this effect, the same element in Figure 4.8 is used, except the applied force of 100-kN is replaced with a specified displacement of 1-mm. Since the 100-kN force produces a 1-mm displacement, a 1-mm specified displacement should produce an internal force of 100-kN for the no-slip case. Figure 4.14 confirms this. But if the element is allowed to slip according to either slippage model I or model II, the internal force is greatly reduced. In Figure 4.14, most of the specified displacement is transferred directly to the slippage component of the total deformation and the internal force remains at or near the slippage load. In fact, if the slippage load was reduced to zero in model I (slippage begins at the onset of loading), the entire specified displacement would be due to slippage and the internal force in the member would be zero. This demonstrates that a slipping connection not only increases

deflections, but can also significantly reduce the connecting member's internal axial force.

4.3.2 Double-Diagonal Plane Truss

The double-diagonal truss example is revisited to investigate the effects of slippage and to compare the results of both slippage models. Just as the results for two different methods of analysis should not be compared directly, the results for instantaneous slippage and continuous slippage should not be compared unless the amount the member slips is equal for both cases. As demonstrated with simple bar elements, the instantaneous and continuous slippage models only agree with each other when all members slip the same amount. The amount the members actually slip was not shown in Table 4.5, since this information was not provided in the literature. When the slippage parameters selected by Kitipornchai are used for verification purposes (Figure 4.1), the deflections using model II are significantly less than the deflections using model I (as seen in Figure 4.2). This does not mean the two models disagree with each other, it means the amount of slip each model produced was not equal. The low m parameter in model II only produced a slippage of 0.044-mm at the final load compared to the fully completed slip of 1.0-mm when using slippage model I.

The maximum slippage, Δ_s, should be set to the difference between the bolt hole and the bolt diameter of a connection, 1-mm was assumed for this example. Once the specified slip is complete, the member stiffness is restored to its original value. If a slipping member does not reach the specified amount when using model I, nothing can be done to increase the slip since the applied load is not large enough to complete the clearance slip. If complete slip is achieved with model I, but not with model II, the m parameter can be increased to achieve complete slip. If the applied load was less than approximately 8-kN (see Figure 4.2) then both models would not be able to complete the specified slip.

In order to produce a 1-mm slippage in the tension member for both models, thus allowing a direct comparison, the m parameter was increased as shown in Figure 4.15. In order to complete the clearance slip with model II, a minimum m parameter of

210 must be selected. Any value above 210 produces an axial slip equal to the specified slip (1-mm), and any value below 210 produces an insufficient amount of slip (less than 1-mm). Figure 4.16 shows that both models predict a very similar load-deflection relationship when the tension member slips the same amount. From approximately 9-kN up to the final applied load of 10-kN, the load-deflection relationship is linear for both models. This represents the transition from slippage stiffness to original stiffness, which occurs once the slippage has reached the maximum specified amount. When analyzing a structure with continuous bolt slippage, it may be necessary to perform several runs of the program, each time modifying the slippage parameters until the member slip is equal to the specified clearance slip, Δ_s.

An interesting consequence of allowing one diagonal to slip while leaving the other diagonal in the no-slip case, is the load-distribution effect. Figure 4.17 illustrates the changes that occur in the diagonal member's axial force when member 4 is allowed to slip according to model I, but member 5 is not. The axial forces of the diagonal members in the no-slip case are included for comparison. When the axial force in tension member 4 exceeds the slippage load (2-kN in this example), the member begins to slip. While slippage is occurring, the axial force in member 4 remains constant while member 5 must take on additional load to maintain equilibrium. Once the prescribed slippage in member 4 has been achieved, both members share the applied force equally and the axial force increases with the applied load at the same rate as the no-slip case (the slopes are equal in Figure 4.17 after the applied load exceeds approximately 8-kN). In this example, slippage of the tension member has decreased the final axial force in member 4 from 14.14-kN to 4.9-kN while the axial force in member 5 has increased from -14.14-kN to -23.38-kN. Almost identical results were achieved using slippage model II.

For this simple example with only 5 members and allowing only one member to slip, the load-distribution effect is easily observed. The effect becomes less noticeable as the number of members in a structure is increased, and as the number of slipping members is increased. If both diagonals are allowed to slip, the axial forces of all members are virtually the same as the no-slip case, but the deflections are significantly larger. Since both diagonals reach their slip load simultaneously, the applied load cannot be distributed from one diagonal to the other, and the reduced stiffnesses only cause

larger deflections. Likewise, if all members in the double-diagonal truss are allowed to slip, the axial forces again are virtually the same as the no-slip case and the deflections are even larger. The larger deflections are due to larger axial elongations comprised of elastic elongation and 1-mm of slip. The results are summarized in Table 4.8.

4.3.3 Double-Diagonal Plane Frame with Semi-Rigid Connections

The double-diagonal truss example, shown originally in Figure 4.1, is re-analyzed with semi-rigid connections to determine if joint slippage is influenced by joint flexibility. The verification is based on a comparison between the perfectly pinned and the perfectly rigid idealizations. TAP models the tangent stiffness of a semi-rigid connection by using the following exponential function

$$R = \frac{dM}{d\theta_r} = C \cdot \exp\left(-\frac{|\theta_r|}{\alpha}\right) \tag{4.1}$$

in which α is a scaling factor, C is a curve fitting constant and θ_r is the relative angle of rotation between connecting members (accumulated at each load increment). When α is large the exponential term approaches unity and the stiffness of the semi-rigid connection becomes equal to the constant C. In order to model a pinned connection a small C value is selected; in this example C=1E-8 was used to represent the truss element solution (C must be small, but greater than 1E-10 in order to prevent a singular stiffness matrix). In order to model a rigid connection a large C value is selected; in this example C=1E20 was used to represent the beam element solution. To investigate the semi-rigid case an intermediate stiffness is selected, in this example a constant connection stiffness of C=1E5 was used. The semi-rigid beam element can easily model nonlinear moment-rotation behavior by decreasing the α factor.

Figure 4.18 shows the vertical deflection of node 2 of the double-diagonal frame for the no-slip case. As expected, the deflection for the frame modeled with semi-rigid beam elements was larger than the beam element (C=1E20) solution but smaller than the truss element (C=1E-8) solution. Figure 4.19 shows the vertical deflection of node 2 of the double-diagonal frame when all elements are allowed to slip 1-mm according to model I and II. Again the semi-rigid beam element solution falls in between the beam

and truss solution. In fact the percent increase in deflection from the beam solution to the semi-rigid beam solution was almost the same for the slip and no-slip cases. Semi-rigid beam elements increased the deflection by 13.9% for the no-slip case and by 12.4% for all members slipping 1-mm. Similarly, the percent increase in deflection from the semi-rigid beam solution to the truss solution was almost the same for the slip and no-slip cases. A 12.0% increase was observed for the no-slip case and an 11.4% increase was observed for all members slipping 1-mm. Model I and model II solutions were identical at the final load – once all members had slipped the same amount. This simple example shows that joint flexibility influences the nodal deflections, but does not influence joint slip behavior.

4.3.4 Simple Transmission Tower

The simple transmission tower (Figure 4.4) is revisited to investigate the effects of slippage and to compare the results of both slippage models. As previously discussed, the instantaneous and continuous slippage models only agree with each other when all members slip an equal amount. By arbitrarily assuming an m parameter of 4 (Kitipornchai, 1994) the amount the members in the tower actually slip is not guaranteed to be equal to the specified 1-mm, and therefore the two models predict different results. That explains why the model II deflection at A (Figure 4.5) is significantly less than the model I deflection.

For model I, as the load factor is increased to a maximum of 30, a total of 44 of the 69 beam elements in the tower exceed their slippage load and undergo a 1-mm slippage. The other 25 elements do not exceed their slippage load and their stiffness does not change. For model II, all the members slip, but the amount each member slips is dependent on its m parameter and its axial force. Table 4.9 shows the axial slippage of 40 tower members for model I and model II. Only with large m values do members slip the specified 1-mm with model II. Since the continuous slip model also depends on the axial force in the member, elements with a small axial force that did not exceed their slippage load for model I (elements 11-20 in Table 4.9 for example) produce a much smaller slippage for model II.

Since the member slippage using model II approaches the member slippage using model I with higher m values, the transverse deflection at A using model II with an m parameter of 100 is almost identical to the model I solution at higher load factors (see Figure 4.20). The two models are not identical, however. For example, in Table 4.9, element number 26 slips 0.24-mm using model II, while in model I this element does not slip at all. Also, at low and intermediate load levels, the two models can predict considerably different deflections (see Figure 4.20 at a load factor of approximately 13). Only when the same members slip the same amount at the same load level, do the two models predict identical deflections and member stresses. Although the deflections increased considerably, the axial stresses in the simple transmission tower were unaffected by axial slippage.

4.4 Structural Analysis of a Full-Scale Transmission Tower

A full-scale transmission tower is shown in Figure 4.21. This tower is located in northern Manitoba and is part of Manitoba Hydro's Nelson River DC transmission system. It is over 60-m tall and is comprised of 494 primary members (not including 12 boundary elements restraining the footing joints in the three global directions for all four main legs), and 217 primary nodes. The actual tower has a total of 708 angle members and 384 connection nodes, but these totals are also including secondary members and secondary nodes. The analysis of this tower does not include secondary members or the joints attached only to secondary members (called secondary nodes). Secondary members are only relevant in compression capacity calculations, since their purpose is to reduce the unbraced length of primary members and not to provide load resistance. The self-weight of these neglected secondary members is accounted for by multiplying the primary member self-weight by an appropriate factor (Yue, 1994). A factor of 1.2 was used in this example.

This tower was designed with 16 different angle sizes: from L51x51x4.8 angles used in the transverse and longitudinal cross-bracing in the upper section of the tower to L152x152x13 angles used in the main legs of the bottom section of the tower. The members are typically assumed to be truss elements, but the TAP program can model the

tower members as truss elements, beam elements, or a combination of the two. The wire loading condition shown in Figure 4.21 is one of several worst-case scenarios tested by Manitoba Hydro's analysis and design program and the output from that program will be used to verify the results of the TAP program.

4.4.1 Linear Analysis

The three-dimensional representation of the tower's upper section, Figure 4.22, best illustrates the staggered bracing pattern used for this tower. The bracing members on the longitudinal face and the transverse face do not meet at a common joint, providing additional stability and strength without increased material costs. The staggered bracing pattern does complicate the analysis however. Each time the bracing members on each face do not meet at a common joint, this additional joint adds three equations (if only truss members are attached to the joint) or six equations (if a beam member is attached to the joint) to the system of equations for the entire tower. For this particular tower, the staggered bracing pattern adds over 60 primary joints to the analysis, or up to 360 additional equations.

These staggered joints also present a mathematical problem besides the increased number of equations that must be solved. At each of these joints, all the members connected to these joints are in the same plane – producing a planar joint and a singular stiffness matrix if the connecting members can only resist an axial force (if they are all truss elements). For example, joint 12 in Figure 4.22 is a planar joint. The elements that are connected to node 12 (elements 6-12, 10-12, 16-12, and 23-12) all lie in the same plane. These planar nodes are common in most transmission towers, not just towers with staggered bracing. In order to solve such a system of equations, artificial restraints must be provided in the direction of instability, or the truss elements must be replaced with beam elements. Both options were tried for this tower, and the solutions were compared with the output of the program that is currently being used by Manitoba Hydro. The deflections for several of the tower's nodes in the upper section (the nodes that are subjected to the largest transverse deflections) are presented in Table 4.10.

The maximum deflections at the very top of the tower (nodes 1-5) were very similar for both programs no matter which element configuration was used with TAP. The deflections are slightly different between the Manitoba Hydro truss model and the TAP truss model since the artificial restraint procedure is not identical. The TAP program restrains the planar node in one of the global coordinates whereas the Manitoba Hydro program calculates the direction normal to the plane of all connecting elements and attaches the restraint in that direction. Also, the self-weight of truss members stabilized with artificial restraints cannot be concentrated at the end nodes since these nodes are not strong enough to resist loading. The artificial cross-sectional area provided at planar nodes is only large enough to prevent a singular stiffness matrix and any applied load would cause very large deflections. Since no load can be applied to a planar node, the self-weight of the connecting members must be distributed to the closest non-planar node. This procedure of redistributing the self-weight (automatically calculated with the Manitoba Hydro program but not with TAP) might contribute to the small discrepancies between the two programs.

There are several serious problems with the artificial restraint method. Most important, the computed deflections at restrained planar nodes are not accurate solutions. The artificial restraint technique allows the program to solve for deflections at non-planar nodes in the tower, but the deflections at restrained nodes should not be considered accurate. For example, when the tower is modeled as a truss, nodes 12-15 and nodes 20-23 (nodes that must be restrained artificially) only deflect 3-mm in the *Y*-direction using the Manitoba Hydro program and less than 1-mm when using TAP. This lack of movement in the unstable direction is what allows the system of equations to be solved, but this lack of movement is not consistent with the nodal deflections near these restrained nodes. The nodes above and below these nodes (nodes that are not restrained artificially in the *Y*-direction) are displacing approximately 500-mm, see Table 4.10. When the main legs are modeled as beam elements, or when all the members are modeled as beam elements, then nodes 12-15 and nodes 20-23 displace an amount similar to their neighboring nodes – approximately 500-mm. When beam elements are used, the *Y*-direction displacements gradually decrease from a maximum amount at the top of the tower to smaller values near the bottom of the tower, predicting a more realistic solution

for nodal displacements than the artificially restrained truss model. This relationship is most pronounced in the *Y*-direction since the applied load causes large displacements in this direction, but the *X*-displacements and *Z*-displacements are also more consistent throughout the tower if beam elements are used, see Table 4.10. Because the internal forces and stresses are calculated based on the nodal displacements, the stresses calculated from a truss/beam model are also more accurate than an artificially restrained truss model.

Of the two methods used, the preferred method is to model the main leg members as beam elements rather than truss elements with artificial restraints. This easily solves the singular matrix problem without having to search for every planar node and attach an artificial restraint element, eliminates the need for dummy members to prevent structural mechanisms, eliminates the incorrect displacements at planar nodes corrected with artificial restraints, eliminates the need to redistribute the self-weight of members attached to planar nodes, and is a more accurate model since the main leg members do resist bending stresses and are continuous through the primary joints.

Modeling the main legs as beam elements does complicate the analysis significantly however, since each node has six degrees of freedom (three translational and three rotational) instead of only three degrees of freedom for truss elements. Also, a third node must be specified for each beam element to describe its orientation completely in three-dimensions. Modeling the main legs as beam elements increases the computation time, but the predicted deflections and stresses are more realistic.

Since the primary members not on the main legs of the tower are also continuous through primary and secondary joints, and can be connected with moment-resisting multiple-bolt configurations, they also could be accurately modeled as beam elements. In fact, some researchers use the beam element to model all members of a transmission tower. The differences in nodal deflections were very small between the full-scale tower modeled with only beam elements in the main legs and the full-scale tower completely modeled with beam elements. In both models, the most significant forces were axial forces. The largest bending moments in members of the full-scale tower were approximately 4-kNm, and axial forces were as high as 700-kN. The largest bending moments occurred in the main leg members in the bottom section of the tower. The

bending stress at the extreme fibers of these angle sections was 60-MPa, compared to the axial stress of 190 MPa. Unlike a truss element, when a tower member is modeled as a beam element, it must be designed to resist axial forces, shearing forces, and bending moments.

4.4.2 Slippage Effects

In the following slippage analysis, the full-scale transmission tower is modeled with beam elements for the main legs and any elements continuous through planar nodes (all horizontal members), and truss elements are used for all of the primary bracing members on the longitudinal and transverse faces. As discussed in the previous section, the final deflections computed by the instantaneous slippage model and the continuous slippage model are nearly identical, as long as the elements slip the same amount in each model. Consequently, only the continuous slippage model is used for this example, with a large m parameter to complete the clearance slip (m=100). Model II also tends to converge with fewer load increments than model I. This tower, with 217 nodes with six degrees of freedom at most nodes, takes about two minutes of computation time per load increment. In order to insure solution convergence, 2000 load increments were used, requiring almost three days of computation time. Figure 4.23 shows the transverse deflection of node 1 converging with increasing load increments.

The slippage model for the full-scale tower assumes that the bolts are not bearing nor in a position of maximum clearance, but that the bolts are centered in the bolt hole. The effect that bolt position has on the analysis can easily be determined by varying the amount of maximum slippage for certain elements. In this example, the slippage parameters used in model II were based on experimental studies conducted by Ungkurapinan (2000). The parameters used for the full-scale tower are summarized in Table 4.11. It should be noted that the maximum slip for the members in the four main legs of the tower is considered between the splicing points of the continuous main leg angles. Since each continuous main leg angle is actually made up of several individual beam elements separated by nodal points that connect transverse and longitudinal bracing members, the total slip per continuous main leg angle must be divided evenly among the

beam elements between the two splice points. For all other members, the maximum slip value can be taken as the actual member maximum slip. It was assumed that the angle members were bolted together using only one bolt, corresponding to a slippage load of 9.29-kN. As demonstrated with the simple bar element, the magnitude of the slippage load does not have an effect on the final deflections, as long as the axial force in each member exceeds the specified slippage load. The final results for a tower assembled with four-bolt connections are the same as a tower assembled with one-bolt connections, as long as the axial forces exceed 46.95-kN (see Table 4.11). The deflections at intermediate load levels are not the same, however, as some elements begin to slip earlier in the tower with only one-bolt connections.

Figure 4.24 shows the transverse deflected shape of the full-scale transmission tower after the final load increment was applied. As expected, the deflections predicted using slippage model II with realistic slippage parameters were greater than the no-slip case. The greatest tower deflection (node 1) increased from 531.29-mm to 780.23-mm when using slippage model II, an increase of over 45%. Despite the significant increases in nodal deflections, the member stresses remained relatively unchanged. Table 4.12 shows the axial stresses of critical members in the full-scale tower. Four members were chosen from the top section, middle section, and bottom section of the tower – these three sections are constructed using three different angle types. The four members chosen in each section represent each of the four main legs. The axial stresses are symmetric (two main legs in equal compression and two main legs in equal tension) since the applied loading does not cause any twisting about the vertical axis of the tower. As Table 4.12 indicates, connection slippage has no effect on member axial stresses, it only adds to the overall flexibility of the tower. This was also observed with the double-diagonal truss and the simplified transmission tower.

However, when a displacement was specified, model II (with the same experimentally determined slippage parameters) significantly changed the axial stresses in critical members when compared to the no-slip case. To investigate a foundation settlement (or heave) the same full-scale transmission tower was used, except the transverse loading was removed. The member's self-weight and the same vertical wire loads were applied along with a specified foundation heave of 100-mm on only one of the

four foundations. Transmission tower foundation movements of up to 150-mm have been observed in northern Manitoba, where seasonal frost and the formation of ice lenses cause significant frost heave. These conditions vary greatly over short distances, producing differential settlements between adjacent footings. Figure 4.25 shows a transmission tower in northern Manitoba leaning to the left due to foundation movement. The critical members for the specified displacement analysis, the members with the highest axial stresses, were all located in the bottom section of the tower. These members are shown in Table 4.13.

The axial stresses in the critical members were greatly reduced when slippage model II was used. Axial stress in the horizontal truss bracing was reduced by 55-Mpa. The axial stresses in the truss members off the main legs were reduced by an average of 40-MPa. But the greatest change was observed in the main leg beam members – the most important structural element in the tower. The main leg axial stresses were reduced by almost 100-Mpa each, a decrease of over 90% in one main leg member.

4.5 Recommended Slippage Model

In the parametric study and slippage investigation in the two previous sections, the following considerations were made:

- Comparing model I, model II, and the no-slip case
- Varying the number of load increments
- Varying the m parameter in slippage model II
- Varying the magnitude of slip, Δ_s
- Varying the magnitude of the slippage load, P_s
- Varying the number of slipping elements in a structure
- Comparing the forces induced in members with and without joint slip
- Comparing the nodal deflections of a structure with and without joint slip
- Examining the axial force-deformation relationship due to support movement with and without slip
- Examining the influence of semi-rigid joints on slip behavior

- Comparing a truss element model with artificial restraints and a beam element model
- Modeling joint slippage with experimentally determined parameters

Based on the results of the above investigations, the following model is recommended for transmission tower analysis:

- A continuous slippage model (model II) with a large enough *m* parameter to complete the required slip
- If the element slip is less than the required bolt clearance, the *m* parameter can be increased
- To accurately model the slippage behavior, the analysis should use experimentally determined values for the magnitude of joint slip and the magnitude of slippage load
- Beam elements should be used to model the main tower legs and wherever a planar node exists (artificial restraints should be avoided)
- The analysis should be repeated with smaller load increments until the solution converges (fewer increments are required for the continuous slippage model)

Element Number	Axial Forces (kN)		
	Method of Joints	PASSFEM	TAP
13	150.0	150.0	150.0
14	150.0	150.0	150.0
15	-134.2	-134.2	-134.2
16	-134.2	-134.2	-134.2
23	0.0	0.0	0.0
24	0.0	0.0	0.0

Table 4.1: Comparison of axial forces in selected members of a plane truss

Element Number	Axial Forces (kN)		
	PASSFEM	SAP IV	TAP
2	-23.7	-23.7	-23.7
3	-19.8	-19.8	-19.8
4	13.0	13.0	13.0
5	16.9	16.9	16.9
22	49.7	49.7	49.7
23	-64.0	-64.0	-64.0
24	42.6	42.6	42.6
25	-71.1	-71.1	-71.1

Table 4.2: Comparison of axial forces in selected members of a space truss

Element Number	End Moments (kN-cm)		
	PASSFEM	SAP IV	TAP
1	2921	2921	2921
7	5949	5949	5949
13	5263	5263	5263
19	-12340	-12340	-12341
25	-9256	-9256	-9256

Table 4.3: Comparison of end moments in selected members of a plane frame

Element Number	End Moments (kN-cm)					
	PASSFEM		SAP IV		TAP	
	My	Mz	My	Mz	My	Mz
1	7.35	-1170.0	7.35	-1170.0	7.35	-1169.8
11	3.27	-697.9	3.27	-697.9	3.27	-697.9

Table 4.4: Comparison of end moments in selected members of a space frame

Computer Program	Node 2 Deflection (mm)		
	No Slip	Instantaneous Slip	Continuous Slip
Tension Diagonal Slips			
AK TOWER (1994)	0.301	0.345	0.339
TAP	0.301	0.467	0.328
Compression Diagonal Slips			
AK TOWER (1994)	0.301	0.333	0.328
TAP	0.301	0.507	0.335

Table 4.5: Comparison of double-diagonal truss deflections at 95% of ultimate load (F = 3.145-kN)

Computer Program	Transverse Deflection at *A* (mm)		
	No Slip	Instantaneous Slip	Continuous Slip
AK TOWER (1994)	15.76	16.44	18.51
TAP	14.54	19.14	15.48

Table 4.6: Comparison of deflections of simple transmission tower at 95% of ultimate load (load factor, λ, of 27.9)

Number of Load Increments	Main Leg Axial Slippage Δ_s (mm)
25	6.79
50	1.68
100	1.52
150	1.25
500	1.01
1000	1.00

Table 4.7: Axial slippage in a typical member of the simple transmission tower for various load increments (maximum slippage = 1.0-mm)

	No Slip	Element 4 Slips	Elements 4 and 5 Slip	All Elements Slip
Node 2				
X-displacement (mm)	0.25	0.41	0.25	1.25
Y-displacement (mm)	0.96	1.58	2.37	3.37
Node 3				
X-displacement (mm)	-0.25	-0.09	-0.25	-1.25
Y-displacement (mm)	0.96	1.75	2.37	3.37
Element 1				
Axial Force (kN)	10.00	16.53	10.02	10.01
Elongation (mm)	0.25	0.41	0.25	1.25
Slip (mm)	0.00	0.00	0.00	1.00
Element 2				
Axial Force (kN)	0.00	6.53	0.02	0.01
Elongation (mm)	0.00	0.16	0.00	0.00
Slip (mm)	0.00	0.00	0.00	0.00
Element 3				
Axial Force (kN)	-10.00	-3.47	-9.98	-9.99
Elongation (mm)	-0.25	-0.09	-0.25	-1.25
Slip (mm)	0.00	0.00	0.00	-1.00
Element 4				
Axial Force (kN)	14.14	4.91	14.12	14.13
Elongation (mm)	0.50	1.17	1.50	1.50
Slip (mm)	0.00	1.00	1.00	1.00
Element 5				
Axial Force (kN)	-14.14	-23.38	-14.17	-14.15
Elongation (mm)	-0.50	-0.83	-1.50	-1.50
Slip (mm)	0.00	0.00	-1.00	-1.00

Table 4.8: Output for several slippage configurations of double-diagonal truss

Element	Model I	Model II m=4	Model II m=10	Model II m=100
1	1.036	0.329	0.735	1
2	1.038	0.274	0.613	1
3	1.034	0.274	0.613	1
4	1.044	0.330	0.737	1
5	0	0.126	0.177	0.155
6	1.003	0.267	0.591	1
7	1.001	0.330	0.737	1
8	1.030	0.274	0.613	1
9	1.010	0.274	0.612	1
10	1.010	0.329	0.733	1
11	0	0.002	0.000	0.002
12	0	0.156	0.275	0.423
13	0	0.016	0.022	0.033
14	0	0.012	0.015	0.021
15	0	0.032	0.038	0.033
16	0	0.030	0.033	0.035
17	0	0.014	0.017	0.023
18	0	0.014	0.020	0.030
19	0	0.003	0.004	0.008
20	0	0.002	0.003	0.005
21	1.015	0.137	0.306	1
22	1.016	0.142	0.317	1
23	1.005	0.141	0.315	1
24	1.022	0.137	0.307	1
25	1.002	0.139	0.308	1
26	0	0.110	0.208	0.240
27	1.005	0.137	0.307	1
28	1.003	0.139	0.307	1
29	1.007	0.142	0.317	1
30	1.028	0.137	0.306	1
31	0	0.069	0.120	0.215
32	0	0.000	0.002	0.007
33	1.048	0.137	0.307	1
34	1.018	0.142	0.317	1
35	1.013	0.142	0.317	1
36	1.005	0.137	0.307	1
37	0	0.031	0.032	0.033
38	0	0.011	0.011	0.014
39	1.161	0.137	0.307	1
40	1.013	0.142	0.317	1

Table 4.9: Axial slippage for members of simple transmission tower (mm)

MB Hydro program, all truss elements			
NODE	X-DISP	Y-DISP	Z-DISP
1	0	531.876	-17.78
2	0	531.876	2.794
3	0	531.876	2.794
4	0	531.876	-17.78
5	0	532.13	-29.972
6	0	514.096	-17.526
7	0	514.096	2.794
8	0	514.096	2.794
9	0	514.096	-17.526
10	0	593.344	-17.78
11	0	592.074	2.794
12	7.62	3.302	-50.292
13	-7.366	2.286	35.56
14	7.366	2.286	35.56
15	-7.62	3.302	-50.292
16	1.27	485.902	-19.05
17	-0.254	485.394	4.572
18	0.254	485.394	4.572
19	-1.27	485.902	-19.05
20	-8.382	3.302	-50.8
21	8.128	2.286	36.322
22	-8.128	2.286	36.322
23	8.382	3.302	-50.8
24	1.27	457.708	-20.32
25	-0.254	458.47	5.842
26	0.254	458.47	5.842
27	-1.27	457.708	-20.32

TAP, all truss elements			
NODE	X-DISP	Y-DISP	Z-DISP
1	-0.042	536.48	-16.919
2	-0.002	536.4	3.930
3	0.002	536.4	3.930
4	0.042	536.48	-16.919
5	-0.000	536.75	-29.423
6	0.029	518.28	-16.851
7	0.009	518.33	3.867
8	-0.009	518.33	3.867
9	-0.029	518.28	-16.851
10	-0.000	598.36	-16.944
11	-0.000	596.78	3.929
12	7.806	-0.015	-50.005
13	-7.472	-0.008	37.146
14	7.472	-0.008	37.146
15	-7.806	-0.015	-50.005
16	-0.001	489.75	-18.255
17	0.001	489.23	5.511
18	-0.001	489.23	5.511
19	0.001	489.75	-18.255
20	-8.477	-0.000	-50.569
21	8.298	-0.000	37.842
22	-8.298	-0.000	37.842
23	8.477	-0.000	-50.569
24	-0.000	461.4	-19.574
25	-0.000	461.98	6.881
26	-0.000	461.98	6.881
27	0.000	461.4	-19.574

TAP, truss cross-bracing and beam main legs			
NODE	X-DISP	Y-DISP	Z-DISP
1	-0.040	531.29	-17.573
2	-0.003	531.21	3.079
3	0.003	531.21	3.079
4	0.040	531.29	-17.573
5	-0.000	531.56	-29.972
6	0.030	513.25	-17.511
7	0.007	513.3	3.022
8	-0.007	513.3	3.022
9	-0.030	513.25	-17.511
10	-0.000	513.19	-17.581
11	-0.000	513.28	3.067
12	0.377	499.02	-18.196
13	-0.226	498.74	3.833
14	0.226	498.74	3.833
15	-0.377	499.02	-18.196
16	0.398	484.94	-18.879
17	-0.268	484.5	4.629
18	0.268	484.5	4.629
19	-0.398	484.94	-18.879
20	0.252	470.75	-19.538
21	-0.181	470.88	5.324
22	0.181	470.88	5.324
23	-0.252	470.75	-19.538
24	0.271	456.96	-20.166
25	-0.199	457.39	6.008
26	0.199	457.39	6.008
27	-0.271	456.96	-20.166

TAP, all beam elements			
NODE	X-DISP	Y-DISP	Z-DISP
1	-0.039	531.1	-17.563
2	-0.003	531.02	3.076
3	0.003	531.02	3.076
4	0.039	531.1	-17.563
5	-0.000	531.37	-29.949
6	0.030	513.08	-17.502
7	0.007	513.12	3.020
8	-0.007	513.12	3.020
9	-0.030	513.08	-17.502
10	-0.000	513.07	-17.567
11	-0.000	513.12	3.062
12	0.370	498.8	-18.192
13	-0.220	498.59	3.829
14	0.220	498.59	3.829
15	-0.370	498.8	-18.192
16	0.369	484.77	-18.874
17	-0.255	484.34	4.627
18	0.255	484.34	4.627
19	-0.369	484.77	-18.874
20	0.255	470.64	-19.528
21	-0.183	470.68	5.325
22	0.183	470.68	5.325
23	-0.255	470.64	-19.528
24	0.288	456.82	-20.156
25	-0.215	457.23	6.006
26	0.215	457.23	6.006
27	-0.288	456.82	-20.156

Table 4.10: Comparison of deflections of full-scale transmission tower using Manitoba Hydro's program and TAP with different element configurations

Member Type	Slippage Load P_s (kN)	Maximum Slippage Δ_s (mm)
Single angle main leg members spliced together	43.28	3.5 (per continuous angle)
Single angle members with one-bolt connections	9.29	1.7 (per member)
Single angle members with two-bolt connections	20.14	1.7 (per member)
Single angle members with three-bolt connections	29.28	1.7 (per member)
Single angle members with four-bolt connections	46.95	1.7 (per member)

Table 4.11: Slippage parameters used in full-scale transmission tower based on load-slip experiments (Ungkurapinan, 2000)

Element Number	Axial Stress (MPa)	
	No Slip	Slippage Model II
Top Section Critical Members		
21	-115.04	-114.78
34	83.37	83.45
47	83.37	83.45
60	-115.04	-114.78
Mid Section Critical Members		
81	-188.8	-188.17
90	129.91	129.76
99	129.91	129.76
108	-188.8	-188.17
Bottom Section Critical Members		
153	-191.7	-189.16
159	138.33	136.97
165	138.33	136.97
171	-191.7	-189.16

Table 4.12: Axial stress in critical members of full-scale transmission tower with and without bolt slippage

Element Number	Axial Stress (MPa)	
	No Slip	Slippage Model II
Main Leg Beam Members		
181	-252.74	-156.65
182	205.99	106.96
183	-265.72	-170.08
184	218.12	119.49
Truss Members off Main Legs		
419	-222.36	-179.24
420	206.65	167.30
421	-215.80	-172.63
422	199.86	160.56
423	-218.06	-175.86
424	200.55	161.23
425	-219.61	-176.46
426	206.47	166.20
Horizontal Truss Bracing		
455	326.14	270.78
456	-326.28	-270.93
457	-326.29	-270.93
458	326.14	270.77

Table 4.13: Axial stress in critical members of full-scale transmission tower with a 100-mm foundation heave with and without bolt slippage

AE = 10000-kN F = 10-kN

Δ_s = 1-mm P_s = 2-kN $m = 4$ $n = 6$

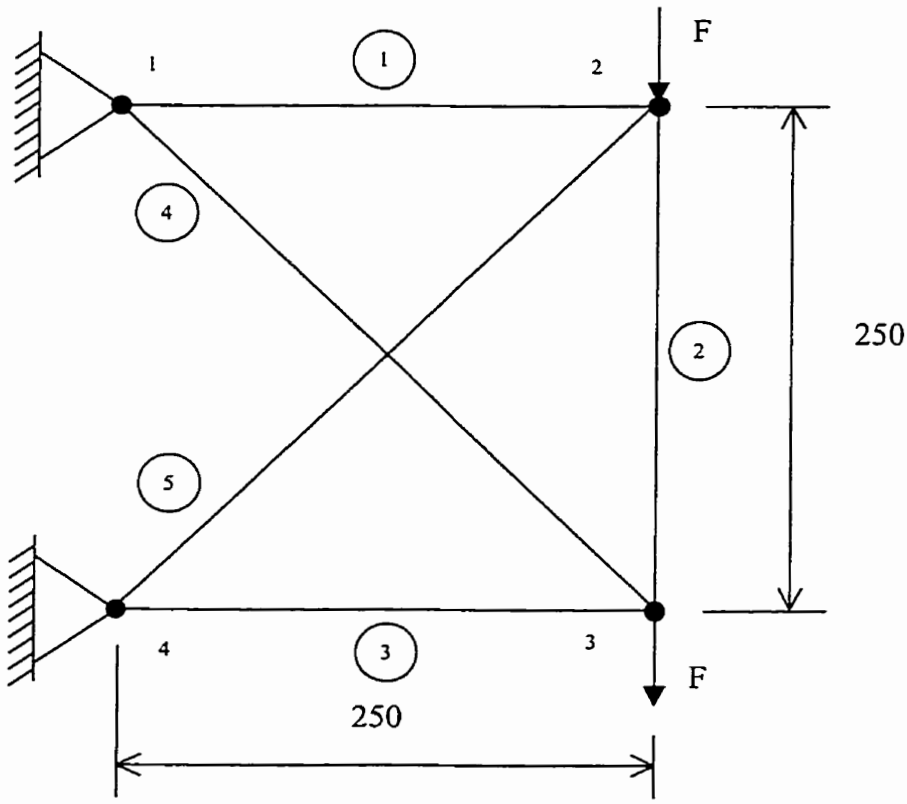

Figure 4.1: Double-Diagonal plane truss

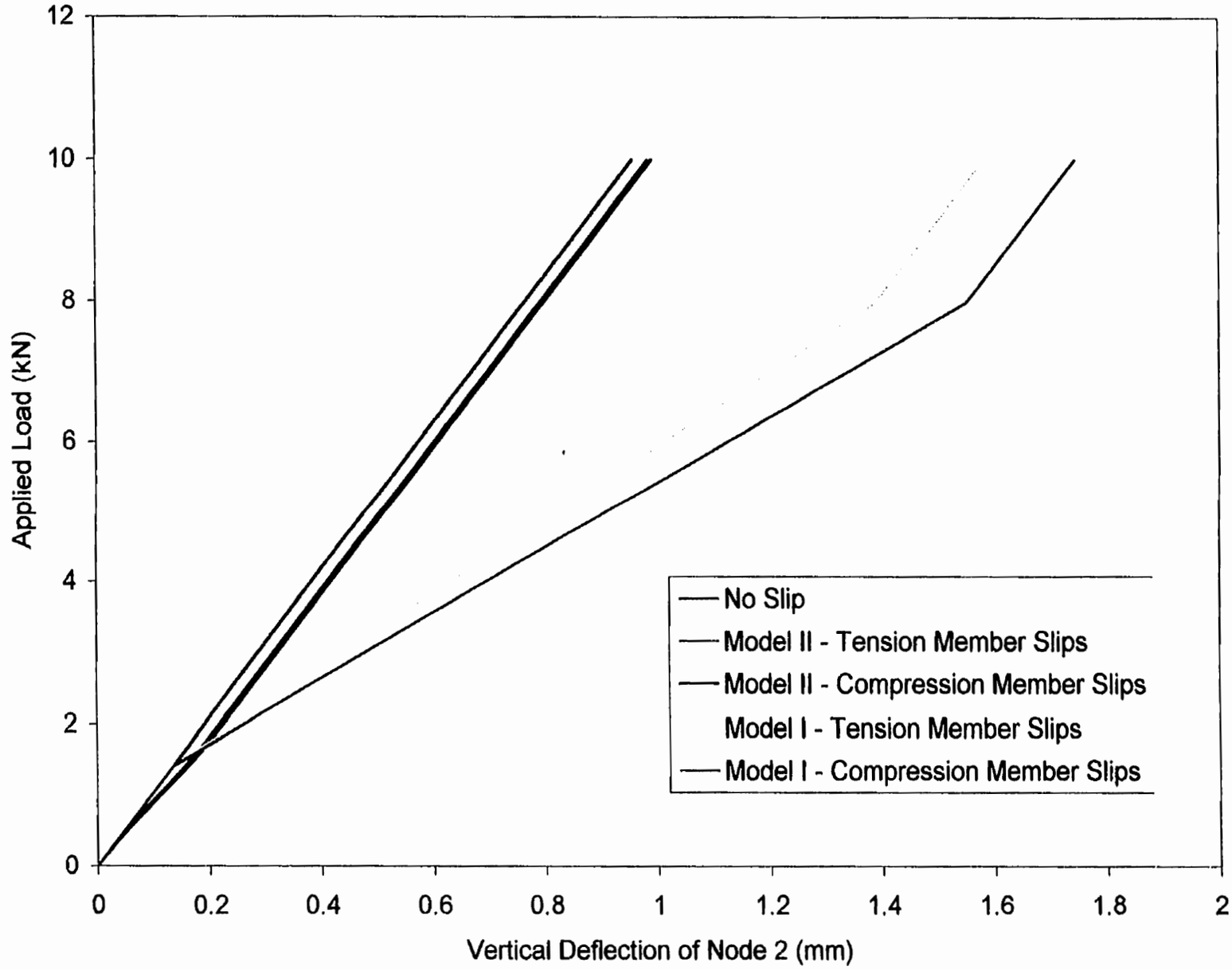

Figure 4.2: Double-Diagonal truss deflection

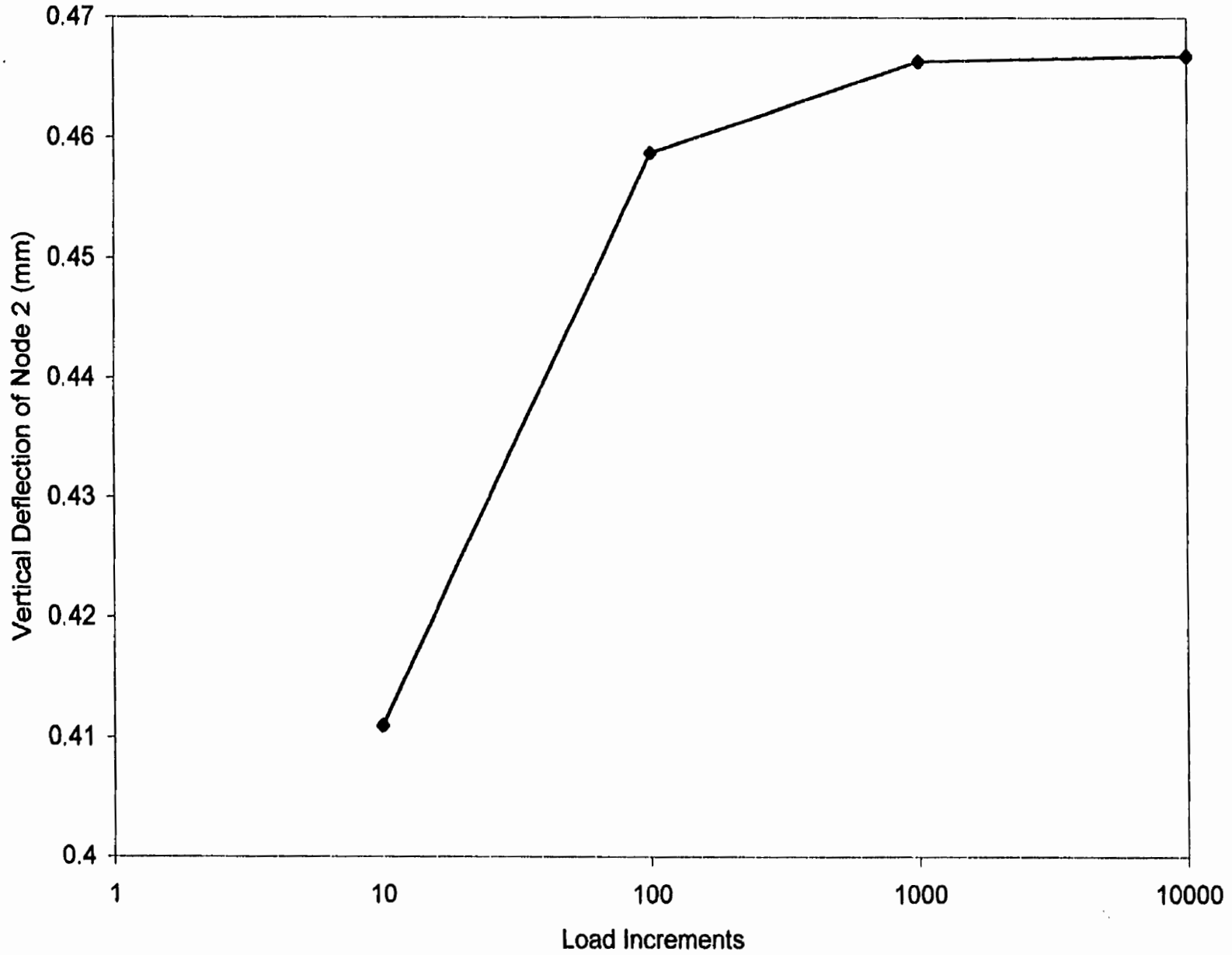

Figure 4.3: Convergence of double-diagonal truss (model I)

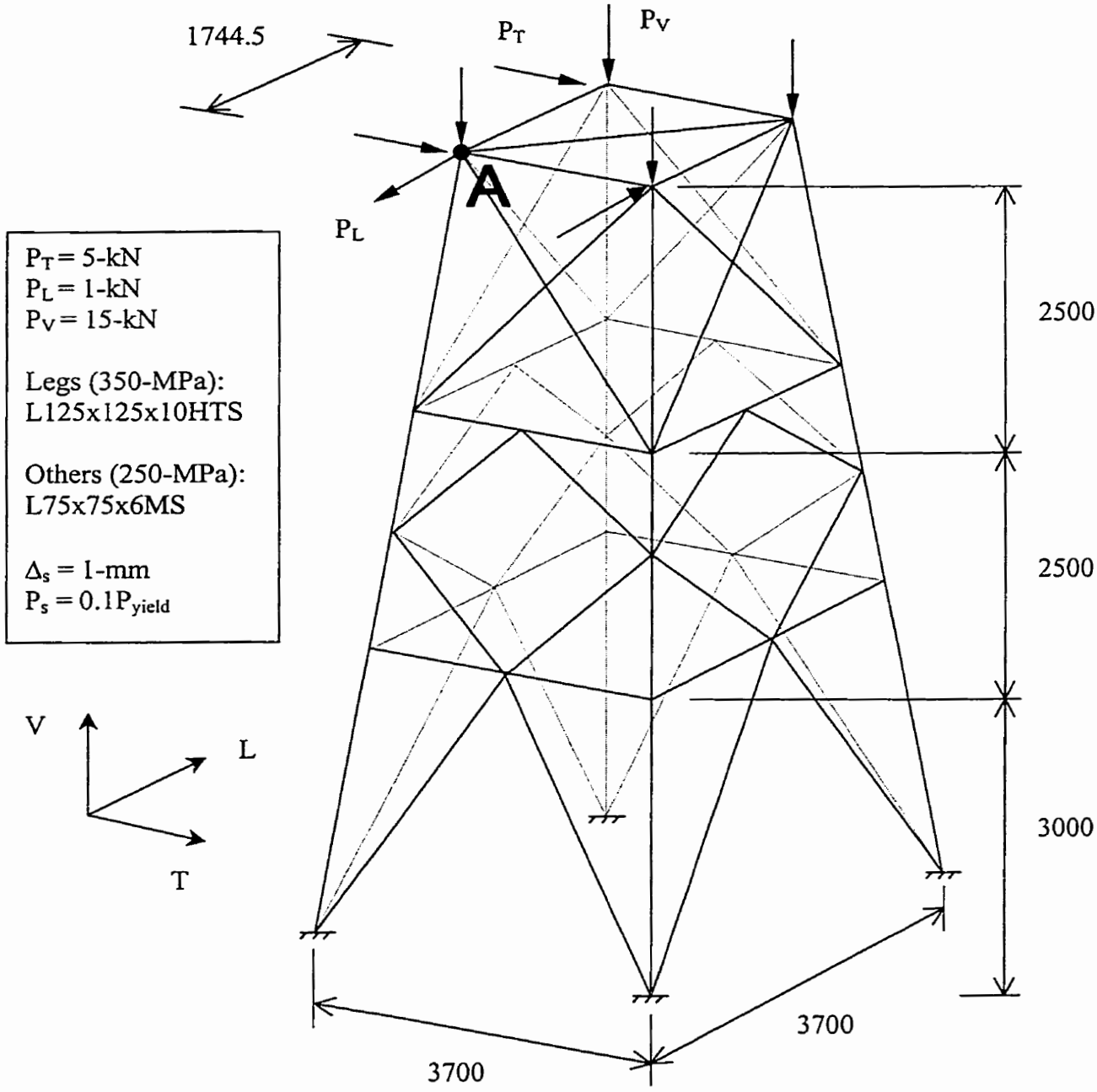

Figure 4.4: Simple transmission tower subassembly

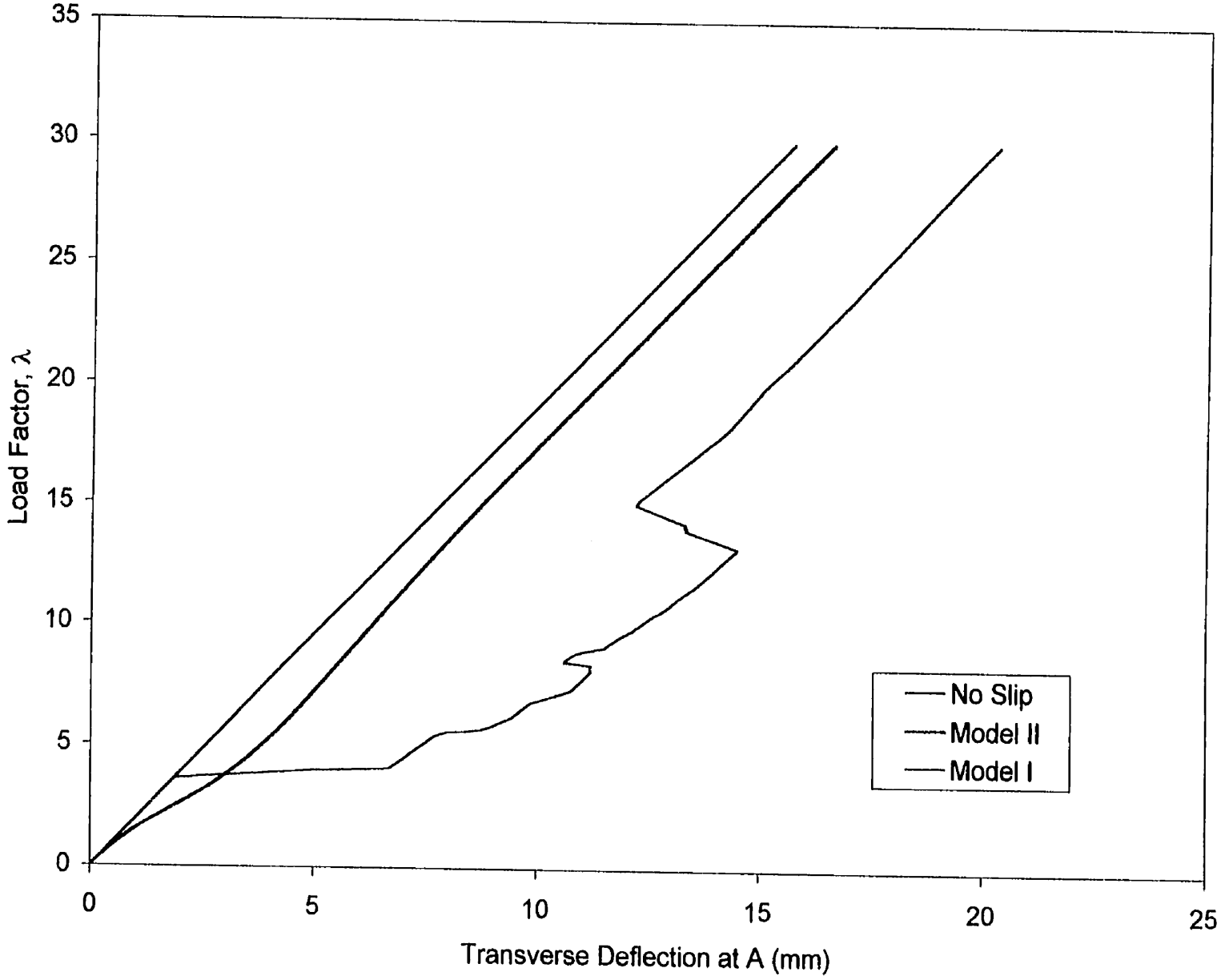

Figure 4.5: Transverse deflection of simple transmission tower for all models

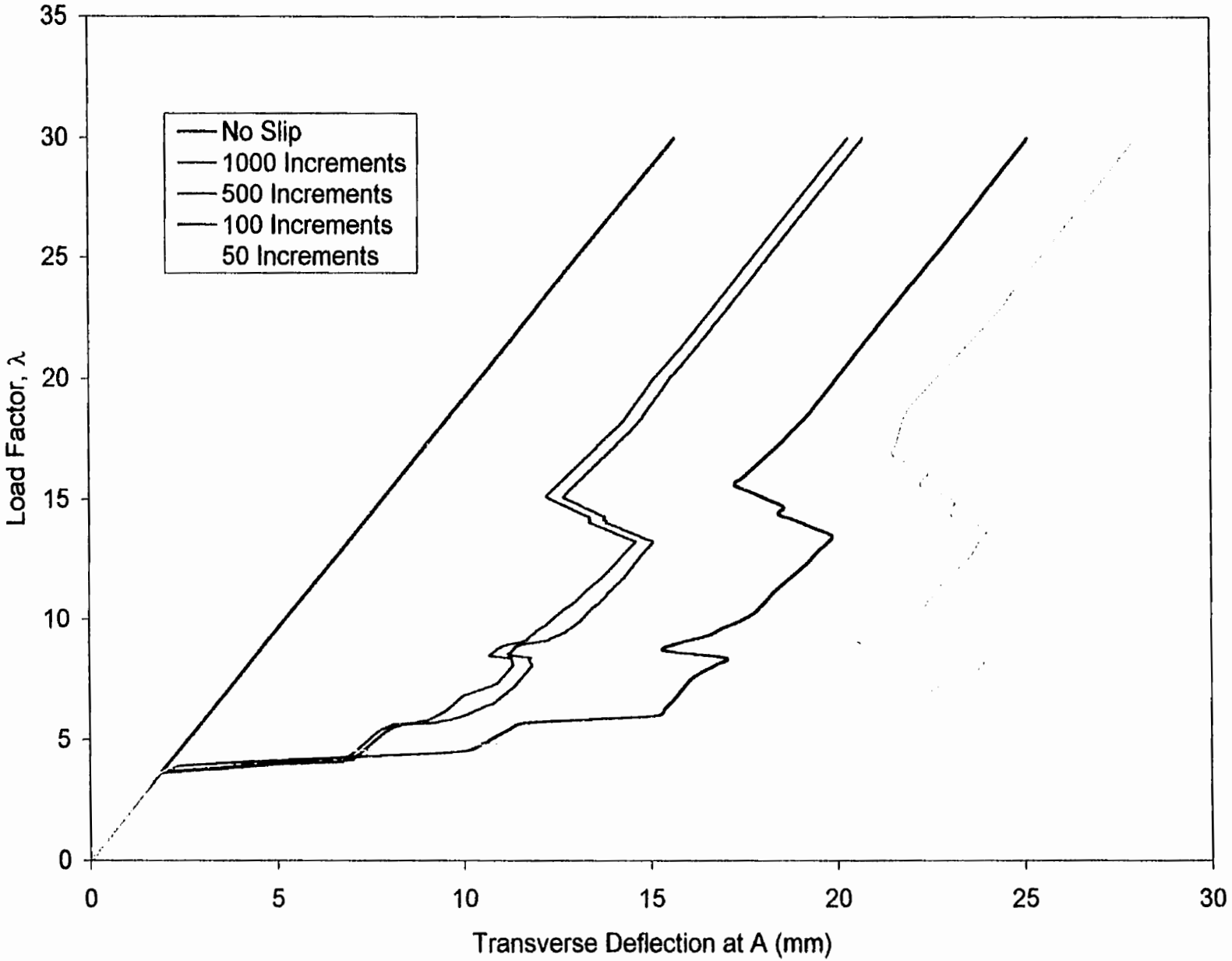

Figure 4.6: Transverse deflection of simple transmission tower for different load increments (model I)

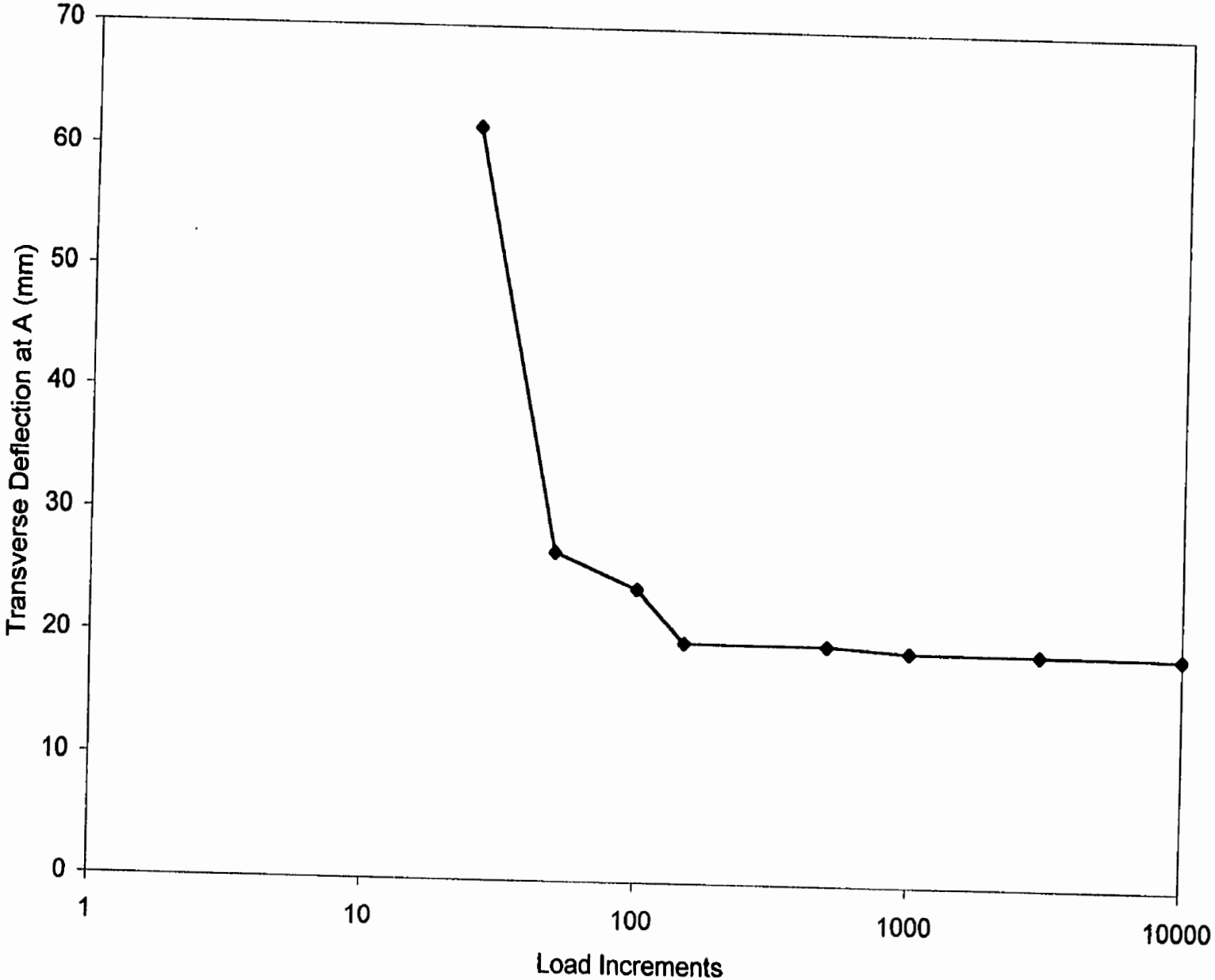

Figure 4.7: Convergence of simple transmission tower (model I)

AE/L = 100-kN/mm F = 100-kN

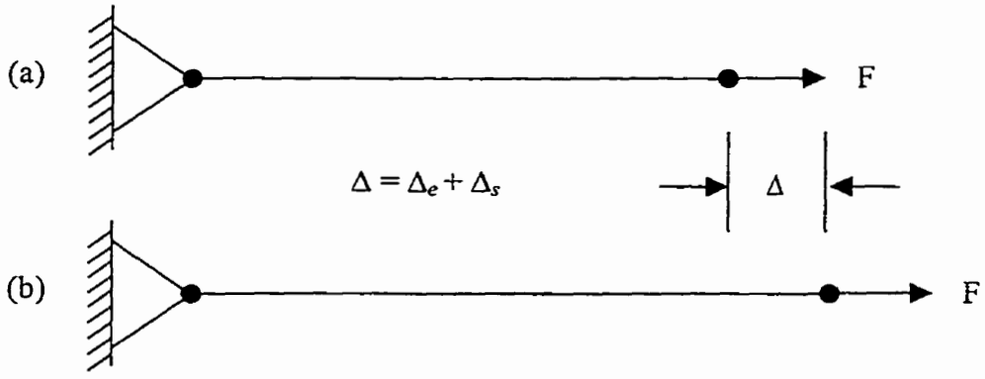

Figure 4.8: 1-D bar element (a) before loading (b) after loading

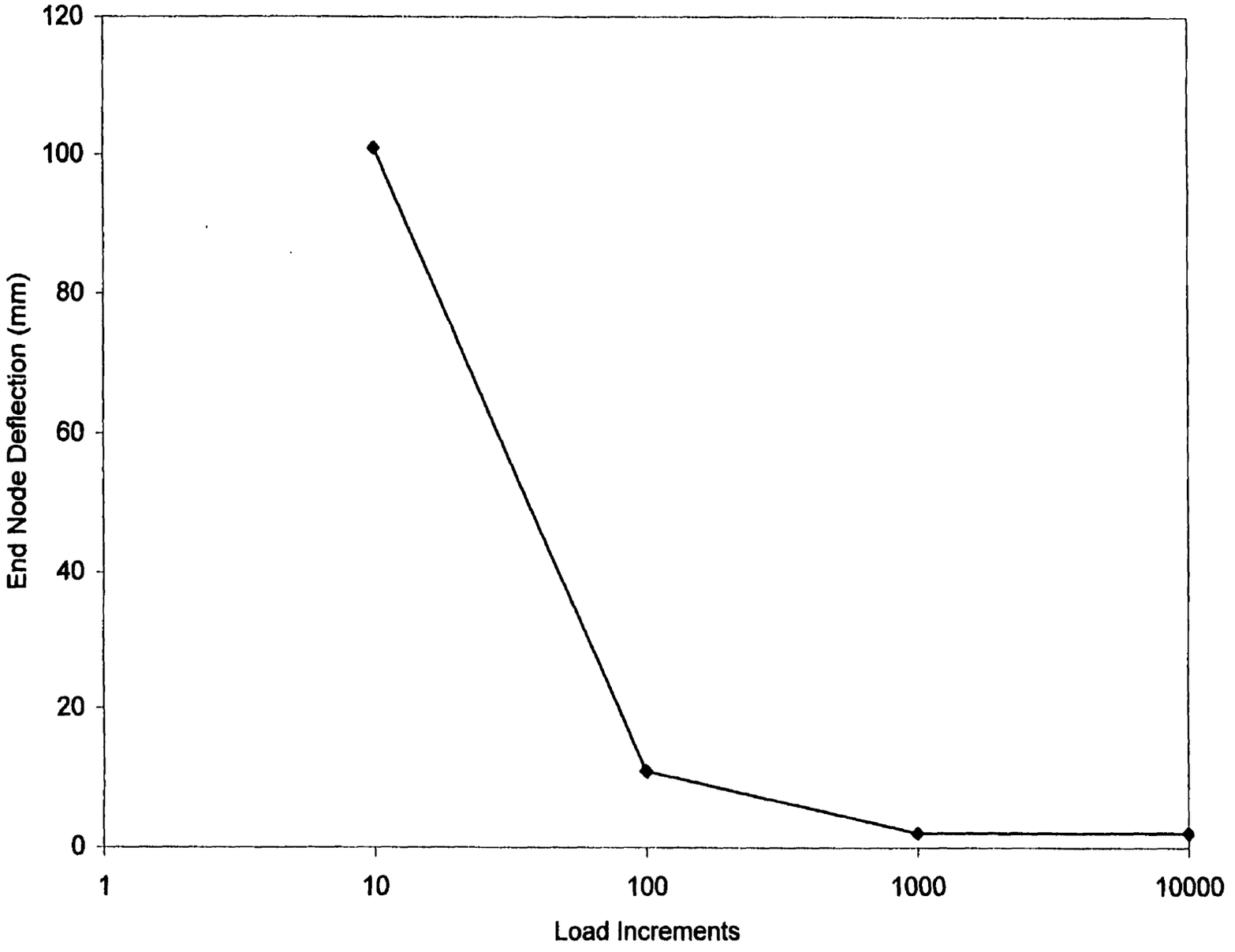

Figure:4.9 Convergence of simple bar element (model I)

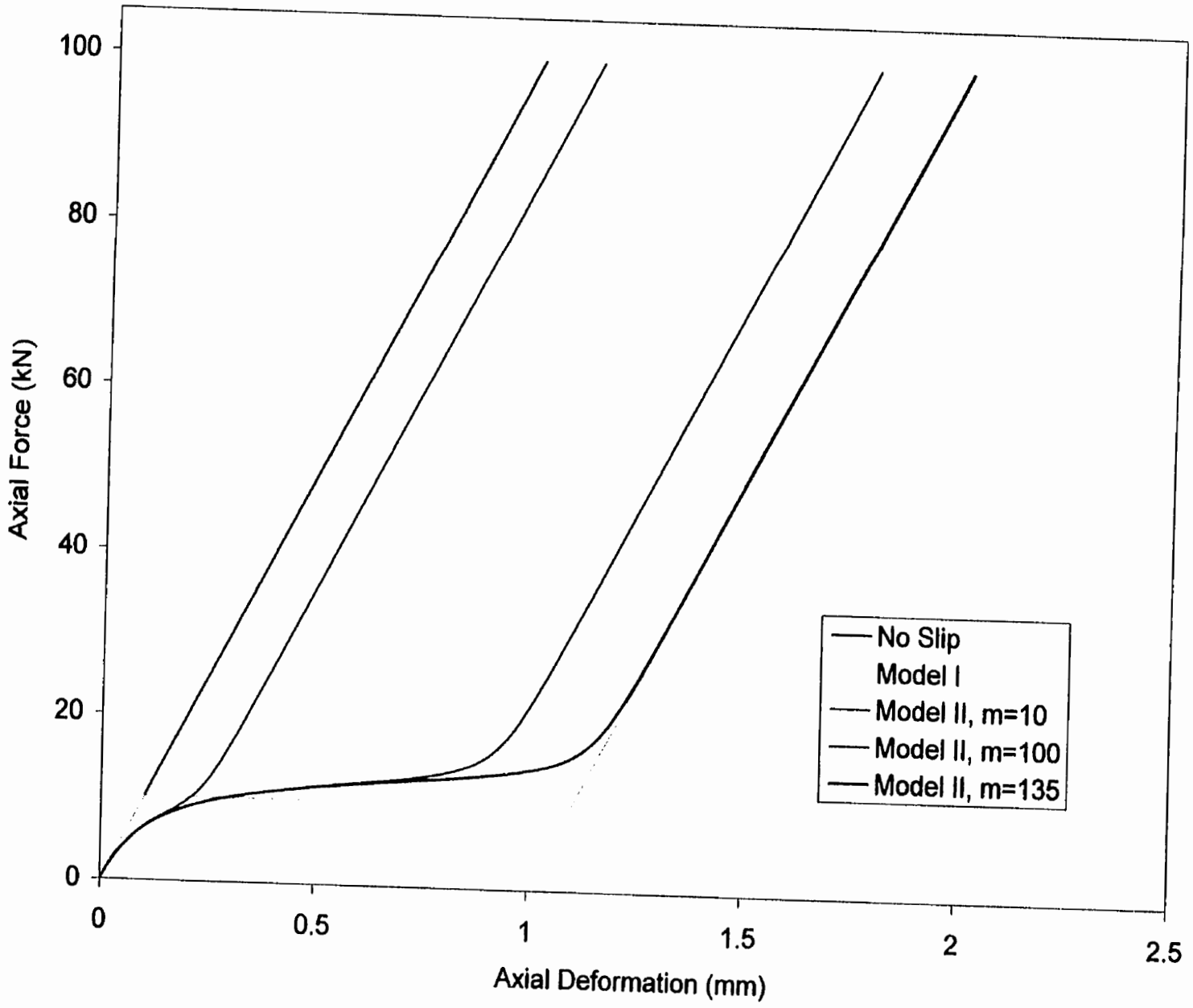

Figure 4.10: Axial force-deformation relationship for simple bar element (Ps=10-kN)

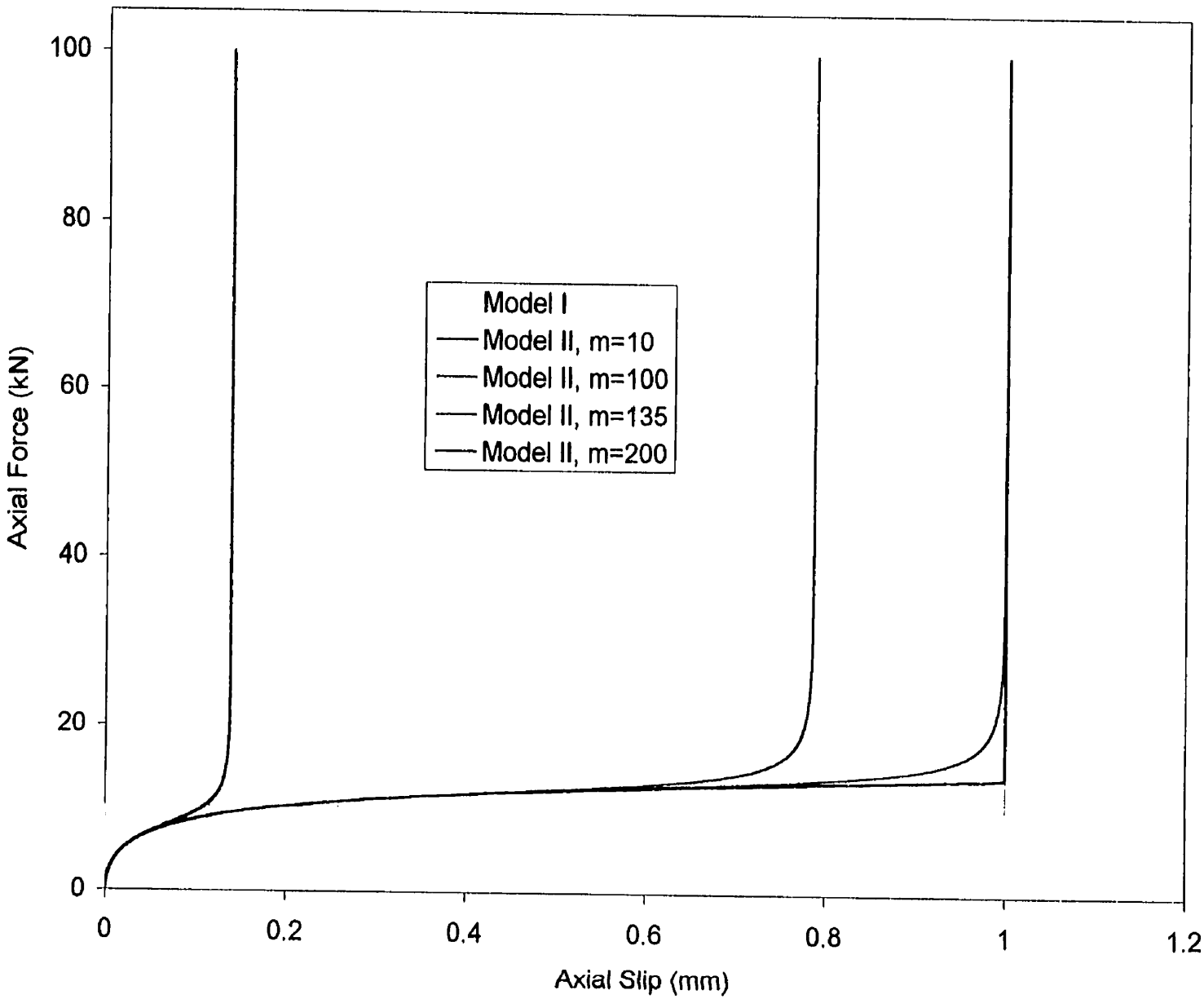

Figure 4.11: Axial force-slip relationship for simple bar element

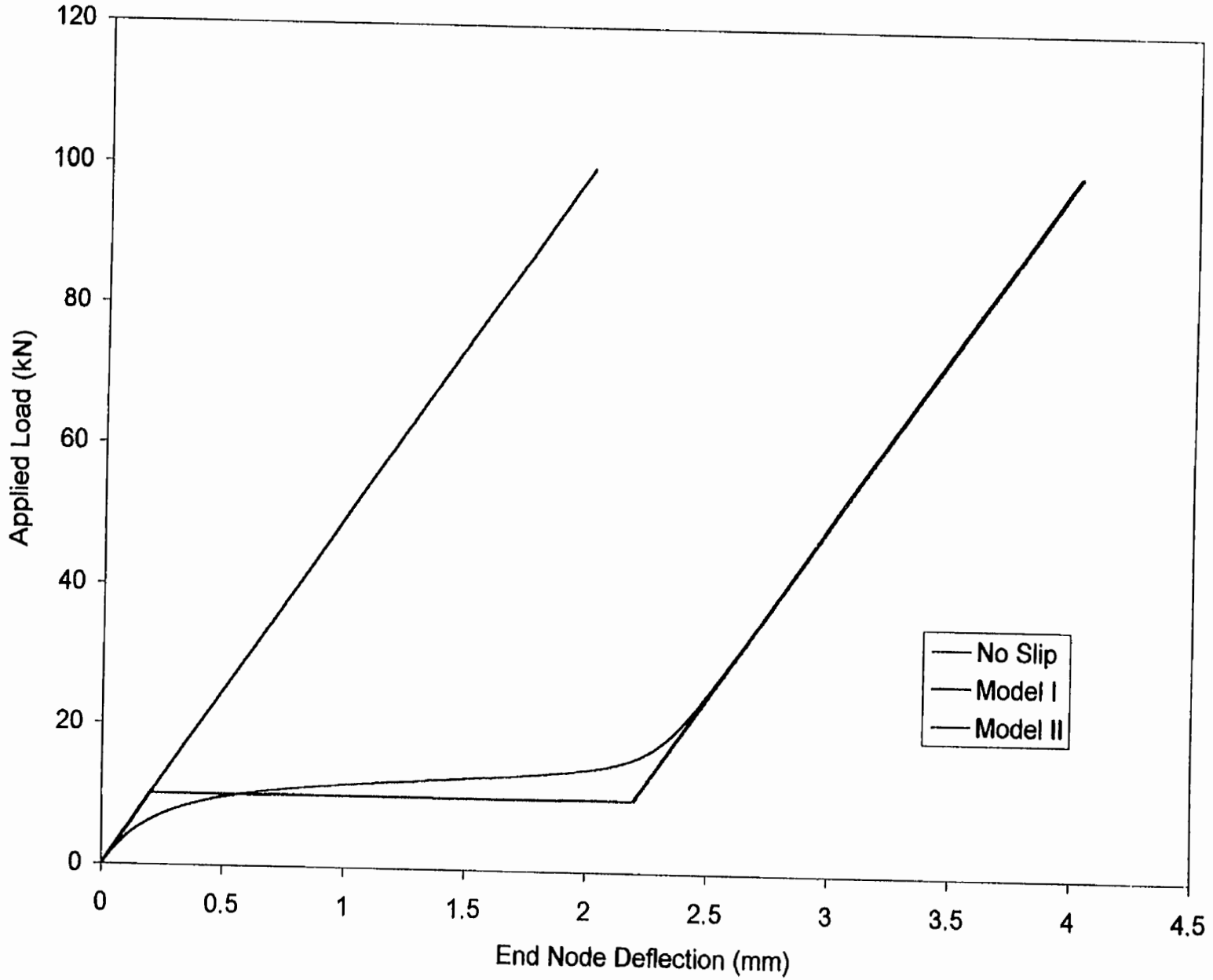

Figure 4.12: End node deflection for two member assembly

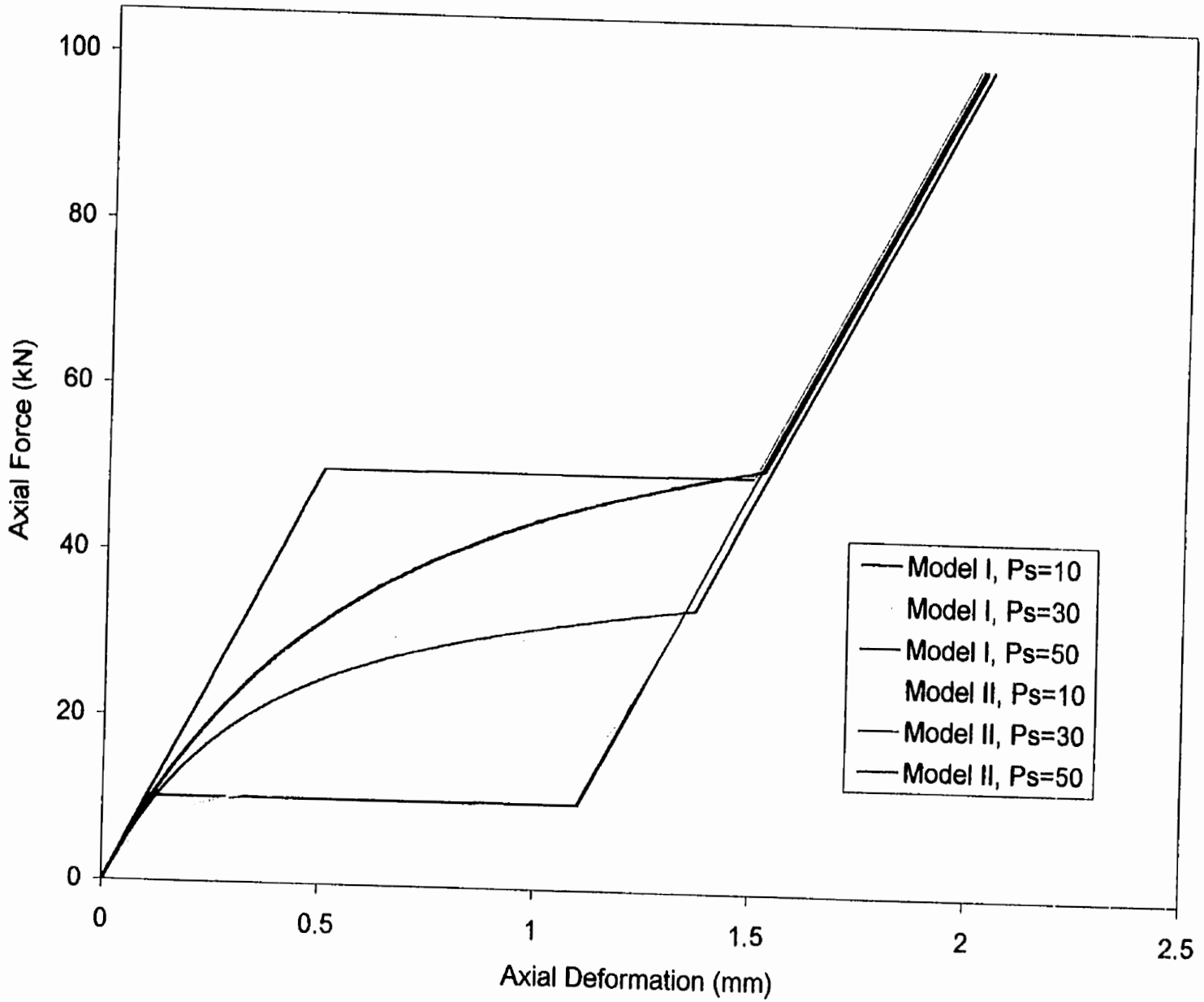

Figure 4.13: Axial force-deformation relationship for simple bar element (m=135)

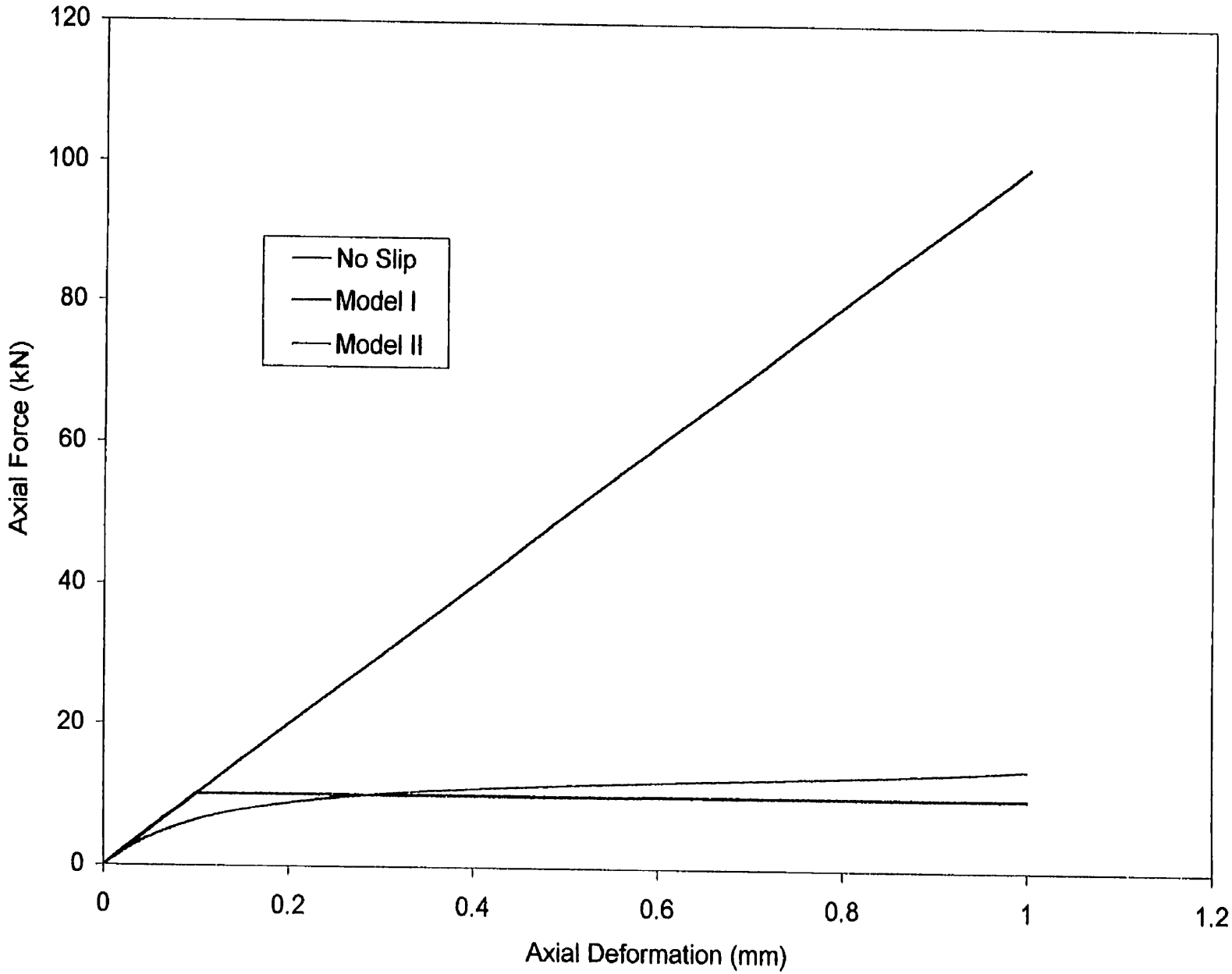

Figure 4.14: Simple bar element with a 1-mm specified displacement (Ps = 10-kN)

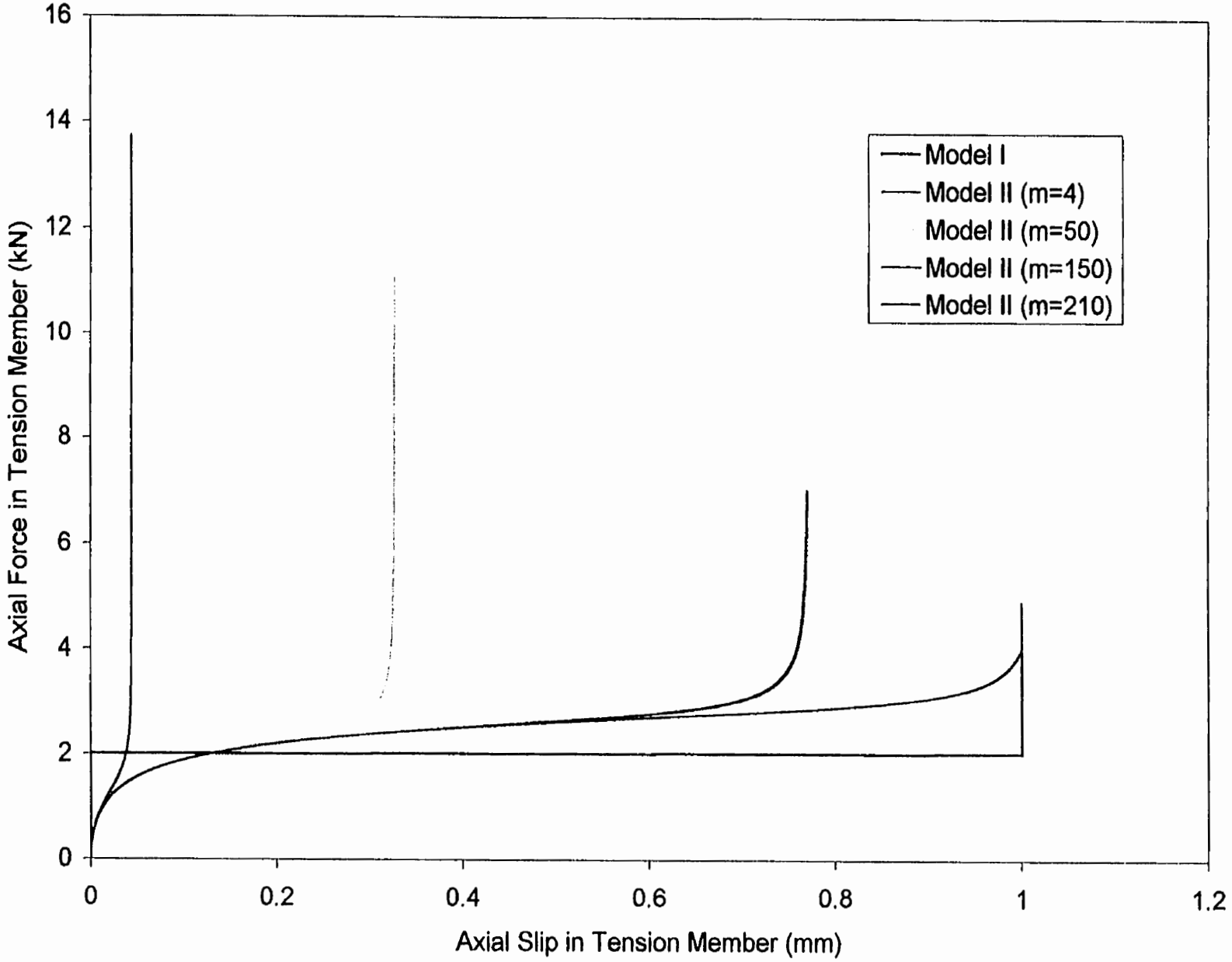

Figure 4.15: Axial force-slip relationship for tension member of double-diagonal truss

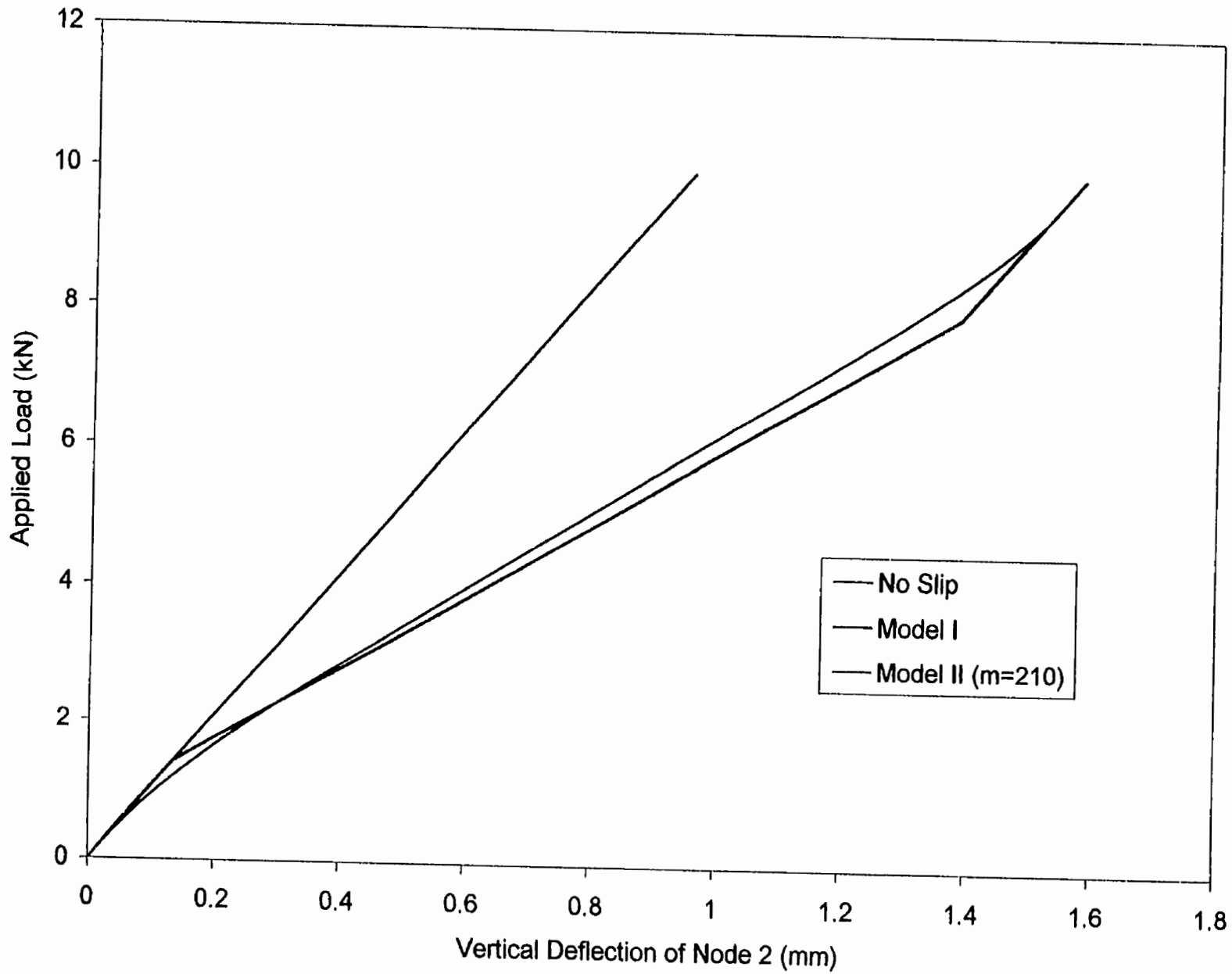

Figure 4.16: Double-Diagonal truss deflection (m=210)

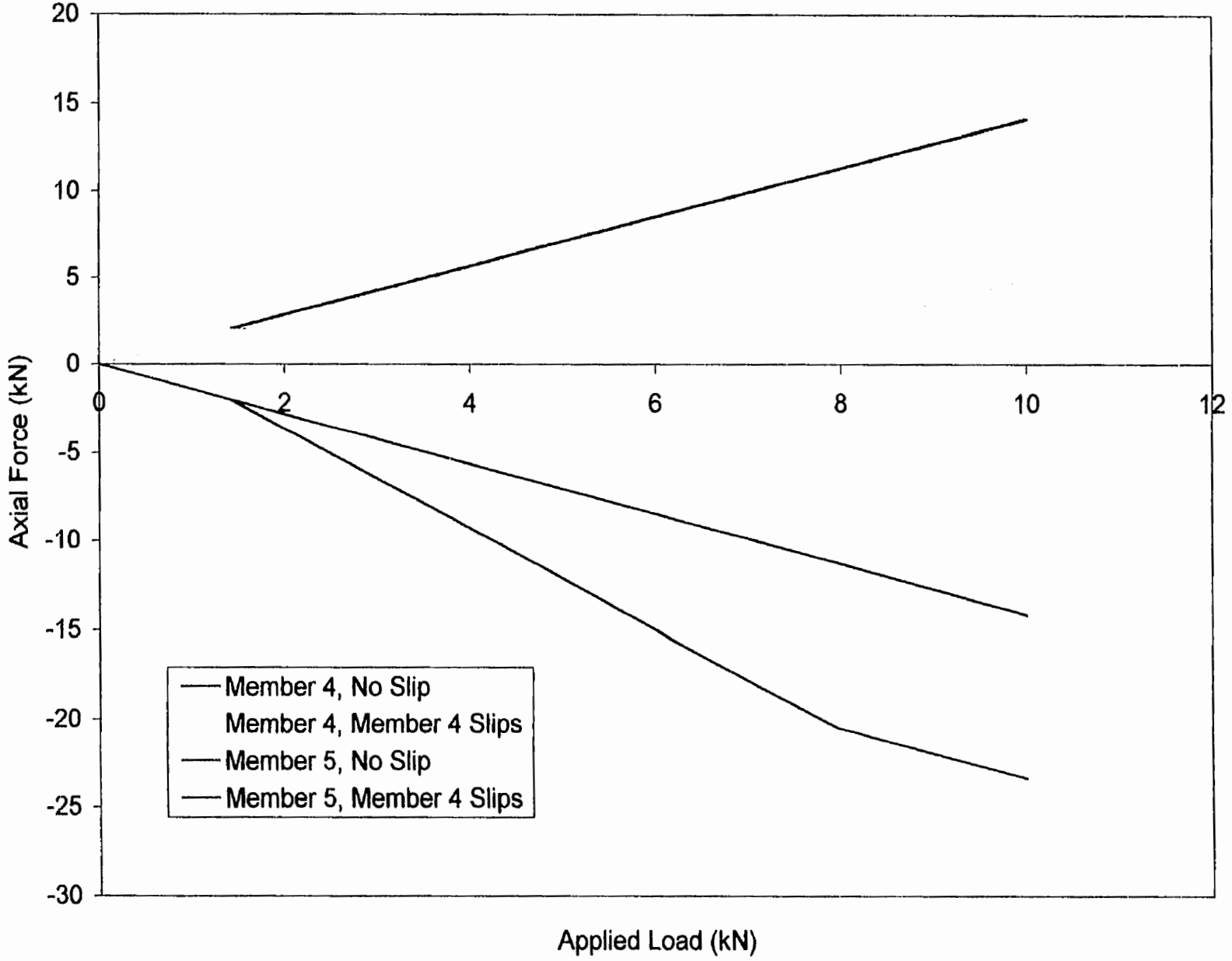

Figure 4.17: Load-Distribution effect for double-diagonal truss (model I)

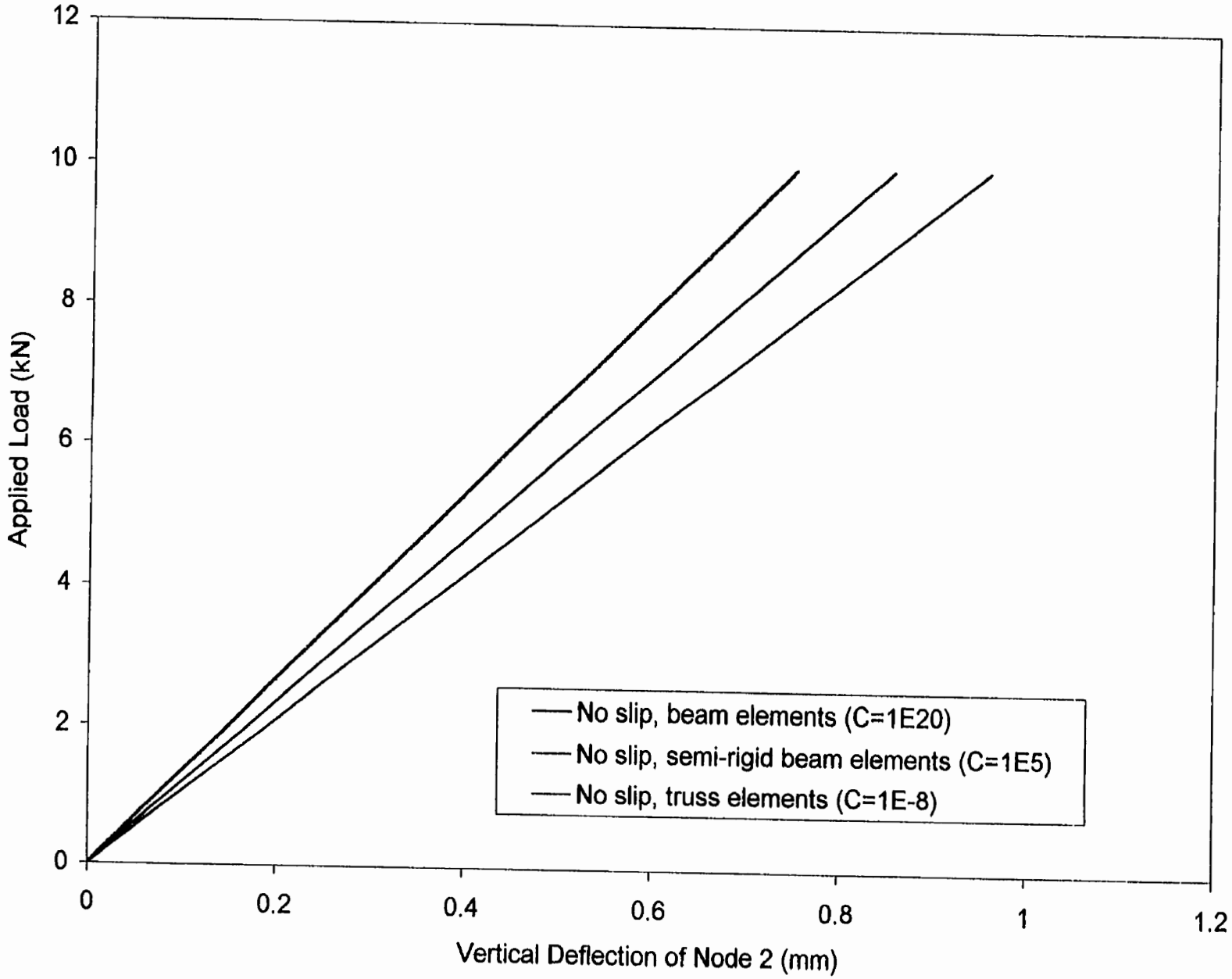

Figure 4.18: Double-Diagonal frame deflection considering joint flexibility

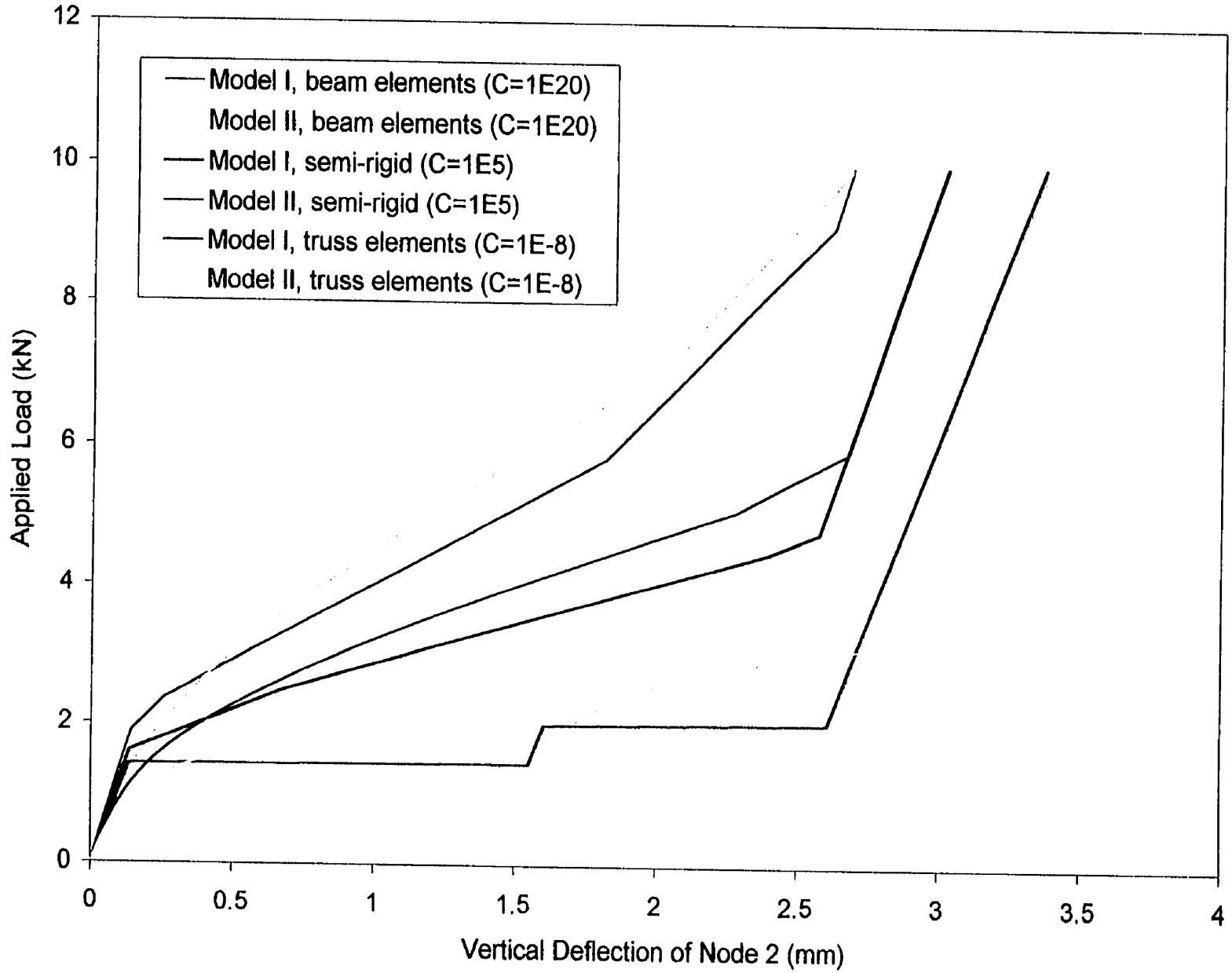

Figure 4.19: Double-Diagonal frame deflection with joint slip and joint flexibility (m=500)

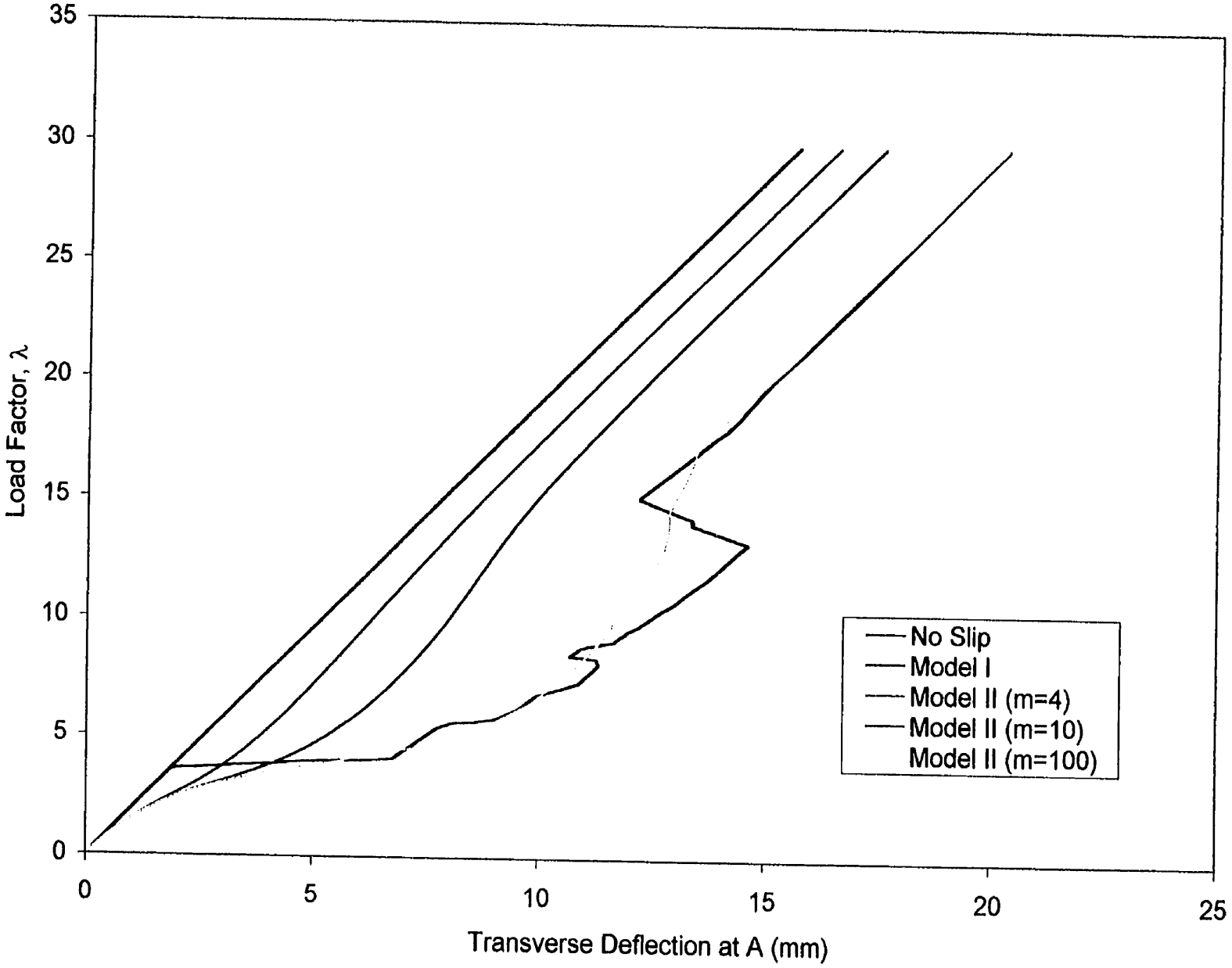

Figure 4.20: Transverse deflection of simple transmission tower for various *m* values

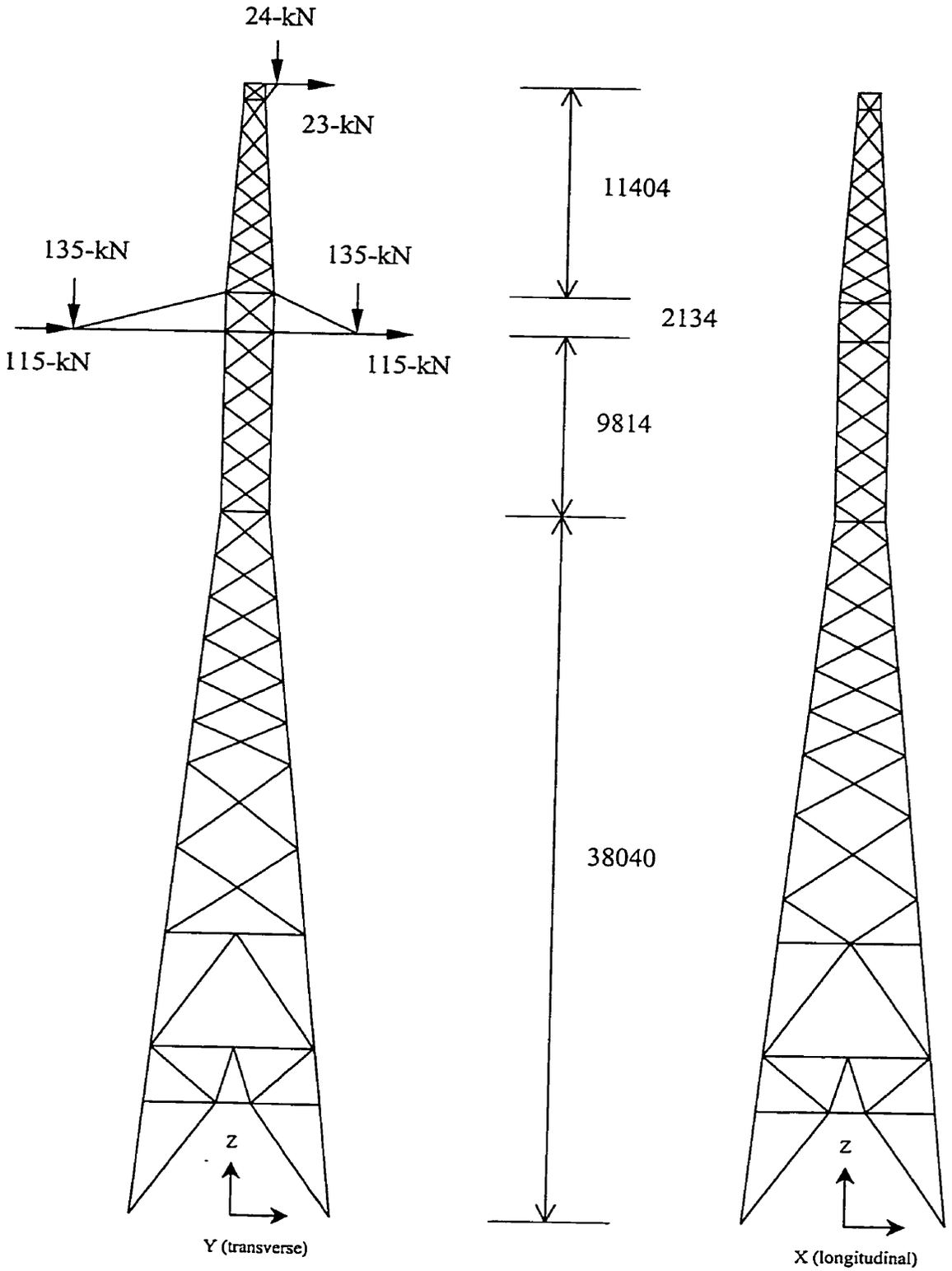

Figure 4.21: Full-Scale transmission tower

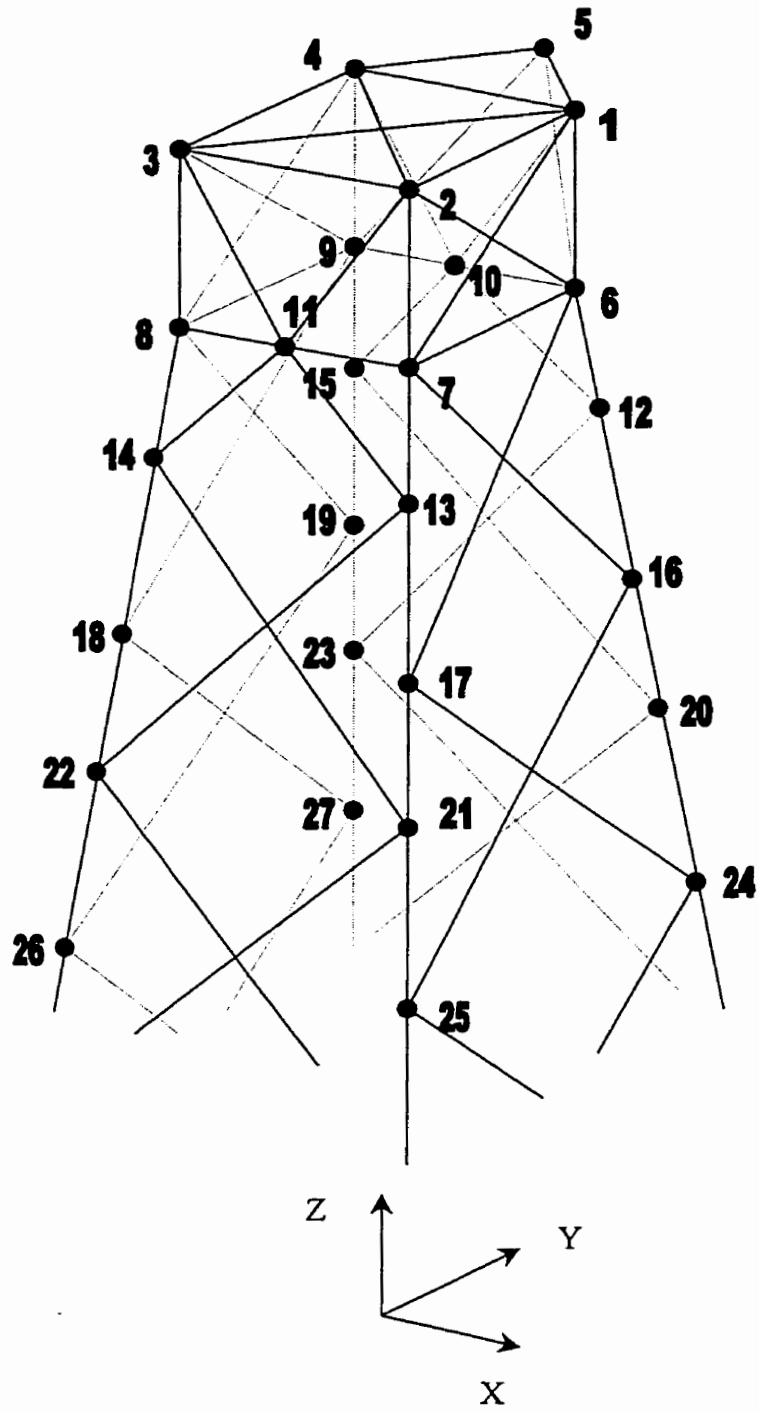

Figure 4.22: Upper section of full-scale transmission tower

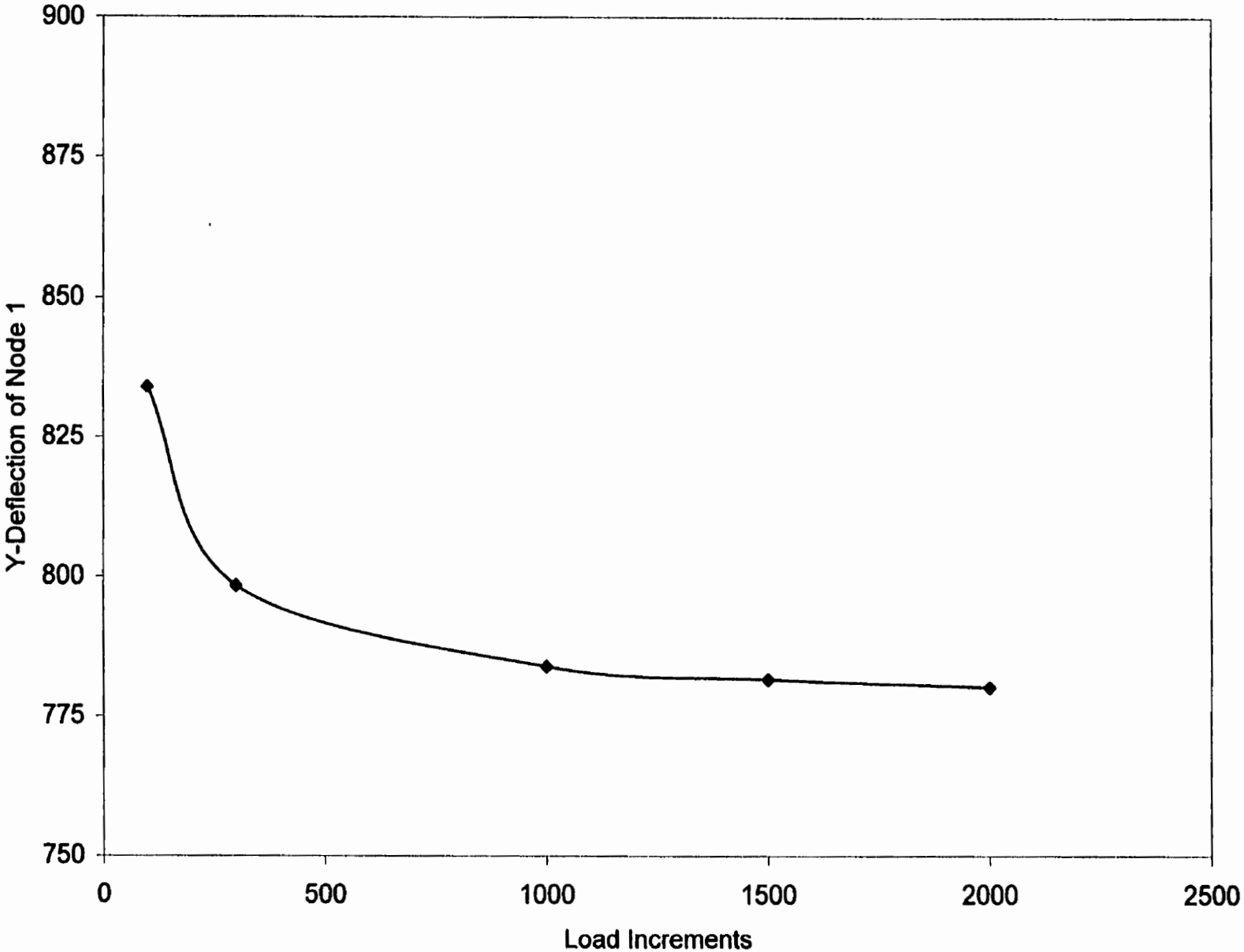

Figure 4.23: Transverse deflection of node 1 of full-scale transmission tower for different load increments

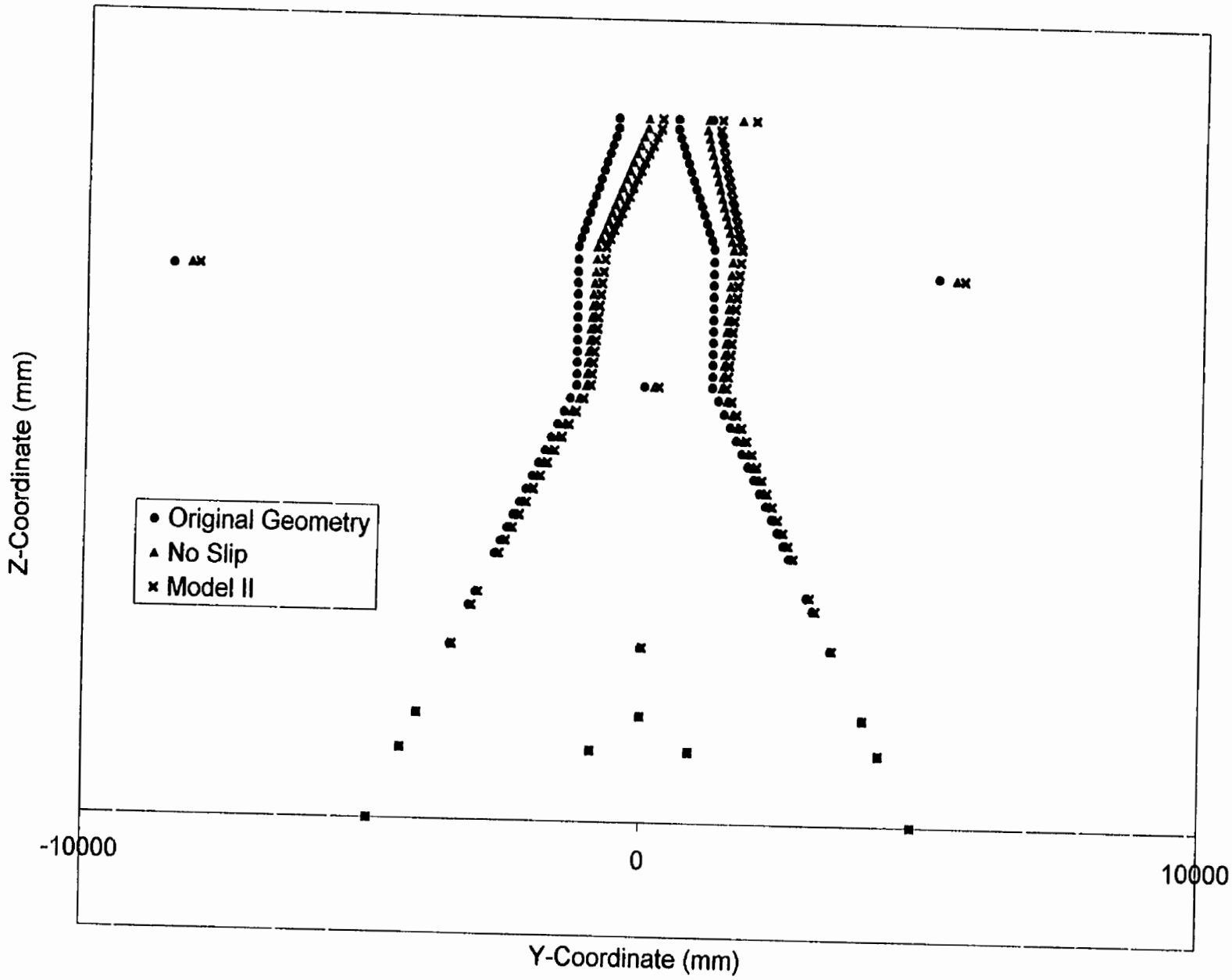

Figure 4.24: Transverse deflected shape of full-scale transmission tower

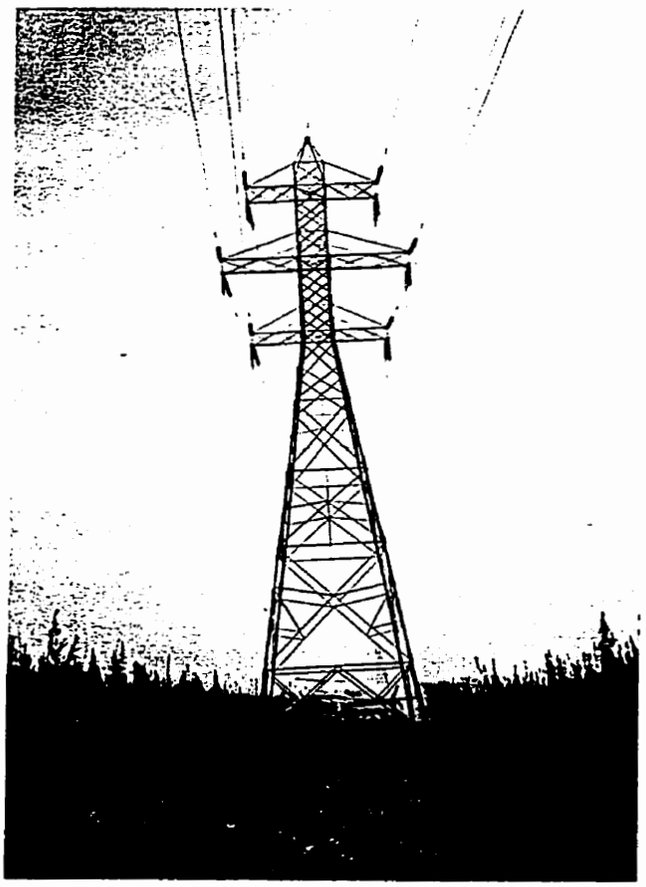

Figure 4.25: Transmission tower subjected to large foundation movement

Chapter 5

SUMMARY AND CONCLUSIONS

5.1 Summary

This study investigated the effect of bolt slippage on the deflections and axial stresses of latticed self-supporting transmission towers. A structural analysis program was developed which could model structural members as truss elements or beam elements, could incorporate bolt slippage using an instantaneous slippage model or a continuous slippage model, and could include the effects of semi-rigid connections provided moment-rotation data were available. The instantaneous slippage model assumes that all of the bolt slip occurs at a certain load level. The ends of a member slip a specified amount when the axial force exceeds the slippage load. The slipping member's stiffness is greatly reduced causing increased joint deflection while the internal force remains relatively constant. The continuous slippage model assumes that bolt slippage occurs once the first load increment is applied and follows a non-linear function throughout the loading process. This function is used to reduce the member stiffness to account for slippage deformation. For both slippage models, the total axial deformation of a member is comprised of elastic deformation and slippage deformation.

The linear no-slip capabilities of the developed program were verified by comparing the output with other structural analysis programs. The only comparison available for verifying the bolt slippage models was the AK TOWER program. Although the analysis techniques were different, the TAP program and the AK TOWER program both predicted significant increases in nodal deflections as a result of bolt slippage. Also, the instantaneous and continuous slippage models predicted identical deflections and stresses when the members in a structure slip the same amount for both models – establishing the validity of the TAP program. The m parameter for the continuous slippage model can be increased until all of the members in a structure slip the specified amount (the experimentally determined clearance if available).

The developed program investigated the slippage behavior of several latticed structures, including a simple one-dimensional bar, a double-diagonal plane truss, a

double-diagonal plane frame with semi-rigid connections, a simplified three-dimensional transmission tower, and a full-scale transmission tower. The full-scale tower used experimentally obtained slippage parameters to accurately model the bolted connections. The most important parameters for a slipping member are the exact amount of clearance slip allowed at a bolted connection and the load that initiates bolt slippage. Both of these parameters can be determined experimentally.

5.2 Conclusions

The results of this study confirm the suspicions of earlier researchers and practicing engineers: bolt slippage has a considerable effect on the behavior of latticed structures. The investigation of slippage behavior has shown that a structure using any bolt slippage model (instantaneous or continuous) will result in larger displacements compared to the same structure without accounting for slippage. Furthermore, as the number of slipping elements increase in a structure, or, as the specified slippage amount for each member increases, slippage deformation accumulates and the nodal displacements become even larger. Self-supporting latticed transmission towers are usually sufficiently rigid to assume small-displacement theory, but since bolt slippage greatly increases nodal displacements, significant secondary stresses may be induced. Latticed towers used to transmit and receive high frequency signals for wireless communication are also at risk. Excessive deflections caused by connection slip can interfere with communications creating a serviceability failure. Increased flexibility, due to the decrease in member stiffness, could also influence a structure's vibration and fatigue characteristics.

The axial stresses in latticed structures are also affected by bolt slippage. The two-dimensional plane truss example illustrated the load-distribution effect caused by bolt slippage. In structures that only experience slippage in certain members, higher stresses are observed in non-slipping members and lower stresses are observed in slipping members, compared to an identical structure without accounting for slippage. In the full-scale transmission tower using realistic slippage parameters, the axial stresses were not significantly affected by bolt slippage. However, the ability of a slipping member to

absorb a specified displacement had a dramatic effect on the axial stresses in the full-scale transmission tower. Bolt slippage increased the structure's ability to withstand differential settlement or heave, by translating the specified displacement into slippage deformation in the tower members. Allowing the members connected to the specified displacement node to slip, greatly reduced their stresses. In the full-scale tower, the axial stress was reduced by as much as 90% in one of the main legs when experimentally determined slippage parameters were used. Bolt slippage, therefore, could explain why the large stresses caused by foundation movements, predicted by software not including slippage effects, do not occur in reality – slippage is reducing the member stresses to realistic, elastic, pre-buckling values.

The parametric studies on the various latticed structures revealed that varying the slippage load effects the axial force-deformation relationship, but the end result is unchanged. As long as a member exceeds its slippage load, no matter what the value, the deflections at the final load will be identical. Members that do not exceed their slippage load cause differences between an instantaneous slippage analysis and a continuous slippage analysis since slippage can occur in the continuous model at loads below the slippage load, but not in the instantaneous model.

Finally, the slippage analysis of the full-scale transmission tower revealed that the three-dimensional truss model, normally used to analyze transmission towers, should be replaced by a truss/beam model. Modeling the main legs as beam elements eliminates the need for dummy members to prevent structural mechanisms, eliminates displacement errors at planar nodes when using a truss model with artificial restraints, and is a more accurate model since the main leg members resist bending stresses and are continuous through bracing members. When incorporating bolt slippage, both models predict identical solutions when all members slip the same amount. The continuous slippage model is preferable since it does not exceed the specified slip amount (as the instantaneous model does with insufficient load increments), and a portion of the total bolt slip can occur below the slippage load, which occurs in experimental testing.

5.3 Recommendations for Future Work

The program developed in this study was intended to accurately predict the behavior of transmission towers under working load conditions. The program could be expanded to predict the behavior up to ultimate load. Considerations for member yielding and buckling could be included, as well as the ability to include material and geometric nonlinearity. Such considerations would require an improved nonlinear solution method, requiring an iteration procedure for each load increment.

The program could also be improved by developing a method to input data faster and easier. Although a sophisticated preprocessor might not improve the efficiency of a linear interpolation data generation scheme since each element has its own specific slippage parameters, connection and orientation nodes, loading conditions, and material properties.

To increase the accuracy of the proposed slippage models, continued experimental testing on typical tower members and connection types could be conducted. A joint element could be formulated to incorporate both rotational slippage and translational slippage by modification of the technique used for semi-rigid joints in the TAP program. The joint element could model the slippage characteristics of a typical tower member up to yielding – not just modeling clearance slip but the entire load-slip relationship. Although, such a model would more accurately represent the experimental data, the conclusions of this study are unlikely to change as a result of a more realistic bolt-slip model.

Appendix A

STIFFNESS MATRICES OF TRUSS AND BEAM ELEMENTS

A.1 Two-Dimensional Truss Element

The stiffness matrix of a two-dimensional truss element in the global axes system is given as

$$[k]=\frac{EA}{L}\begin{bmatrix} C_x^2 & C_xC_y & -C_x^2 & -C_xC_y \\ C_xC_y & C_y^2 & -C_xC_y & -C_y^2 \\ -C_x^2 & -C_xC_y & C_x^2 & C_xC_y \\ -C_xC_y & -C_y^2 & C_xC_y & C_y^2 \end{bmatrix} \tag{A.1}$$

where C_x, C_y, C_z are the direction cosines of the element in the x, y, and z directions respectively.

A.2 Three-Dimensional Truss Element

The stiffness matrix of a three-dimensional truss element in the global axes system is given as

$$[k]=\frac{EA}{L}\begin{bmatrix} C_x^2 & C_yC_x & C_zC_x & -C_x^2 & -C_yC_x & -C_zC_x \\ C_xC_y & C_y^2 & C_zC_y & -C_xC_y & -C_y^2 & C_zC_y \\ C_xC_z & C_yC_z & C_z^2 & -C_xC_z & -C_yC_z & -C_z^2 \\ -C_x^2 & -C_yC_x & -C_zC_x & C_x^2 & C_yC_x & C_zC_x \\ -C_xC_y & -C_y^2 & -C_zC_y & C_xC_y & C_y^2 & C_zC_y \\ -C_xC_z & -C_yC_z & -C_z^2 & C_xC_z & C_yC_z & C_z^2 \end{bmatrix} \tag{A.2}$$

A.3 Two-Dimensional Beam Element

The stiffness matrix of a two-dimensional beam element in the member axes system is given as

$$[k_m]=\begin{bmatrix} \frac{EA}{L} & 0 & 0 & -\frac{EA}{L} & 0 & 0 \\ 0 & \frac{12EI_z}{L^3} & \frac{6EI_z}{L^2} & 0 & -\frac{12EI_z}{L^3} & \frac{6EI_z}{L^2} \\ 0 & \frac{6EI_z}{L^2} & \frac{4EI_z}{L} & 0 & \frac{6EI_z}{L^2} & \frac{2EI_z}{L} \\ -\frac{EA}{L} & 0 & 0 & \frac{EA}{L} & 0 & 0 \\ 0 & -\frac{12EI_z}{L^3} & -\frac{6EI_z}{L^2} & 0 & \frac{12EI_z}{L^3} & -\frac{6EI_z}{L^2} \\ 0 & \frac{6EI_z}{L^2} & \frac{2EI_z}{L} & 0 & -\frac{6EI_z}{L^2} & \frac{4EI_z}{L} \end{bmatrix} \quad \text{(A.3)}$$

To obtain the stiffness matrix in the global axes system $[k_m]$ must be transformed using the following expression

$$[k]=[T]^T\cdot[k_m]\cdot[T] \quad \text{(A.4)}$$

where

$$[T]=\begin{bmatrix} C_X & C_Y & 0 & 0 & 0 & 0 \\ -C_Y & C_X & 0 & 0 & 0 & 0 \\ 0 & 0 & 1 & 0 & 0 & 0 \\ 0 & 0 & 0 & C_X & C_Y & 0 \\ 0 & 0 & 0 & -C_Y & C_X & 0 \\ 0 & 0 & 0 & 0 & 0 & 1 \end{bmatrix} \quad \text{(A.5)}$$

A.4 Three-Dimensional Beam Element

The stiffness matrix of a three-dimensional beam element in the member axes system is given as

$$[k_m]=\begin{bmatrix}
\frac{EA}{L} & 0 & 0 & 0 & 0 & 0 & \frac{EA}{L} & 0 & 0 & 0 & 0 & 0 \\
0 & \frac{12EI_z}{L^3} & 0 & 0 & 0 & \frac{6EI_z}{L^2} & 0 & \frac{12EI_z}{L^3} & 0 & 0 & 0 & \frac{6EI_z}{L^2} \\
0 & 0 & \frac{12EI_y}{L^3} & 0 & \frac{6EI_y}{L^2} & 0 & 0 & 0 & \frac{12EI_y}{L^3} & 0 & \frac{6EI_y}{L^2} & 0 \\
0 & 0 & 0 & \frac{GI_x}{L} & 0 & 0 & 0 & 0 & 0 & \frac{GI_x}{L} & 0 & 0 \\
0 & 0 & \frac{6EI_y}{L^2} & 0 & \frac{4EI_y}{L} & 0 & 0 & 0 & \frac{6EI_y}{L^2} & 0 & \frac{2EI_y}{L} & 0 \\
0 & \frac{6EI_z}{L^2} & 0 & 0 & 0 & \frac{4EI_z}{L} & 0 & \frac{6EI_z}{L^2} & 0 & 0 & 0 & \frac{2EI_z}{L} \\
\frac{EA}{L} & 0 & 0 & 0 & 0 & 0 & \frac{EA}{L} & 0 & 0 & 0 & 0 & 0 \\
0 & \frac{12EI_z}{L^3} & 0 & 0 & 0 & \frac{6EI_z}{L^2} & 0 & \frac{12EI_z}{L^3} & 0 & 0 & 0 & \frac{6EI_z}{L^2} \\
0 & 0 & \frac{12EI_y}{L^3} & 0 & \frac{6EI_y}{L^2} & 0 & 0 & 0 & \frac{12EI_y}{L^3} & 0 & \frac{6EI_y}{L^2} & 0 \\
0 & 0 & 0 & \frac{GI_x}{L} & 0 & 0 & 0 & 0 & 0 & \frac{GI_x}{L} & 0 & 0 \\
0 & 0 & \frac{6EI_y}{L^2} & 0 & \frac{2EI_y}{L} & 0 & 0 & 0 & \frac{6EI_y}{L^2} & 0 & \frac{4EI_y}{L} & 0 \\
0 & \frac{6EI_z}{L^2} & 0 & 0 & 0 & \frac{2EI_z}{L} & 0 & \frac{6EI_z}{L^2} & 0 & 0 & 0 & \frac{4EI_z}{L}
\end{bmatrix} \tag{A.6}$$

To obtain the stiffness matrix in the global axes system, $[k_m]$ must be transformed using equation A.4, where

$$[T]=\begin{bmatrix}
[T'] & 0 & 0 & 0 \\
0 & [T'] & 0 & 0 \\
0 & 0 & [T'] & 0 \\
0 & 0 & 0 & [T']
\end{bmatrix} \tag{A.7}$$

and

$$[T']=\begin{bmatrix}
C_x & C_y & C_z \\
\frac{-C_x \cdot C_y \cdot \cos\alpha - C_z \cdot \sin\alpha}{\sqrt{C_x^2+C_z^2}} & \sqrt{C_x^2+C_z^2}\cdot\cos\alpha & \frac{-C_y \cdot C_z \cdot \cos\alpha + C_x \cdot \sin\alpha}{\sqrt{C_x^2+C_z^2}} \\
\frac{C_x \cdot C_y \cdot \sin\alpha - C_z \cdot \cos\alpha}{\sqrt{C_x^2+C_z^2}} & -\sqrt{C_x^2+C_z^2}\cdot\sin\alpha & \frac{C_y \cdot C_z \cdot \sin\alpha + C_x \cdot \cos\alpha}{\sqrt{C_x^2+C_z^2}}
\end{bmatrix} \tag{A.8}$$

in which

$$\sin\alpha = \frac{z_{kr}}{\sqrt{y_{kr}^2 + z_{kr}^2}} \qquad \text{and} \qquad \cos\alpha = \frac{y_{kr}}{\sqrt{y_{kr}^2 + z_{kr}^2}} \tag{A.9}$$

The coordinates y_{kr}, and z_{kr} locate the point k (used to define the principal planes of bending) in the y_m-z_m plane. For more detail see Krishnamoorthy, C. S. (1996). In case of a vertical member (parallel to the global y-axis) the transformation must be modified as

$$[T]_{vert} = \begin{bmatrix} 0 & C_y & 0 \\ -C_y \cdot \cos\alpha & 0 & \sin\alpha \\ C_y \cdot \sin\alpha & 0 & \cos\alpha \end{bmatrix} \tag{A.10}$$

Appendix B

STIFFNESS MATRICES OF SEMI-RIGID BEAM ELEMENTS

B.1 Two-Dimensional Semi-Rigid Beam Element

The following formulation is based on the work of Al-Bermani and Kitipornchai (1992) and Chen and Lui (1987). The tangent stiffness relation of a connection element at end i of a beam element is given as

$$\begin{Bmatrix} M_{Ti} \\ M_{ei} \end{Bmatrix} = \begin{bmatrix} R_i & -R_i \\ -R_i & R_i \end{bmatrix} \begin{Bmatrix} \theta_{Ti} \\ \theta_{ei} \end{Bmatrix} \tag{B.1}$$

where M_{Ti} is the total end moment, M_{ei} is the element end moment, R_i is the rotational stiffness of the connection element, θ_{Ti} is the total nodal rotation, and θ_{ei} is the element nodal rotation (see Figure B.1). The relative joint rotation used in equations 2.16 and 2.17 is found using

$$\theta_{ri} = \theta_{Ti} - \theta_{ei} \tag{B.2}$$

The tangent stiffness relationship in the global coordinates of the beam element with connection elements at end i and end j can be written as

$$\begin{Bmatrix} M_{Ti} \\ M_{ei} \\ \{F_e\} \\ M_{Tj} \\ M_{ej} \end{Bmatrix} = \begin{bmatrix} R_i & -R_i & & & \\ -R_i & R_i & & & \\ & & [K_e] & & \\ & & & R_j & -R_j \\ & & & -R_j & R_j \end{bmatrix} \begin{Bmatrix} \theta_{Ti} \\ \theta_{ei} \\ \{r_e\} \\ \theta_{Tj} \\ \theta_{ej} \end{Bmatrix} \tag{B.3}$$

where $\{F_e\}$, $[K_e]$, $\{r_e\}$ are the element nodal forces of the beam element, the stiffness matrix of the beam element (see Appendix A), and the beam element end displacements respectively. Equation B.3 can be rewritten as

$$\{{}_cF_{ec}\} = [{}_cK_{ec}] \cdot \{{}_cr_{ec}\} \tag{B.4}$$

where $[{}_cK_{ec}]$ is a 10 x 10 stiffness matrix of a beam element with connection elements at both ends. The subscripts imply a connection element on the left end and right end of the beam element.

In order to enforce compatibility at the junctions between the connection element and the beam element, the 10 x 10 stiffness matrix must be transformed into an 8 x 8 stiffness matrix. This transformation ensures that the element rotations at both ends of the beam only appear once in the nodal displacement vector. The following kinematic relations can be written

$$\{{}_c r_{ec}\} = [{}_c T_c] \cdot \{{}_c r_{Tc}\} \tag{B.5}$$

$$\{{}_c r_{ec}\} = \langle \theta_{Ti} \quad \theta_{ei} | u_i \quad v_i \quad \theta_{ei} \quad u_j \quad v_j \quad \theta_{ej} | \theta_{Tj} \quad \theta_{ej} \rangle^T \tag{B.6}$$

$$\{{}_c r_{Tc}\} = \langle u_i \quad v_i \quad \theta_{Ti} \quad u_j \quad v_j \quad \theta_{Tj} | \theta_{ei} \quad \theta_{ej} \rangle^T \tag{B.7}$$

where the 10 x 8 kinematic transformation matrix is given as

$$[{}_c T_c] = \begin{bmatrix} 0 & 0 & 1 & 0 & 0 & 0 & 0 & 0 \\ 0 & 0 & 0 & 0 & 0 & 0 & 1 & 0 \\ 1 & 0 & 0 & 0 & 0 & 0 & 0 & 0 \\ 0 & 1 & 0 & 0 & 0 & 0 & 0 & 0 \\ 0 & 0 & 0 & 0 & 0 & 0 & 1 & 0 \\ 0 & 0 & 0 & 1 & 0 & 0 & 0 & 0 \\ 0 & 0 & 0 & 0 & 1 & 0 & 0 & 0 \\ 0 & 0 & 0 & 0 & 0 & 0 & 0 & 1 \\ 0 & 0 & 0 & 0 & 0 & 1 & 0 & 0 \\ 0 & 0 & 0 & 0 & 0 & 0 & 0 & 1 \end{bmatrix} \tag{B.8}$$

The resulting transformation gives

$$[{}_c K'_{ec}] = [{}_c T_c]^T \cdot [{}_c K_{ec}] \cdot [{}_c T_c] \tag{B.9}$$

where $[{}_c K'_{ec}]$ is now an 8 x 8 matrix. The stiffness relationship of the transformed semi-rigid beam element can be partitioned as

$$\begin{bmatrix} [k_{11}] & [k_{12}] \\ [k_{21}] & [k_{22}] \end{bmatrix} \begin{Bmatrix} \{d_1\} \\ \{d_2\} \end{Bmatrix} = \begin{Bmatrix} \{Q_1\} \\ \{Q_2\} \end{Bmatrix} \tag{B.10}$$

where

$$\{d_1\} = \langle u_i \quad v_i \quad \theta_{Ti} \quad u_j \quad v_j \quad \theta_{Tj} \rangle^T \tag{B.11}$$

and

$$\{d_2\} = \langle \theta_{ei} \quad \theta_{ej} \rangle^T \tag{B.12}$$

The degrees of freedom at the junction between the beam element and the connection element (θ_{ei} and θ_{ej}) are internal degrees of freedom and can be condensed out using static condensation. Since there are no applied moments on the internal degrees of freedom, $\{Q_2\}$ is a zero vector, and by using static condensation

$$[K]=[k_{11}]-[k_{12}]\cdot[k_{22}]^{-1}\cdot[k_{21}] \tag{B.13}$$

where $[K]$ is the 6 x 6 stiffness matrix for a semi rigid beam element in two dimensions. It is easier to implement the above transformations into a computer program by using an alternate condensation procedure. It can be shown that equation B.13 is identical to the following expression

$$[K]=[{}_cC_c]^T\cdot[{}_cK'_{ec}]\cdot[{}_cC_c] \tag{B.14}$$

where

$$[{}_cC_c]=\begin{bmatrix}[I]\\ [{}_cQ_c]\end{bmatrix} \tag{B.15}$$

in which $[I]$ is a 6 x 6 identity matrix and $[{}_cQ_c]$ is a 2 x 6 matrix containing the condensation terms

$$[{}_cQ_c]=-[k_{22}]^{-1}\cdot[k_{21}] \tag{B.16}$$

Therefore the transformation from a beam element with connection elements on both ends can be reduced to a semi-rigid beam element in one step

$$[K]=[{}_cC_c]^T\cdot[{}_cT_c]^T\cdot[{}_cK_{ec}]\cdot[{}_cT_c]\cdot[{}_cC_c] \tag{B.17}$$

Now the stiffness relationship is

$$[K]\cdot\{d_1\}=\{Q_1\} \tag{B.18}$$

and the displacements and total rotations in $\{d_1\}$ can be found. To solve for the element rotations use

$$\{d_2\}=-[k_{22}]^{-1}\cdot[k_{21}]\cdot\{d_1\} \tag{B.19}$$

or simply

$$\{d_2\}=[{}_cQ_c]\cdot\{d_1\} \tag{B.20}$$

Since the total rotation and element rotation at a semi-rigid joint are now known, the relative rotation can be calculated using equation B.2 and the rotational stiffness of the connection element can be updated in equations B.1 and B.3 for the next load increment.

B.2 Three-Dimensional Semi-Rigid Beam Element

The formulation of the semi-rigid beam element in three dimensions is identical to the formulation in two dimensions, only there are now three rotational degrees of freedom for each connection element. The tangent stiffness relation of a connection element at end i of a beam element is now given as

$$\begin{Bmatrix} M_{xTi} \\ M_{xei} \\ M_{yTi} \\ M_{yei} \\ M_{zTi} \\ M_{zei} \end{Bmatrix} = \begin{bmatrix} R_{xi} & -R_{xi} & & & & & & & & & & \\ -R_{xi} & R_{xi} & & & & & & & & & & \\ & & R_{yi} & -R_{yi} & & & & & & & & \\ & & -R_{yi} & R_{yi} & & & & & & & & \\ & & & & & & R_{zi} & -R_{zi} & & & & \\ & & & & & & -R_{zi} & R_{zi} & & & & \end{bmatrix} \begin{Bmatrix} \theta_{xTi} \\ \theta_{xei} \\ \theta_{yTi} \\ \theta_{yei} \\ \theta_{zTi} \\ \theta_{zei} \end{Bmatrix} \tag{B.21}$$

and $\left[{}_{c}K_{ec}\right]$ in equation B.4 is now a 24 x 24 stiffness matrix. The 24 x 18 kinematic transformation matrix is now written as

$$[{}_cT_c]=\begin{bmatrix}
0&0&0&1&0&0&0&0&0&0&0&0&0&0&0&0&0&0\\
0&0&0&0&0&0&0&0&0&0&0&0&1&0&0&0&0&0\\
0&0&0&0&1&0&0&0&0&0&0&0&0&0&0&0&0&0\\
0&0&0&0&0&0&0&0&0&0&0&0&0&1&0&0&0&0\\
0&0&0&0&0&1&0&0&0&0&0&0&0&0&0&0&0&0\\
0&0&0&0&0&0&0&0&0&0&0&0&0&0&1&0&0&0\\
1&0&0&0&0&0&0&0&0&0&0&0&0&0&0&0&0&0\\
0&1&0&0&0&0&0&0&0&0&0&0&0&0&0&0&0&0\\
0&0&1&0&0&0&0&0&0&0&0&0&0&0&0&0&0&0\\
0&0&0&0&0&0&0&0&0&0&0&0&1&0&0&0&0&0\\
0&0&0&0&0&0&0&0&0&0&0&0&0&1&0&0&0&0\\
0&0&0&0&0&0&0&0&0&0&0&0&0&0&1&0&0&0\\
0&0&0&0&0&0&1&0&0&0&0&0&0&0&0&0&0&0\\
0&0&0&0&0&0&0&1&0&0&0&0&0&0&0&0&0&0\\
0&0&0&0&0&0&0&0&1&0&0&0&0&0&0&0&0&0\\
0&0&0&0&0&0&0&0&0&0&0&0&0&0&0&1&0&0\\
0&0&0&0&0&0&0&0&0&0&0&0&0&0&0&0&1&0\\
0&0&0&0&0&0&0&0&0&0&0&0&0&0&0&0&0&1\\
0&0&0&0&0&0&0&0&0&1&0&0&0&0&0&0&0&0\\
0&0&0&0&0&0&0&0&0&0&0&0&0&0&0&1&0&0\\
0&0&0&0&0&0&0&0&0&0&1&0&0&0&0&0&0&0\\
0&0&0&0&0&0&0&0&0&0&0&0&0&0&0&0&1&0\\
0&0&0&0&0&0&0&0&0&0&0&1&0&0&0&0&0&0\\
0&0&0&0&0&0&0&0&0&0&0&0&0&0&0&0&0&1
\end{bmatrix} \qquad \text{(B.22)}$$

Equation B.15 can also be applied to the three-dimensional semi-rigid beam, only now the identity matrix, $[I]$, is a 12 x 12 matrix and $[{}_cQ_c]$ is a 6 x 12 matrix. Again the stiffness of the three-dimensional semi-rigid beam element is written as

$$[K]=[{}_cC_c]^T\cdot[{}_cT_c]^T\cdot[{}_cK_{ec}]\cdot[{}_cT_c]\cdot[{}_cC_c] \qquad \text{(B.20)}$$

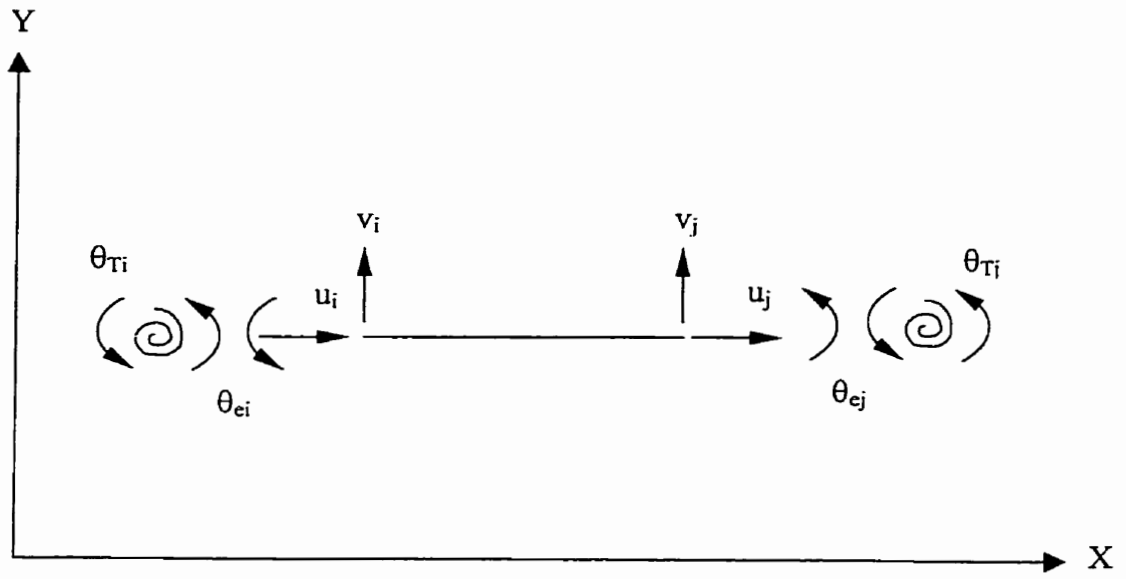

Figure B.1: 2-D Beam Element with Semi-Rigid joints at Both Ends

Appendix C

STRUCTURES FOR LINEAR VERIFICATION

C.1 Plane Truss

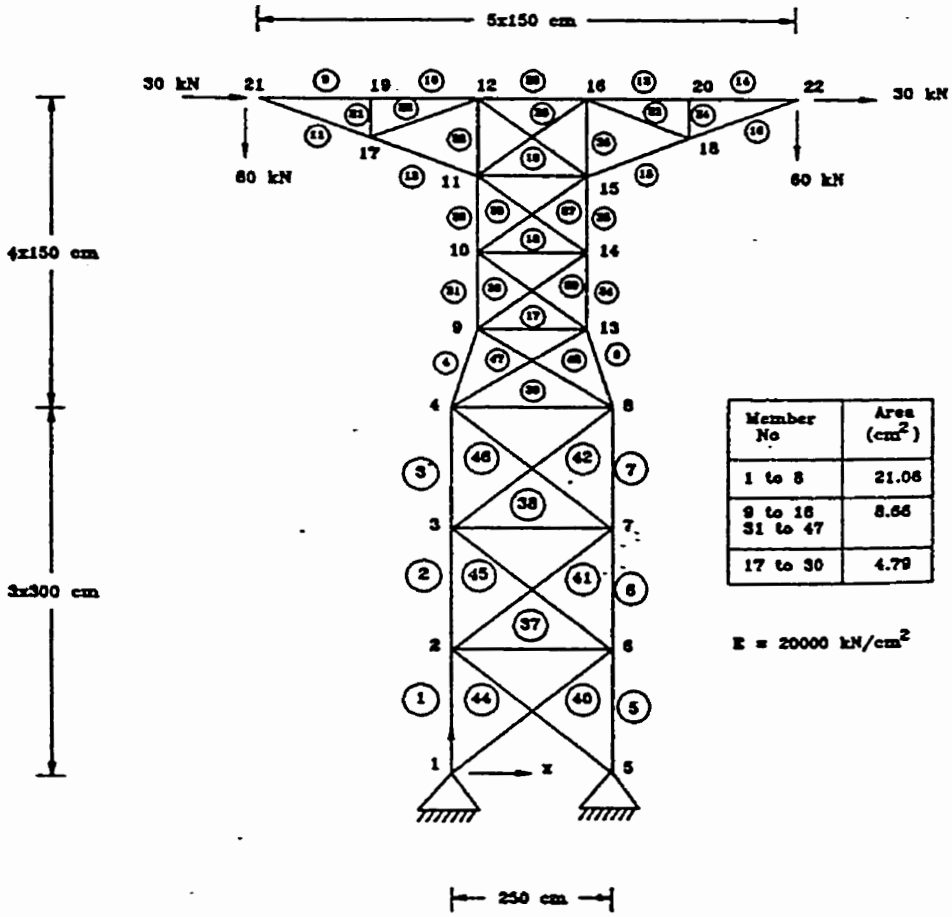

Member No	Area (cm^2)
1 to 8	21.06
9 to 16 31 to 47	8.66
17 to 30	4.79

E = 20000 kN/cm^2

C.2 Space Truss

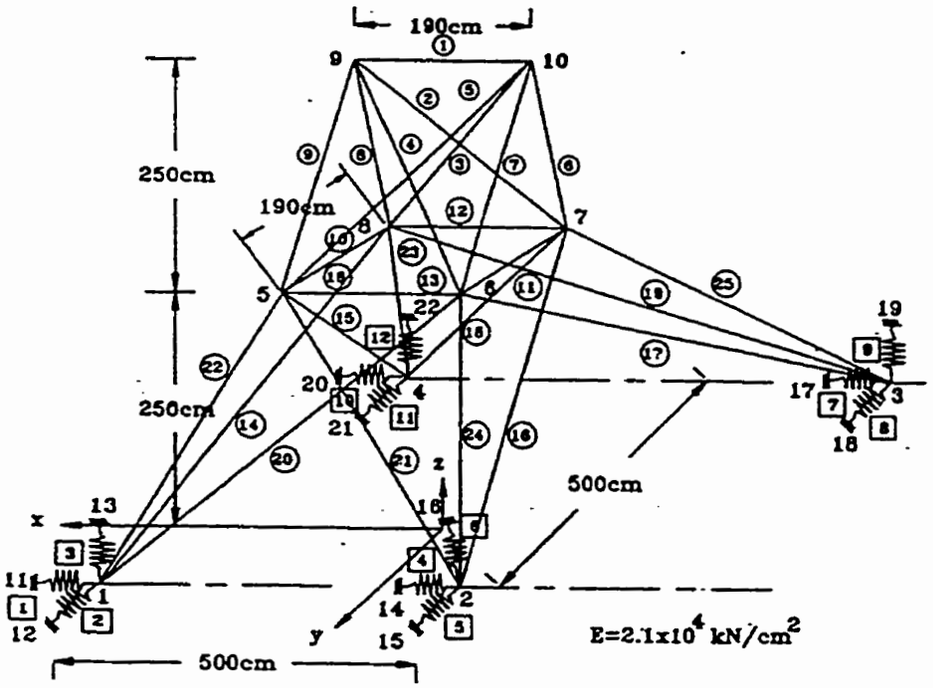

Member No.	Area (cm^2)
1 to 5	10.47
6 to 9	19.03
10 to 21	21.06
22 to 25	42.12

	Load (kN)		
Node	x-direction	y-direction	z-direction
5	−2.30	–	–
8	−2.30	–	–
9	−4.50	−45.0	−23.0
10	–	−45.0	−23.0

C.3 Plane Frame

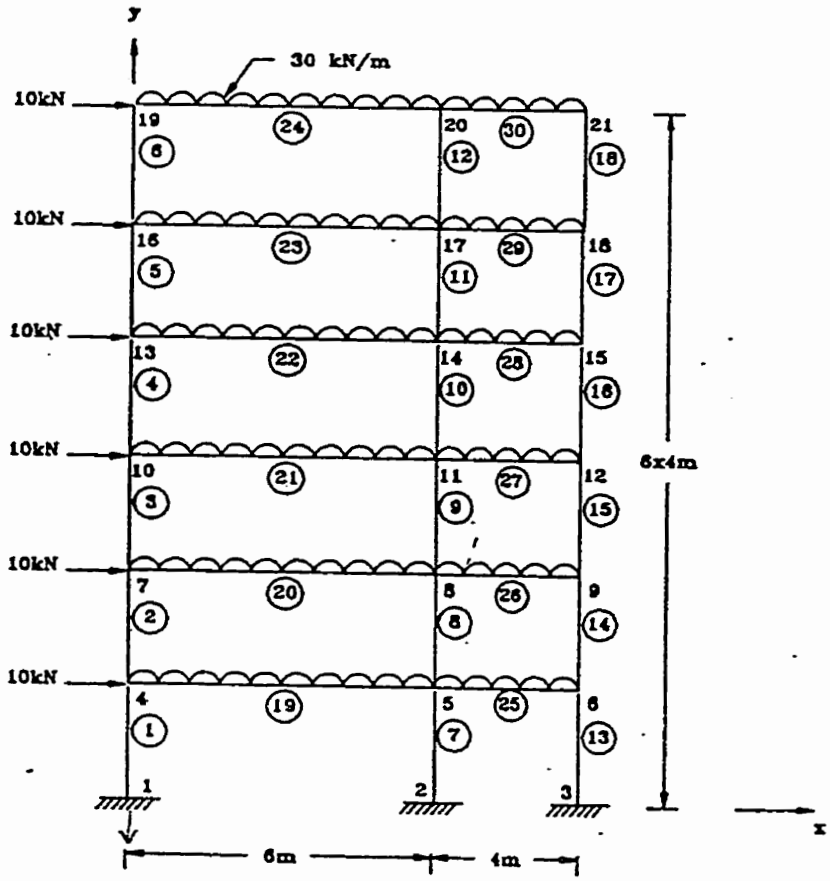

All Columns: 30 x 50*cm*
All beams : 30 x 60*cm*

$$E = 2 \times 10^3 \text{ kN/cm}^2$$

C.4 Space Frame

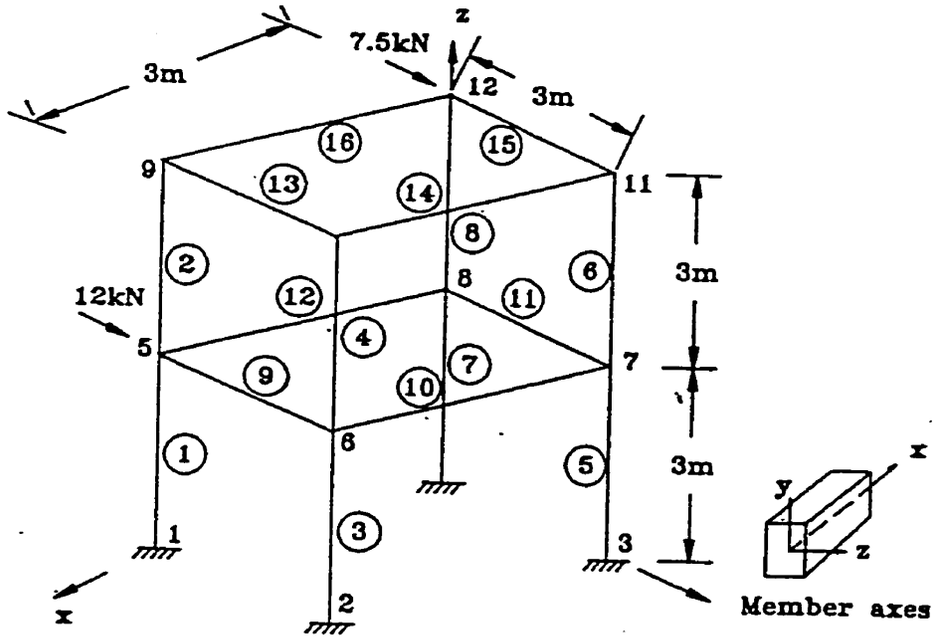

$E = 2.1 \times 10^4$ kN/cm^2

$\mu = 0.3$

	Area (cm^2)	I_x (cm^4)	I_y (cm^4)	I_z (cm^4)
All beams -	19.0	3.24	52.6	726.4
All columns -	32.33	10.0	150.0	2235.4

Fig. 7.37 Space frame 2

Member No.	Node No. (for 'k' node)
1,2	2
3,4	1
5,6	4
7,8	3
9,10	10
11,12	12
13,14	6
15,16	8

References

Alam, M. J., Santhakumar, A. R. (1996). "Reliability Analysis and Full-Scale Testing of Transmission Tower." *Journal of Structural Engineering*, 122(3), 338-344.

Al-Bermani, F. G. A., Kitipornchai, S. (1990A). "Nonlinear Analysis of Thin-Walled Structures Using Least Element/Member." *Journal of Structural Engineering*, 116(1), 215-234.

Al-Bermani, F. G. A., Kitipornchai, S. (1990B). "Elasto-plastic Large Deformation Analysis of Thin-Walled Structures." *Engineering Structures*, 12(1), 28-36.

Al-Bermani, F. G. A., Kitipornchai, S. (1992A). "Nonlinear Analysis of Transmission Towers." *Engineering Structures*, 14(3), 139-151.

Al-Bermani, F. G. A., Kitipornchai, S., Chan, S. L. (1992B). "Formex Formulation of Transmission Tower Structures." *International Journal of Space Structures*, 7(1), 1-10.

Al-Bermani, F. G. A., Kitipornchai, S. (1992C). "Elastoplastic Nonlinear Analysis of Flexibly Jointed Space Frames." *Journal of Structural Engineering*, 118(1), 108-127

ASCE. (1988). *Guide for Design of Steel Transmission Towers*, ASCE Manual 52, 2nd edition, New York.

ASCE. (1991). *Guidelines for Electrical Transmission Line Structural Loading*, ASCE Manual 74, New York.

Beck, C. F. (1971). "Computer's Role in Transmission Line Design." *Journal of the Structural Division*, ASCE, 97(1), 63-79.

Bergstrom, R. N., Arena, J. R., Kramer, J. M. (1960). "Design of Self Supported Steel Transmission Towers." *Journal of the Power Division*, ASCE, 86(3), 55-88.

Chen, W., Lui, E. (1987). "Effects of Joint Flexibility on the Behavior of Steel Frames." *Computers and Structures*, 26(5), 719-732

Delvecchio, J. N., Soom, A. (1991). "Tolerances and Available Relative Motions in Bolted Connections." *Advances in Design Automation*, ASME, 2, 177-183.

Dutson, J. D., Folkman, S. L. (1996). "A Nonlinear Finite Element Model of a Truss Using Pinned Joints." *American Institute of Aeronautics and Astronautics Journal*, 793-803.

Federal Highway Administration (FHWA). (1981). Report No. FHWA/RD-81/147 "Friction-Type Bolted Connections with A588 Weathering Steel." Offices of Research & Development, Structures and Applied Mechanics Division, Washington D.C.

Ghali, A., Neville, A. M. (1978). *Structural Analysis – A Unified Classical and Matrix Approach*, Chapman and Hall, London.

Gilchrist, R. T., Chong, K. P. (1979). "Thin Light-Gage Bolted Connections Without Washers." *Journal of the Structural Division*, ASCE, 105(1), 175-183.

Kitipornchai, S., Al-Bermani, F. G. A. (1992). "Nonlinear Analysis of Lattice Structures." *Journal of Constructional Steel Research*, 23, 209-225.

Kitipornchai, S., Al-Bermani, F. G. A., Peyrot, A. H. (1994). "Effect of Bolt Slippage on Ultimate Behavior of Lattice Structures." *Journal of Structural Engineering*, ASCE, 120(8), 2281-2287.

Kitipornchai, S., Zhu, K., Xiang, Y., Al-Bermani, F. G. A. (1991). "Single-Equation Yield Surfaces for Monosymmetric and Asymmetric Sections." *Engineering Structures*, 13(10), 366-370.

Kitipornchai, S., Chan, S. L. (1987). "Nonlinear Finite Element Analysis of Angle and Tee Beam-Columns." *Journal of Structural Engineering*, 113(4), 721-739.

Knight, G. M. S., Santhakumar, A. R. (1993). "Joints Effects on Behavior of Transmission Towers." *Journal of Structural Engineering*, 119(3), 698-712.

Krishnamoorthy, C. S. (1996). *Finite Element Analysis - Theory and Programming*, 2nd edition, Tata McGraw-Hill Publishing Company Limited, New Delhi.

Lo, D. L. C., Morcos, A., Goel, S. K. (1975). "Use of Computers in Transmission Tower Design." *Journal of the Structural Division*, ASCE, 101(7), 1443-1453.

Lobb, V., Stoller, F. (1971). "Bolted Joints Under Sustained Loading." *Journal of the Structural Division*, ASCE, 97(3), 905-933.

Marjerrison, M. (1968). "Electric Transmission Tower Design." *Journal of the Power Division*, ASCE, 94(1), 1-23.

Mercadal, M., Vander Velde, W. E. (1989). "Analysis of Limit Cycle in Control Systems for Joint-Dominated Structures." *Journal of Guidance*, 12(3), 388-395.

Onada, J., Sano, T., Minesugi, K. (1994). "Passive Damping of Truss Vibration Using Preloaded Joint Backlash." *American Institute of Aeronautics and Astronautics Journal*, 33(7), 1335-1341.

Owen, D. R. J., Hinton J. (1980). *Finite Elements in Plasticity*, Pineridge Press Limited, U.K.

Petersen, W. (1962). "Design of EHV Steel Tower Transmission Lines." *Journal of the Power Division*, ASCE, 88(1), 39-65.

Rossow, E. C., Lo, D. L. C., Chu, S. (1975). "Efficient Design-Analysis of Physically Nonlinear Trusses." *Journal of the Structural Division*, ASCE, 101(4), 839-853.

Roy, S., Fang, S., Rossow, E. C. (1984). "Secondary Stresses on Transmission Tower Structures." *Journal of Energy Engineering*, 110(2), 157-173.

Shi, G., Atluri, S. N. (1991). "Nonlinear Dynamic Response of Frame-Type Structures with Hysteretic Damping at the Joints." *American Institute of Aeronautics and Astronautics Journal*, 30(1), 234-240.

Ungkurapinan, N. (2000). "A Study of Joint Slip in Galvanized Bolted Angle Connections." Masters thesis presented to the University of Manitoba, Winnipeg.

Williams, D. C. J., Brightwell, I. W. (1987). "Stochastic Method of Assessing the Effect of Joint Deformation on Bolted Lattice Towers" *Probabilistic Methods Applied to Electric Power Systems, Proceedings of the First International Symposium*, 365-373.

Winter, G. (1956). "Tests on Bolted Connections in Light Gage Steel." *Journal of the Structural Division*, ASCE, 82(2), paper 920, 1-25.

Yue, B. (1994). *Tower Design and Analysis Program Users Manual*. Manitoba Hydro-Transmission and Civil Design Department.

Zienkewicz, O. C., Taylor, R. L. (1989). *The Finite Element Method*, 4th edition, McGraw-Hill Book Company, London.